UNIVERSITY OF CALGARY

Determination and Application of Asphaltene Property Distributions for Native and Refined Crude Oils

by

Diana Maria Barrera

A THESIS

SUBMITTED TO THE FACULTY OF GRADUATE STUDIES

IN PARTIAL FULFILMENT OF THE REQUIREMENTS FOR THE

DEGREE OF MASTER OF SCIENCE

DEPARTMENT OF CHEMICAL AND PETROLEUM ENGINEERING

CALGARY, ALBERTA

July, 2012

Abstract

Asphaltenes are the heaviest and most polar components of crude oils and they present a number of challenges during production and processing of crude oil, particularly due to precipitation which is a first step towards deposition and fouling. In order to understand and model asphaltene precipitation, it is necessary to determine basic physical properties such as the density and molecular weight. However, asphaltenes are a mixture of hundreds of thousands of chemical species some of which self-associate, and it has proven challenging to determine these properties. The challenge is even greater for refined materials because the molecules and their self-association behavior have been altered via reaction. The objectives of this thesis are: 1) to develop a methodology to determine the density and molecular weight distributions of asphaltenes from both native and refined crude oils; 2) model asphaltene precipitation from native and reacted streams.

Asphaltenes from a given feedstock were fractionated into different solubility cuts in solutions of *n*-heptane and toluene. At a given *n*-heptane/toluene (HT) mass ratio, the asphaltenes were divided into a soluble (light) cut and an insoluble (heavy) cut. The fractionation was repeated at different HT ratios to obtain a series of light and heavy cuts. The density of each cut was determined indirectly from the densities of solutions of asphaltenes and toluene at 23°C measured with an Anton Paar density meter. The apparent molecular weight of each cut was measured for asphaltene concentrations up to 60 kg/m^3 in toluene at 50°C using a Jupiter vapor pressure osmometer.

In theory, the property distributions of the whole asphaltenes can be reconstructed from the properties of the cuts. However, since asphaltenes self-associate, the molecular weight of the fractions will likely change when the cuts are redissolved in toluene. Therefore, the molecular weight data were modeled with a previously developed association model. The model assigns a mole fraction of molecules that propagate self-association and a mole fraction of molecules that terminate the self-association. Once mole fractions are known, the mole fraction of each class of molecule in the whole

asphaltene can be reconstructed from material balances of the cuts. Ultimately, a self-consistent distribution of molecular classes was obtained from which a molecular weight distribution was calculated using the model. The distribution was then used as an input into a previously developed regular solution model for asphaltene precipitation. Predictions of asphaltene yield from solutions of asphaltenes in *n*-heptane and toluene were compared against experimental data.

Molecular weight and density distributions from four native and four refined crude oils were determined. The density and molecular weight data together suggest that approximately 90 wt% of the asphaltenes in any sample self-associate. The density data also indicated that asphaltene aggregates have a nearly uniform average density.

The previously developed regular solution model, using a Gamma distribution to represent the asphaltene molecular weight distribution, was able to predict the solubility of native, non-reacted asphaltenes even with the default property correlations. Nonetheless, the model and its solubility parameter correlation were updated based on the new density data. A new solubility parameter correlation was required for the native asphaltenes. The same correlation was successfully applied to all of the reacted samples. The solubility predictions were sensitive to the shape of the molecular weight distribution of the aggregated asphaltenes. Therefore, a different set of solubility parameter correlations was required for the distribution predicted by the self-association model versus the Gamma distribution. Overall, it was demonstrated that the regular solution approach can be applied to determine the solubility of reacted asphaltenes.

Acknowledgements

I want to express my special gratitude to my supervisor, Dr. Harvey W. Yarranton, for giving me the opportunity to join his team and for believing in me, even in the most difficult moments. I admire how, with his calm, I always ended up doing more work than I wanted to do and I did not even notice it. Thanks for giving me space to think and work by myself, even if that meant random meetings with crazy amounts of results that neither of us could understand. Working with him made me improve in so many areas of my life that it is not possible to move to the next stage of my life without missing him and his group.

I would like to thank my committee, Dr. Josephine Hill, Dr. Pedro Pereira and Dr. Ed Ghent for taking the time to participate in this thesis. I would also want to thank the University of Calgary, the Faculty of Graduate Studies and the Department of Chemical and Petroleum Engineering for giving me the opportunity of continue my studies and achieve one of the biggest achievements in my career. Thanks to Shell Global Solutions for the financial support to this project and for the interest that showed in the results of this research.

I also would like to thank all the people from the Asphaltene and Emulsion Research group, especially to Elaine Baydak, who was one of the biggest supports when I was lost and could not understand where I was going; she was always there with a big smile cheering me up and helping me to continue learning every day. Some of her ideas and comments are also expressed in this thesis, because she was the one accompanying me during my writing. I would like to thank Diana Ortiz for her time teaching me all the characterization techniques and for her help with some of the samples.

I want to thank all my family and friends because they let me talk about asphaltenes even if they do not understand, and they also turned the grey and cold days into amazing moments with their messages and calls. Thanks to all the people that I met since I came

here, because they showed me that it was worthy to create new bonds with people completely different than me. Thanks to my grandmother Aura who taught me to give everything in all that I do and who was the one reminding me that it is important to be not only an excellent professional but also an amazing person, in that way we will always be with the ones that we love, even if they cannot see us. Thanks to my mom Gladys, because she never complained about my crazy calls in the moments that I needed the most and the only thing that I wanted was her hug, and I want to congratulate her for letting me to grow up on my peace and because I cannot see how someone could be a better support in my life than her. Thanks to my dad Manuel, because even with his crazy way of loving me, today I can say that I am just like him, and I am proud of that. And, thanks to my sister Natalia for being always there, always listening to me, always trusting me; hopefully one day I will be as good sister as her.

To Aura who was the light guiding me in the darkness

To Gladys for being my biggest fan

To Natalia, who always makes me feel closer to home

To Manuel because my work is the result of his amazing work

Table of Contents

List of Tables

List of Figures

List of Symbols and Nomenclature

A	Coefficient in VPO calibration equation
A	Fitting parameter from Equation 4.31
A	Parameter in solubility parameter expression
a	Fitting parameter from Equation 5.17
B	Fitting parameter of Equation 4.31
C	Concentration
C	Fitting parameter of Equation 4.31
c	Fitting parameter from Equation 5.21
cumf	Cumulative mass fraction in molecular weight distribution
cumw	Cumulative mass fraction in density distribution
D	Fitting parameter of Equation 4.31
d	Fitting parameter from Equation 5.21
E	Voltage
f	Fugacity
H	Heat
HT##	Heptol ratio with ##% of *n*-heptane
HT##L	Light fraction soluble in *HT##*
HT##H	Heavy fraction precipitated using *HT##*
I	Intercept in the specific volume plot
K	Association constant in the single-end termination model
K	Equilibrium ratio
K	Proportionality constant from the VPO
l	Interaction parameter
MW	Molecular weight
N	Neutral molecules
n	Number of fractions in calculation of molecular weight distribution
P	Pressure
P	Propagator molecules

R	Universal gas constant
S	Slope in the specific volume plot
T	Terminator molecules
T	Absolute temperature
w	Mass fraction
x	Molar fraction

Greek Symbols

Γ	Gamma function
Δ	Difference
α	Parameter of the Gamma distribution
β	Binary interaction parameter for non-ideal systems
β	Parameter of the Gamma distribution
γ	Activity coefficient
δ	Solubility parameter
ρ	Density
υ	Molar volume
ϕ	Volume fraction

Superscripts

^{0}	Standard
$^-$	Average
H	Heavy phase
L	Light phase

Subscripts

0	Initial
1, 2, 3, …	1^{st}, 2^{nd}, 3^{rd}, …
2	Solute
A	Asphaltenes

avg	Average
H	Heavy phase
HT##L	Light fraction soluble in *HT##*
HT##H	Heavy fraction precipitated using *HT##*
i, j, k	i^{th} , j^{th} and k^{th} components
incr	Increment or cut
L	Light phase
m	Mixture
mono	Monomer
n	Number of monomers in an aggregate.
N	Neutral molecules
P	Propagators molecules
s	Solvent
T	Terminator molecules
T	Toluene
vap	Vapour

Chapter 1: Introduction

The global demand of petroleum products continues to increase throughout the world even as traditional light sources of crude oil are depleting. Hence, there is a demand to exploit reservoirs containing heavier oil. Heavy oil usually requires thermal stimulation or dissolution with solvents for recovery and is more challenging to process (Speight, 2007). Some of the solvents used in recovery and processing, especially paraffinic solvents, can cause asphaltene precipitation leading to deposition and fouling which can reduce production and increase operating costs (Agrawala *et al.*, 2001; Andersen, 2008; Leontaritis *et al*., 1987; Leontaritis, 1989). The stability of blended, partially reacted streams against asphaltene precipitation is a concern for refineries. The introduction of heavy oil feedstocks may exacerbate this issue.

Asphaltenes are defined as the fraction of crude oil that is insoluble in aliphatic compounds, but soluble in aromatic solvents (Speight, 2007; Andersen, 2008). They precipitate from petroleum upon changes of temperature, pressure and composition as a solid-like phase. They are a complex mixture of millions of structural types and, to date, the distribution of asphaltene molecular structures cannot be specifically characterized due to their variety and complexity. However, it has been shown that asphaltenes consist of condensed aromatic nuclei linked to alkyl and cycloalkyl systems with heteroatoms such as oxygen, nitrogen and sulfur (Sheremata *et al*., 2004, Speight, 2007; Kuznicki *et al*., 2008).

When asphaltenes precipitate during petroleum processing, they plug pores in oil reservoir rocks, oil wells and surface equipment. They also create stable water-in-oil emulsions and precipitate as a solid-like phase in pipelines and vessels. During refining of petroleum, asphaltenes increase coke formation, fouling of heat exchangers and separation equipment and poisoning of catalysts. These problems are sources of economic losses in the oil industry, thus a better understanding of asphaltene behavior is required in order to avoid operational problems (Birdi, 2008).

Asphaltenes in solution also form aggregates of molecules. The exact mechanism of association has not been established, but involves a combination of aromatic π-π stacking, hydrogen bonding and van der Waals forces (Yen *et al.*, 1961; Speight, 1994; Andersen, 2008). Associated asphaltenes in crude oil have been modeled as colloids, reverse micelles, or macromolecules in a non-ideal solution (Pfeiffer, 1940; Ravey *et al*., 1988; Speight, 1994; Martin, 1996; Yarranton *et al*., 2000; Agrawala *et al*., 2001; Murgich *et al*., 2002; Merino-Garcia *et al.*, 2004, Friberg, 2007; Merino-Garcia *et al*., 2007; Hammami *et al*., 2007; Merino-Garcia *et al*., 2007).

Several models of asphaltene precipitation have also been developed based on these different concepts of asphaltene self-association. Colloidal models (Leontaritis *et al*., 1987; Leontaritis, 1989) have had limited application. The most successful models are phase equilibrium models that treat asphaltenes as molecular-scale aggregates in solution. The two most common approaches are the regular solution (Fussel, 1979; Hirschberg *et al*. 1984; Kawanaka *et al*., 1991; Alboudwarej *et al*., 2003; Akbarzadeh *et al*., 2005) and the equation of state models (Gupta, 1986; Ting *et al*., 2003; Sabbagh *et al*., 2006; Li and Firoozabadi, 2010). This thesis uses the modified regular solution approach from Akbarzadeh *et al.* (2005). This model requires the density, molecular weight, and solubility parameter distributions of the asphaltenes as inputs.

Since asphaltenes self-associate, it is the property distribution of the aggregated material that is required for phase behavior modeling. One approach to determine asphaltene properties is to fractionate them in different solvents, obtaining smaller cuts of still heterogeneous material but with systematic differences in properties. Fractionation methods include separation with *n*-heptane/toluene, *n*-hexane/toluene and CH_2Cl_2/*n*-pentane mixtures, or direct precipitation from crude oil. Fractions obtained with these methods demonstrate an increase in molecular weight, density, heteroatom content, aromaticity, and polarity from the most soluble to the least soluble fraction. The properties from solubility fractions have been used to estimate the molar mass and density distributions of a limited number of native petroleum asphaltenes (Yarranton *et*

al., 1996; Tojima *et al*., 1998; Kaminski *et al*., 2000; Spiecker *et al*., 2003; Trejo *et al*., 2004; Fossen *et al*., 2007; Ancheyta *et al*., 2009). While data for properties distributions from native crude oils are scarce, there are no such data for asphaltenes from reacted streams. In order to improve the prediction of asphaltene precipitation, there is a need to determining these property distributions for a variety of asphaltenes, particularly those from reacted streams.

1.1. Objectives of the Present Thesis

The main objective of this thesis is to characterize asphaltenes from native oils and reacted streams and to model their property distributions including density, molecular weight, and solubility parameters. Asphaltenes from a variety of sources are fractionated into solubility cuts by selective precipitation from solutions of *n*-heptane and toluene. The amount that is precipitated depends on the ratio of *n*-heptane-to-toluene in the solution. The average molecular weight and density of each cut are measured. Molecular weight data are fitted using the single-end termination model, which was previously developed to study asphaltene self-association (Agrawala *et al.*, 2001). Molecular weight distributions are constructed from the fitted model. Density data are used to calculate the density distribution and to correlate the experimental values with the molecular weight measurements. Finally asphaltene precipitation data are collected and modeled using the modified regular solution model (Akbarzadeh *et al.*, 2005) with the molecular weight and density distributions as inputs. Asphaltene solubility parameters are adjusted to fit the precipitation data and are correlated to density and molecular weight.

1.2. Thesis Structure

The thesis is organized into seven chapters. Chapter 2 provides a brief background to crude oil refining and introduces heavy oil characterization including the nature of asphaltenes and methods of characterization based on asphaltene fractionation. Asphaltene self-association and phase behavior models are also reviewed.

Chapter 3 presents the experimental methods used in this thesis including the precipitation of asphaltenes from crude oil, solids removal, the determination of their solubility in *n*-heptane/toluene mixtures, and their fractionation in heptol. Finally, the methods used to measure asphaltene density and molecular weight are explained.

Chapter 4 explains the self-association model for asphaltenes previously developed by Agrawala and Yarranton (2001). The chapter explains the concepts and parameters of the original model and then describes the adjustments performed for the introduction of the non-associating material present in asphaltenes.

Chapter 5 describes the regular solution model previously used to predict asphaltene phase behavior in *n*-heptane/toluene mixtures (Akbarzadeh *et al.*, 2005). Two asphaltene molecular weight distribution inputs (the output of the single-end termination model and the Gamma distribution) are presented and discussed. The chapter finishes with the presentation of the methodology for the use of the regular solution model and presents some modifications to the model.

Chapter 6 presents the results and discussion for the nine samples used in this thesis, starting with an explanation about how properties of the asphaltenes fractions were used to reconstruct the molecular weight and density distributions of the whole material. Experimental evidence indicating the presence of non-aggregating material in asphaltenes is shown and a correlation of asphaltene density as a function of molecular weight is developed. The use of the single-end termination model to fit molecular weight data and calculate the distribution is described. Differences between the calculated distribution and the Gamma distribution are discussed and their effects on the asphaltene fractional precipitation are tested using the regular solution model.

Chapter 7 summarizes the findings of this study and presents recommendations for the continuation of this project and some possible future modifications to the asphaltene association model.

Chapter 2: Literature Review

This chapter explains basic concepts related to heavy oil with a focus on asphaltenes. Heavy oil chemistry is reviewed and different models for the asphaltene structure are discussed. The concept of asphaltene association is introduced and various approaches to describe aggregation phenomena are explained. Several techniques for the fractionation of asphaltenes are shown, and the importance of this method for asphaltene property determination is discussed. Asphaltene precipitation and some of the models for the prediction of asphaltene phase behavior are summarized. Finally, the chemical changes in asphaltenes that can occur in refining are discussed.

2.1. Petroleum Chemistry

2.1.1. Heavy Oil Characterization

Crude petroleum is a naturally occurring mixture of hydrocarbon compounds present in sedimentary rock deposits. It also contains compounds of nitrogen, oxygen, sulfur, metals and other elements, and usually it is in liquid state at reservoir conditions. It has different boiling temperatures ranging from about 20°C to above 350°C, and can be separated into fractions by distillation up to 350°C; higher temperatures would risk decomposition and are usually avoided.

Petroleum properties and composition vary widely depending on the source of the material. Some crude oils contain a higher proportion of lower boiling compounds, and others contain higher amounts of higher boiling material (Speight, 2007). The physical properties of the oil such as density and viscosity vary accordingly. Petroleums are classified based on density and viscosity as follows:

- Conventional petroleum is a petroleum that can be recovered by conventional pumping operations as a free-flowing liquid. It has viscosity below 100 mPa.s at ambient temperature, and API gravity higher than 30°.

- Heavy oils are more difficult to obtain than light oils because they require thermal stimulation of the reservoir during recovery. They have a much higher viscosity than conventional petroleum (100 to 10,000 mPa.s at ambient temperature) and their API gravity is lower than 20.

- Extra heavy oils or bitumen are highly viscous and can be semisolid. Bitumen usually has API gravity in the range of 5° to 10° and a viscosity higher than 10,000 mPa.s at ambient temperature (Speight, 2007).

Petroleum can be characterized by a variety of physical techniques. The most common methods are distillation, gas chromatography and solubility based separations. Each is described below.

Distillation curves are a plot of boiling temperature versus the mass or volume distilled. The curves represent the distribution of species in the crude oil by their volatility and are used to divide a crude oil into a number of fractions each representing a different boiling range. This method is also a separation by molecular weight since the boiling temperature is proportional to the molecular mass of organic compounds. Distillation can be carried out up to 350°C at which point the material thermally decomposes. Depending on the nature of the petroleum, non-distillable material can make up as much as 60 wt% of the original crude oil, which limits the characterization of heavy oils due to the inability to determine properties of higher cuts (Speight, 2007).

Simulated distillation (SimDist) measures the retention time of petroleum components in a packed column. The retention time is calibrated to molecular weight or boiling point. SimDist provides similar information as distillation (Altgelt *et al.*, 1994). In general, distillation methods can only provide a limited characterization for heavy fluids, mainly due to the high complexity of crude oil in which the number of components in a specific molecular weight range increases markedly as molecular weight increases. There is not a

pronounced difference in physical properties among the chemical species making it impossible to differentiate the chemical species with high complexity (Speight, 2007).

Solubility based methods of characterization are based on the affinity of petroleum components with solvents and adsorbents. The most common example is SARA fractionation. This systematic extraction separates the crude oil fractions into SARA fractions (Saturates, Aromatics, Resins and Asphaltenes) following the ASTM D2007M method. Asphaltenes are a true solubility class and include all the material that is insoluble in a paraffinic hydrocarbon (*i.e.*, *n*-pentane or *n*-heptane) but soluble in an aromatic hydrocarbon (toluene). The remaining SARA fractions are adsorption classes. The saturate fraction corresponds to the non-polar material, including linear, branched, and cyclic paraffins; it is not adsorbed on polar adsorbents and is recovered with *n*-pentane as the initial eluent from a silica gel/attapulgus clay adsorption column. Aromatic compounds contain aromatic rings, they are adsorbed on a column packed with silica gel and are eluted using a mixture of *n*-pentane/toluene and by Soxhlet extraction in toluene at 30°C. Resins are adsorbed on a clay-packed column and are eluted with a mixture of acetone/toluene (Fan, 2002). The interest of this thesis is in the asphaltene fraction precipitated with *n*-heptane, designated as "C7-asphaltenes".

2.1.2. Asphaltenes

As stated above, asphaltenes are defined as the fraction from a crude oil insoluble in aliphatic compounds (such as pentane and heptane), but soluble in aromatic compounds (*i.e.*, benzene and toluene). They are dark brown to black friable solids with no definite melting point and when heated, they decompose and produce coke.

Asphaltenes are a complex mixture of thousands of structural types and the determination of an actual molecular structure is a difficult task. Data obtained from spectroscopic techniques show that asphaltenes consist of condensed aromatic nuclei bearing alkyl and cycloalkyl systems containing heteroatoms such as oxygen, nitrogen and sulfur, which in some cases are located in the ring systems. The elemental composition of asphaltenes

shows that the amounts of carbon and hydrogen usually vary in a narrow range, with a hydrogen-to-carbon atomic ratio of 1.15 ± 0.05%, but it is possible to find values outside of this range, as shown in Table 2.1. Heteroatom concentration varies notably with oxygen content varying from 0.3% to 4.9%, sulphur content ranging from 0.3% to 10.3% and nitrogen content varying from 0.6% to 3.3% (Speight, 2007).

Table 2.1. Elemental Composition of C5-Asphaltenes from Canadian Samples (Speight, 1994)

Source	Atomic Ratios				Molecular Weight
	H/C	N/C	O/C	S/C	
Athabasca	1.26	0.013	0.018	0.037	5100
Peace River	1.23	0.011	0.017	0.036	7800
Cold Lake	1.23	0.012	0.024	0.033	6860

There is not a particular molecular model that represents asphaltene molecules because a single structure cannot represent both all the characteristics and location of functional groups in an effective manner and be in agreement with field observations (Speight, 1994). However, results from investigations have given some ideas about asphaltene structure. Two extreme views are commonly used to represent asphaltene molecules: the continental- and archipelago- type architectures.

The continental or island molecular model consists of a core aromatic cluster with a large number of fused rings linked to aliphatic bridges, as shown in Figure 2.1. This pericondensed structure contains all the aromatic carbon atoms in a single aromatic group holding more than ten rings, with alkyl chains located in the periphery. This structure gives a relatively flat disk-like molecule (Kuznicki *et al*., 2008). Fluorescence depolarization results showed that asphaltene molecules contain at maximum two highly condensed aromatic clusters per molecule, supporting this structure (Sheremata *et al*., 2004).

The archipelago model (Figure 2.2) represents an asphaltene structure with small aromatic groups linked by aliphatic chains. This model is supported by results from pyrolysis, oxidation, thermal degradation and small angle neutron scattering analyses. All these techniques showed that aromatic groups present in asphaltenes contain one to four aromatic rings and are linked by aliphatic bridges up to 24 carbons long (Sheremata *et al*., 2004).

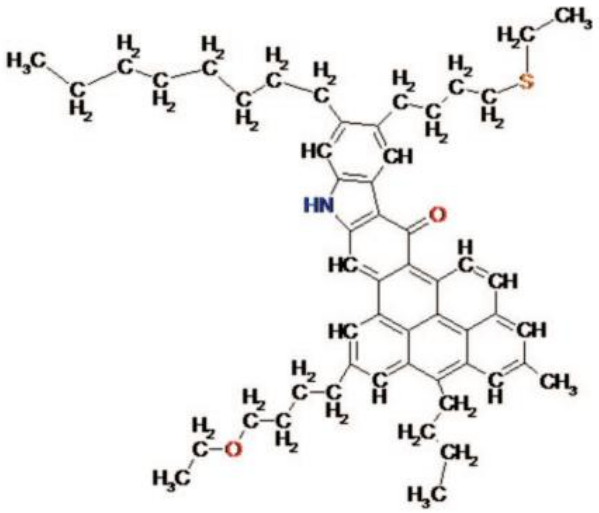

Figure 2.1. Continental model asphaltene structure (Kuznicki *et al*., 2008).

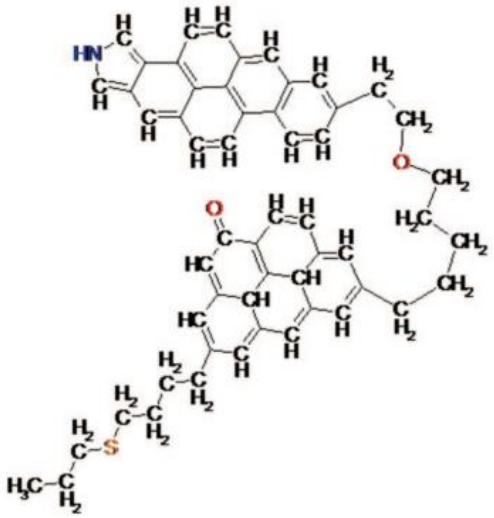

Figure 2.2. Archipelago model asphaltene structure (Kuznicki *et al.*, 2008).

2.1.3. Measurement of Asphaltene Molecular Weight

Asphaltene molecular weight can be measured using different methods, including ultracentrifuge, osmotic pressure, monomolecular film, ebullioscopy, cryoscopy, viscometry, light absorption coefficient, vapor pressure osmometry, equal osmotic pressure and equal vapor pressure. Measurement of asphaltene molar mass is not exact because of the self-association of asphaltenes. Results reported in literature may range from 600 to as high as 300,000 g/mol (Moschopedis *et al.*, 1976). The method used to determine their molecular weight must take into account the low volatility of asphaltenes and their aggregation behavior in solution.

Two of the most common techniques used to measure aggregate molar mass are gel permeation chromatography (GPC) and vapor pressure osmometry (VPO). GPC is an approach which is not limited by the low vapor pressure of asphaltenes. However, results obtained using this method are affected due to the tendency of asphaltenes to adsorb and aggregate, which affects the determination of a calibration curve at high molecular weight values (Speight, 2001). VPO allows the measurement of asphaltene molar mass as

a function of concentration in a defined solvent. Results from VPO have shown that the apparent molar mass of asphaltenes is affected by asphaltene concentration, nature of the solvent used (especially polarity) and temperature at which measurements are performed (Speight, 1994). Yarranton et al., (2000) demonstrated that VPO measures the number average molecular weight of the population of monomers and aggregated asphaltenes.

2.2. Asphaltene Association

Asphaltenes form aggregates of molecules in solution, even at low concentration. The exact mechanism of association has not been established, but possible causes of asphaltene interaction are aromatic π-π stacking, hydrogen bonding, Van der Waals forces or a combination of the different mechanisms (Speight, 2007).

According to x-ray measurements, aromatic sheets tend to stack one on top of the other to a maximum of five, creating larger particles. When heteroatoms or saturations are present in the asphaltene structure, the sheets tend to bend preventing a close approach and creating an amorphous structure. However, there is no evidence that π-π stacking is the main interaction involved in asphaltene aggregation (Yen *et al.*, 1961; Speight, 1994; Andersen, 2008).

Intermolecular hydrogen bonds can be formed between the OH, NH, and COOH functional groups present in asphaltenes. The importance of this mechanism depends on the arrangement and size of the molecules because, in large molecules, the hydrogen bonding sites can be sterically hindered (Andersen, 2008).

Ultimately, the means by which asphaltenes are dispersed in the petroleum is not clear. It has been proposed that associated asphaltenes may exist in crude oil as colloids, as reverse micelles, or as macromolecules in a non-ideal solution. Each one of these postulates leads to different asphaltene precipitation models.

2.2.1. Micellar Model

The term "micelle" has often been used to describe asphaltene aggregates when in fact the term "colloid" or "macromolecule" better fits the authors' meaning. Strictly speaking a micelle is a cluster of surface active molecules in aqueous solution arranged such that the hydrophobic non-polar groups are in the centre of the structure and the hydrophilic polar groups are towards the outer surface in contact with the polar solvent (such as water). Micellization can be considered as a separate phase that forms above a critical micelle concentration (cmc) of surfactant. The cmc is determined experimentally as a change in the slope of the plot of surface tension for an aqueous solution against the logarithm of the surfactant concentration (Friberg, 2007).

In a reverse micelle where the solvent is now organic, the polar groups are sequestered in the core and the non-polar groups are extended away from the centre. For the case of asphaltenes, polynuclear aromatic groups with the higher strength of intermolecular forces and the lowest solubility in aliphatic compounds would be located in the core, and would be surrounded by chains with lower aromaticity. A composition change or the application of an external potential can disturb the balance of forces between the micelles and cause an irreversible asphaltene flocculation.

Results from interfacial tension and isothermal titration calorimetry (Yarranton *et al*., 2000) showed that there is not a critical micelle concentration (cmc) for asphaltenes in solution for the range of concentration measured (down to 2 g/L). They speculated that the aggregation number is too small to consider asphaltenes as typical micelles and they noted that asphaltenes associate in a stepwise manner rather than the sudden transition characteristic of micelles. These observations indicate that micellar model may not apply for asphaltene aggregates (Yarranton *et al*., 2000; Merino-Garcia *et al*., 2007).

2.2.2. Colloidal Model

This model posits that asphaltenes create stacked structures held together by p-p bonding and that aromatic hydrocarbons of lower molecular weight such as resins adsorb, or

simply surround these colloidal structure. This surrounding layer acts as a peptizing agent and maintains the asphaltenes as a colloidal dispersion within the crude oil. These molecules are also surrounded by subsequently lighter compounds, until the molecules become predominantly aliphatic. This gradual transition creates a non-defined interphase between asphaltenes and petroleum.

Changes of pressure, temperature or concentration cause desorption of resins and generate attraction forces between asphaltene molecules, creating larger structures that precipitate depending on their size (Pfeiffer, 1940; Speight, 1994). For example, the addition of a normal alkane liquid to a crude oil makes it lighter and reduces its viscosity, but at the same time affects the equilibrium, which can be re-established with the desorption of resins from the asphaltene surface. A higher degree of desorption produces the agglomeration of asphaltenes as an attempt to reduce the overall surface free energy. If sufficient amount of alkane is added, asphaltene molecules aggregate to such a point where they begin to precipitate (Hammami *et al*., 2007).

The asphaltene colloidal model is supported by small-angle neutron scattering and small-angle X-ray scattering measurements, showing that asphaltenes consist of stacked aromatic sheets held together by π-π bonding. Small angle x-ray and neutron scattering experiments also showed spherical or disk-shaped particles dispersed in crude oil and in asphaltene-toluene mixtures (Ravey *et al*., 1988; Yarranton *et al*., 2000). The colloidal model is complex due to the use of a large number of parameters used to account for asphaltene association. Most colloidal models predict that asphaltene precipitation is irreversible which is not the case, and have yet to predict a wide range of asphaltene phase behaviour.

2.2.3. Oligomerization Model

This model posits that asphaltenes aggregate in a manner analogous to polymerization except that aggregates are held together by dispersion forces rather than covalent bonds. The aggregates are considered to be macromolecules that are part of the solution that is a

crude oil. Aggregation is based on the equilibrium between propagating species and the aggregates formed as follows:

$$P_n + P_1 \leftrightarrow P_{n+1} \qquad [P_{n+1}] = K_{n+1}[P_n][P_1] \qquad (2.1)$$

where P_n is an asphaltene aggregate with n monomers linked and K_n is the association constant of reaction n. The aggregation reactions are assumed to be first order with respect to both the propagating molecules and the aggregates.

The stepwise association models based on this approach vary depending on the parameters used to fit the experimental data. One option is to consider that only dimers are formed (P_2) and the fitting parameters are the equilibrium constant and the enthalpy of self-association (Murgich *et al*., 2002). Other models allow the formation of larger aggregates, but assume that all equilibrium constants and enthalpies are the same for all the reactions (Martin, 1996). An additional approach decreases the value of the equilibrium constant as asphaltene aggregates grow (Martin, 1996).

Another way of looking at asphaltenes is to consider them as a mixture of two types of molecules: propagators, which have multiple active sites and allow the growing of asphaltene aggregates, and terminators, which have only one interaction site and limits the size of the final aggregate (Agrawala *et al*., 2001). In this case, a new parameter is added to the model: the ratio of terminators to propagators, $(T/P)_o$ (Merino-Garcia *et al.*, 2004, Merino-Garcia *et al*., 2007). This model can fit asphaltene molar mass data with few parameters, and the results can be used directly in a thermodynamic model to predict asphaltene molar mass distribution and asphaltene solubility (Agrawala *et al*., 2001). Additionally, this approach fits with excellent results the experimental data obtained from isothermal titration calorimetry (Merino-Garcia *et al*., 2007). This model is presented in detail in Chapter 4.

2.3. Asphaltene Property Distributions

Since asphaltenes are a mixture of millions or more species with a wide range of properties, the amount and type of species that precipitate depend strongly on the conditions at which the precipitation occurs. For example, Figure 2.3 shows that as higher molecular weight paraffinic solvents are used for asphaltene precipitation, the amount of precipitated asphaltenes decreases until a limiting value is reached above *n*-octane (Mitchell *et al*., 1973). Asphaltenes precipitated with *n*-heptane have a higher degree of aromaticity and a higher content of heteroelements than those precipitated with *n*-pentane (Speight, 1994; Speight *et al*., 1981). The amount of precipitated asphaltenes also decreases as temperature increases (Speight, 2007) but is less sensitive to pressure.

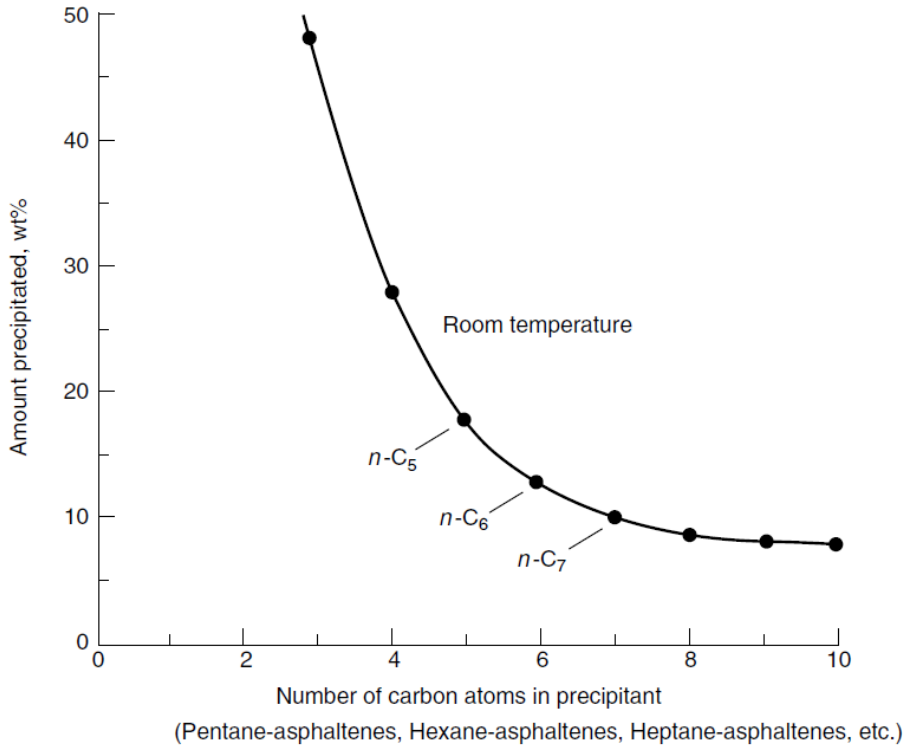

Figure 2.3. Change in asphaltene yield with carbon number of paraffin used (Speight, 2007).

The variation in properties with precipitation conditions provides an opportunity to fractionate asphaltenes in order to examine property distributions or separate particular types of species. Most of the asphaltene fractionation procedures reported in the literature

are performed by solvents. Allowing the precipitation or dissolution of asphaltenes, different fractions can be obtained, reducing the heterogeneity of the components comprised in asphaltenes (Ancheyta *et al*., 2009).

Asphaltene fractionation can be performed using mixtures of different ratio of toluene/*n*-heptane (sometimes called heptol). Tojima *et al*. (1998) divided asphaltenes into heavy and light fractions according to their solubility and obtained four fractions, each one corresponding approximately to 25% of the original asphaltenes. They found that the least soluble fraction (the first insoluble fraction separated) contained the heaviest and most aromatic asphaltenes. This indicates that the heavier asphaltene material precipitates first. The light asphaltenes (soluble fractions) had similar properties to resins.

Trejo *et al*. (2004) precipitated C7-asphaltenes by Soxhlet extraction from dilutions in toluene and the addition of *n*-heptane. They varied the heptane/toluene ratio of the mixture and obtained three different fractions. Results showed that the least soluble fraction contained the heaviest material and had the highest heteroatom content. They observed that unfractionated asphaltenes and fractions exhibit different properties and structural parameters, and they found a linear relationship between the amount of asphaltenes precipitated and heptane–toluene concentration, which is in disagreement with other results (Yarranton, 1996; Spiecker, 2003).

Spiecker *et al*. (2003) dissolved the C7-asphaltenes in toluene and then added heptane. The precipitated asphaltenes were dissolved in methylene chloride and the soluble asphaltenes were isolated. Varying the heptol ratio, they obtained different soluble and precipitate asphaltenes. They observed an increase in the amount of precipitated asphaltenes as the heptane concentration in heptol increased. The precipitated fractions were less soluble in methylene chloride than the whole asphaltenes, indicating that the precipitate had a higher degree of aggregation. Solubility curves showed that precipitated asphaltenes had the lowest solubility and that soluble fractions might help solubilize the precipitated aromatic and polar compounds in heptol. It was found that soluble

asphaltenes were less aromatic, had lower molecular weights and lower metals content than precipitated asphaltenes.

Yarranton *et al*. (1996) used mixtures of hexane–toluene at different ratios. Results showed that asphaltene precipitation increased with the hexane ratio in the solvent mixture. They also found that asphaltenes precipitated at the lowest hexane ratio had the highest molar mass and density of the fractions. Using the properties from the fractions, molar mass and density distributions for asphaltene could then be calculated.

Kaminski *et al*. (2000) fractionated asphaltenes using mixtures of CH_2Cl_2–pentane at different concentrations, obtaining four different fractions. Results showed that the least soluble fraction, corresponding to the most polar asphaltenes, have a crystalline microstructure, contrasting with the completely amorphous nature from the least polar fraction. Results also showed a higher concentration of metals and chlorine in the most polar fraction which matched with its low solubility in the solvents, suggesting that heteroatom content might have a direct effect on asphaltene solubility. They also stated that asphaltenes might behave as a sum of their fractions.

Fossen *et al*. (2007) used a 3:1 *n*-pentane to crude oil ratio, separating a smaller percentage of the asphaltenes, and then by successively increasing the *n*-pentane ratio, they fractionated asphaltenes into four fractions. They measured the onset point of precipitation in *n*-heptane–toluene mixtures and found that the first asphaltenes precipitating from crude oil are the least soluble fraction in the binary mixture, followed by the other fractions in the same order as in the separation with *n*-pentane. Interfacial tension was also measured and results showed a non-homogeneous behavior for this property. Thus problems caused by asphaltene precipitation from crude oil might be caused by just one of the fractions and this cannot be recognized when properties of the whole asphaltenes are measured.

In summary, many attempts have been made to fractionate asphaltenes in order to measure property distributions or selectively separate particular components such as

metals or highly heteroatom species. However, the distribution of composition and properties appears to be gradual throughout the asphaltenes. There is a gradual increase in size, density, aromaticity, and heteroatom content from the least to most soluble asphaltene but no sudden change of properties or concentration of a given type of species. The relationship between self-association and the property distributions in asphaltenes has not been addressed explicitly.

2.4. Asphaltene Phase Behaviour Modeling

It is desirable to predict the conditions that promote or prevent asphaltene precipitation. Modeling of asphaltene deposition gives information about the onset point and amount of precipitated material and this knowledge helps to reduce industry operational problems and costs. The choice of model depends on the perceived asphaltene aggregate structure. The two main approaches are colloidal models and solution models. Colloidal models have had limited success to date and most models in the literature are solution models. There have been two main solution based approaches for asphaltene precipitation: regular solution models and equation of state models. Regular solution models have proven the most successful for fitting and predicting asphaltene precipitation. A regular solution model is used in this thesis and only these models are reviewed here.

Hirschberg *et al*. (1984) considered asphaltenes as monodisperse polymeric molecules dissolved in the crude oil. This dissolution depends on pressure, temperature and composition of the system. They assumed the asphaltenes were a liquid phase in equilibrium with the bulk crude oil liquid phase. They used a three phase model and assumed that the vapour-liquid equilibrium is independent of the liquid-liquid equilibrium. The vapour-liquid equilibrium was calculated using the Soave equation of state while the liquid-liquid equilibrium based on the Flory-Huggins model (Flory, 1953; Huggins, 1941).

Kawanaka *et al*. (1991) considered asphaltenes as polydisperse polymers. They including the entropy of mixing based on the Scott and Magat theory (Scott *et al*., 1945, Scott,

1945). Inputs for the model were composition of the light phase and asphaltene properties; asphaltene properties were represented with an arbitrary molecular weight distribution, in this case the Gamma distribution. They assumed solid-liquid equilibrium and assumed that asphaltenes behaved as heterogeneous polymers.

Yarranton et al. (1996) and Alboudwarej *et al*. (2003) also used a molecular weight distribution for the associated asphaltenes but assumed a liquid-liquid equilibrium. They also used regular solution theory combined with Scott and Magat theory. This model was tested on Western Canadian heavy oils and bitumens with only one fitting parameter, the average molar mass of the asphaltenes in bitumen. Akbarzadeh *et al*. (2004, 2005) generalized the model to international bitumen and heavy oil samples over a range of temperatures and pressures. Details of this model are provided in Chapter 5.

2.5. Refining

During the refining process, crude oil is treated and separated to obtain marketable products which can be divided into three main groups: naphtha (the light and middle distillate cuts used as feedstock in the petrochemical industry), kerosene (compounds with middle boiling range used to produce solvents, diesel, fuel oil and light gas oil), and the residue (the non-volatile fraction used for lubricating oils, gas oil and waxes). The proportion of each of the fractions depends on the quality of the crude oil and the type of refinery it is processed in (Speight, 2007).

The main product of the refining process is gasoline, followed by other types of fuels and light components used in the petrochemical industry. Since light components are in high demand, refineries must convert the heavy material from crude oil into lighter products, which increases the complexity of the refining process.

The initial stage in the refining process is the removal of water and brine carried from the reservoir during the recovery; desalting is an operation where crude oil is washed with water in order to avoid operational problems such as corrosion and plugging, and is

followed by the dewatering stage which is a separation based on difference of densities. After this early stage, the stages present in the refining process vary and may include one or more of the following processes: (Speight, 2007): distillation, thermal cracking, catalytic cracking, hydrogenation, coking, deasphalting and hydrocracking. Some of these processes alter the chemistry of the petroleum feed.

Thermal cracking is a decomposition of the higher-boiling components at elevated temperature into light and heavy gas oil, and a residue which is used as fuel. It involves the thermal breaking of the heavy and complex molecules into smaller chains with a higher value for the petrochemical industry. The inlet for this refining stage is the residue from the distillation stage, which is cracked and separated. Conditions of the process range from 455°C to 540°C and 100 psi to 1000 psi. The operating conditions affect the conversion, the composition of the products, and the percentage of coke generated from the residue.

During catalytic cracking, the gas oil fraction is in contact with a catalyst in order to produce gasoline and lower-boiling products. The catalyst can be arranged in a fixed or fluidized bed and in form of pellets, beads or microspheres. Conditions of temperature and pressure vary according to the catalyst selected for the process. Many types of catalyst are employed but the most common are hydrated aluminum silicates with oxides of zirconium, boron, or thorium. The main problem for catalytic methods is the deactivation of the catalyst due to deposition of carbonaceous material.

In hydrogenation processes, a mixture of the feedstock and hydrogen is fed into the reactor charged with a catalyst (such as cobalt–molybdenum–alumina, tungsten–nickel sulfide, nickel oxide–silica–alumina, and platinum–alumina catalysts). Conditions of the process range from 260°C to 345°C and 500 psi to 1000 psi. The advantages of this process are increased conversion, an increase in the quality of the products, removal of sulphur, and a reduction in the amount of coke produced.

Coking processes convert heavy material to lighter products and solid coke by thermal processing (450°C to 525°C). The generated gases and volatile material leave the reactor, while the solid coke remains. The volatile products are hydrotreated to remove heteroatoms, saturate olefins, and aromatic rings. This process has a high conversion (Wiehe, 2008).

Solvent deasphalting precipitates asphalt from vacuum resid with the addition of *n*-propane, *n*-butane, *i*-butane or *n*-pentante at high solvent to oil ratios. The process temperature is varied between 38°C and 82°C at pressures from 200 psig to 400 psig to maintain a liquid regime. The deasphalted oil is usually mixed with vacuum gas oil and sent to hydrotreating and catalytic cracking (Wiehe, 2008).

During gas oil hydrocracking, the aromatic rings are hydrogenated and the resulting naphthenes are cracked, generating paraffinic products. Hydrocracking also allows the removal of vanadium, nickel and olefins. This process is usually carried in a fixed-bed reactor at high pressure (600 psig to 2500 psig) and high temperature (370°C to 430°C), reaching high conversions.

Optimization of crude oil refining requires knowledge about asphaltene properties and the changes that occur to this class of compounds as refining proceeds. Groenzin *et al*. (2007) studied asphaltenes from a hydrocracked stream in a thermal hydrotreatment process. Results showed that asphaltenes subject to cracking temperatures became similar to coal asphaltenes in terms of molecular size and aromatic ring size. A decrease in asphaltene molecular weight and number of aromatic rings in the structure was observed as the thermal process proceeded and temperature increased. An increase in temperature also promoted the cracking of peripheral alkyl chains. These alkyl side chains are the groups that make the fused rings soluble. Therefore, thermal cracking decreases asphaltene solubility (Buch *et al.*, 2003). Those effects may be due to the extreme reactions that occur at high temperatures and which cannot be controlled during oil refining.

2.6. Summary

Asphaltenes are the densest, most aromatic, most heteroatomic, and least soluble fraction of crude oils. Some or perhaps all of the asphaltenes self-associate and therefore it is challenging to determine the property distribution within the asphaltenes and also to model their phase behavior. Asphaltene self-association has been treated as an oligomerization-like process and a model based on this assumption has successfully represented molecular weight data. Asphaltene precipitation has been modeled using regular solution theory but usually with assumed molecular weight distributions. Self-association models and precipitation models have not been rigorously linked. Nor have such models been applied to refined asphaltenes which may have been chemically altered via thermal cracking or hydrogenation.

Chapter 3: Experimental Methods

This chapter presents the experimental techniques for the separation of asphaltenes, determination of the asphaltene solubility curve, fractionation of asphaltenes and measurement of asphaltene density and molecular weight.

3.1. Chemicals and Materials

Nine samples of asphaltenes from different sources were obtained. Table 3.1 shows all the samples used in this thesis.

Table 3. 1. Bitumen and oils used in this project.

Sample	Supplier
Athabasca bitumen	Syncrude Canada Ltd.
Peace River bitumen	Shell Global Solutions
Arabian crude oil	Shell Global Solutions
Gippsland crude oil	Shell Global Solutions
Cliffdale bitumen	Shell Global Solutions
27034-87	Shell Global Solutions
27034-113	Shell Global Solutions
26845	Shell Global Solutions
27-168-178	Shell Global Solutions

Asphaltene precipitations, solids removal, solubility experiments, and asphaltene fractionations were performed using ACS grade solvents *n*-heptane and toluene obtained from VWR International, LLC. Asphaltene molecular weight measurements were carried out with Omnisolv high purity toluene (99.99%) obtained from VWR; sucrose octaacetate (98%), octacosane (99%) and polystyrene standard (99%) were obtained from

Sigma-Aldrich Chemical Company. Reverse osmosis water was provided by the University of Calgary physical plant.

3.2. Experimental Techniques

3.2.1. Asphaltene Precipitation from Crude Oil

Asphaltenes were extracted from crude oil or bitumen using a 40:1 ratio (mL/g) of *n*-heptane to heavy oil. The mixture was sonicated in an ultrasonic bath for 60 minutes at room temperature and left to settle without disturbing for a total contact time of 24 hours. The supernatant was filtered through a Whatman #2 filter paper until approximately 20% of the solution remained in the beaker. 10% of the original volume of the solvent was added to the remaining asphaltenes in the beaker, and then it was sonicated for 60 minutes and left to settle overnight for a contact time of approximately 18 hours. The remaining mixture was filtered through the same filter paper. The filter cake was washed using 25 mL of *n*-heptane each time at least three times per day over five days until the effluent from the filter was almost colorless. The filter cake was dried in a closed fume hood until the weight of the filter did not change significantly. The dry filter cake consists of asphaltenes and inorganic solids which are collected with the precipitated asphaltenes. The material extracted with n-heptane is termed "C7-asphaltenes+solids". Asphaltenes+solids yields were reported as the mass of asphaltenes recovered after the washing and drying stages divided by the original mass of heavy oil used.

The filtrate consists of maltenes and n-heptane. The maltenes were recovered by evaporating the *n*-heptane in a rotary evaporator at vacuum conditions and temperature between 40 to 60°C, and then dried in a vacuum oven until the weight did not change significantly.

3.2.2. Solids Removal from Asphaltenes

Solids correspond to mineral material like sand, clay, ashes and adsorbed organics that precipitate along with the asphaltenes without affecting the onset or percentage of

precipitated asphaltenes (Mitchell *et al.*, 1973, Alboudwarej *et al*., 2003). In the case of downstream samples, solids may include traces of catalysts and other solids present in different stages and coke, all produced during the refining of crude oil.

Solids are removed from asphaltenes dissolving the C7-asphaltenes+solids in toluene and centrifuging to separate out the solids. A solution of asphaltenes in toluene was prepared at 10 kg/m^3 and at room temperature. The mixture was sonicated in an ultrasonic bath for 20 minutes or until all asphaltenes were dissolved, and then the solution was settled for 60 minutes. The mixture was divided into centrifuge tubes and centrifuged at 4000 rpm for 6 minutes. The supernatant (solids-free asphaltene solution) was decanted into a beaker and set into the fume hood to dry for 4 days or until constant weight, and then solids-free asphaltenes were recovered and stored in a jar. The non-asphaltenic solids, corresponding to the remaining material in the centrifuge tubes, were dried and weighed to calculate the solids content as the mass of solids divided by the mass of the original asphaltene sample. The asphaltenes extracted with n-heptane and treated with toluene to remove solids are termed "C7-asphaltenes".

3.2.3. Asphaltene Solubility

The asphaltene solubility curve is a plot that shows the change in the yield of precipitated asphaltenes in a *n*-heptane-toluene solution (known as heptol solution) as the ratio of heptol changes. The measurements for the amount of precipitated asphaltenes were performed at an asphaltene concentration of 10 kg/m^3 and at room temperature. C7-asphaltenes were first dissolved in toluene by sonicating for 20 minutes. The appropriate amount of *n*-heptane was added and then the mixture was sonicated for 45 minutes and left to settle for 24 hours. The solution was centrifuged at 4000 rpm for 6 minutes. The supernatant was carefully decanted and discarded. Precipitated asphaltenes at the bottom of the vials were washed with a heptol solution at the initial heptol ratio and then sonicated for 5 minutes and centrifuged at 4000 rpm for 6 minutes. The supernatant was again decanted and discarded. The washing was repeated until the supernatant was colorless. The sediments of precipitated asphaltenes were dried under vacuum at 60°C for

2 days. Asphaltene precipitation yields were calculated as the mass of precipitated asphaltenes divided by the initial mass of asphaltenes. The yields were all determined on a solids-free basis. The main source of error is the consistency of the washing procedure and the repeatability for this experiment was approximately ±6%.

3.2.4. Asphaltene Fractionation

The methodology for the fractionation of asphaltenes was similar to that of the solubility experiments. C7-asphaltenes were divided into two fractions based on the solubility curve: a light cut corresponding to the soluble asphaltenes in the specified solution of heptol, and a heavy cut with the asphaltenes precipitated from the same heptol mixture. The asphaltene fractions are termed "HT##L" or "HT##H" where ## is the volume percent of *n*-heptane in the heptol solution, "L" indicates the light soluble asphaltenes, and "H" indicates the heavy insoluble asphaltenes. Unless otherwise indicated, the heptol ratios were chosen such that 25%, 50% and 75% of precipitated asphaltenes were recovered in each experiment. The C7-asphaltenes are termed "whole", indicating that they have not been fractionated.

The fractionations were performed in 10 kg/m^3 solutions of asphaltenes with heptol. Asphaltenes were first combined with toluene and sonicated for 20 minutes, then the corresponding amount of *n*-heptane was added and the mixture was sonicated for 45 minutes. After settling for 24 hours, the solution was centrifuged at 4000 rpm for 6 minutes. The supernatant was transferred to a beaker and the precipitated material (corresponding to the heavy cut) was washed with the same solvent until the supernatant was colorless and then dried in a vacuum oven at 60°C. The supernatant material (corresponding to the light cut) was recovered and dried in a fume hood until the weight change was negligible. The fractional yield of each cut was calculated as the mass of the cut divided by the total mass of asphaltenes. The repeatability for this experiment was approximately ±6%.

3.2.5. Molecular Weight Measurement

Vapor Pressure Osmometry (VPO) was used to measure asphaltene molecular weight. This technique is based on the difference in the vapor pressure between a solute-solvent mixture and the pure solvent at the same temperature and pressure. Inside the instrument, two separate thermistors are placed in a chamber saturated with pure solvent vapor. When droplets of solvent are placed on both thermistors, there is no difference of temperature. If a droplet of sample solution is placed on one of the thermistors, a difference in vapor pressure between the two droplets generates a difference in temperature. The temperature difference causes a resistance change (or voltage difference) in the thermistors, which is related to the molecular weight of the solute, M_2, as follows (Prausnitz *et al.*, 1999; Peramanu *et al*., 1999):

$$\frac{\Delta E}{C_2} = K\left(\frac{1}{M_2} + A_1 C_2 + A_2 C_2^{\,2} + \ldots\right) \tag{3.1}$$

where ΔE is the voltage difference between the thermistors, C_2 is the solute concentration, K is the proportionality constant, and A_1 and A_2 are coefficients arising from the non-ideal behavior of the solution.

To calibrate the apparatus, the solutes chosen form nearly ideal mixtures with the solvent at low concentrations. In this case, most of the higher order terms become negligible:

$$\frac{\Delta E}{C_2} = K\left(\frac{1}{M_2} + A_1 C_2\right) \tag{3.2}$$

For the calibration, the molecular weight of the solute is known, and the proportionality constant, *K*, was calculated by extrapolation in a plot of $\Delta E/C_2$ versus C_2 to zero concentration.

For a non-ideal solution, the molecular weight of an unknown solute is also calculated from the intercept of a plot of $\Delta E/C_2$ versus C_2 this time solving for M_2. For an ideal system, the second term in Equation 3.2 is zero and $\Delta E/C_2$ is constant. In this case, the molecular weight is determined from the average $\Delta E/C_2$ as follows:

$$M_2 = \frac{K}{\left(\Delta E / C_2\right)} \tag{3.3}$$

Asphaltene molecular weights were measured using a Jupiter Model 833 vapor pressure osmometer with toluene as the solvent at 50°C. This instrument has a detection limit of $5\ 10^{-5}$ mol/L when used with toluene or chloroform. The instrument was calibrated with sucrose octaacetate (679 g/mol) as solute and octacosane (395 g/mol) was used to check the calibration.

During the asphaltene molecular weight measurements, there were slight fluctuations in the voltage at any given condition, likely caused by slight variations in local temperature and atmospheric pressure. Therefore, two readings were taken at each concentration to obtain an accurate voltage response for that concentration. Note that the molecular weight is determined from the voltage difference between a sample run and a blank run base line. If the base line voltage is incorrect, the calculated molecular weight will be systematically incorrect at all concentrations. If the sample run voltage is incorrect, only that run is affected. The measured molecular weight of octacosane was within 3% of the correct value. The repeatability of the molecular weight measurements was approximately ±12% for all the samples.

Since asphaltenes self-associate, it is not obvious if they form ideal or non-ideal solutions with toluene. In a separate project, Sanchez (2012) examined the molecular weights of several distillation fractions from Peace River bitumen. She confirmed that the distillation fractions formed non-ideal solutions with toluene, Figure 3.1, and found that the non-ideality decreased towards the heavier fractions. The light fractions contain more paraffinic and naphthenic components which are less likely to form ideal solutions with toluene than the more aromatic heavy fractions. It was not possible to determine from these data if the asphaltenes form ideal or slightly non-ideal solutions with toluene.

If the asphaltenes both self-associate and form non-ideal solutions, the asphaltene molecular weights must be calculated at each concentration as follows:

$$M_2 = \frac{1}{\Delta E / KC_2 - A_1 C_2} \tag{3.4}$$

where the calibration constant is determined from the standards and A_1 must be determined independently. Figure 3.2 shows the effect of different values of A_1 on the calculated molecular weight of one of the Peace River asphaltene fractions (HT92H). There is almost no effect at asphaltene concentrations below 10 kg/m^3 but there is a dramatic effect at concentrations above 20 kg/m^3. If the value of A_1 is set above -0.001 mol·m^3/kg², then the calculated molecular weights reach a maximum at a concentration of 10 kg/m^3 and decrease at higher concentrations. This behaviour is non-physical and therefore it can be concluded that A_1 has a value between zero and approximately -0.001 mol·m^3/kg² for asphaltenes.

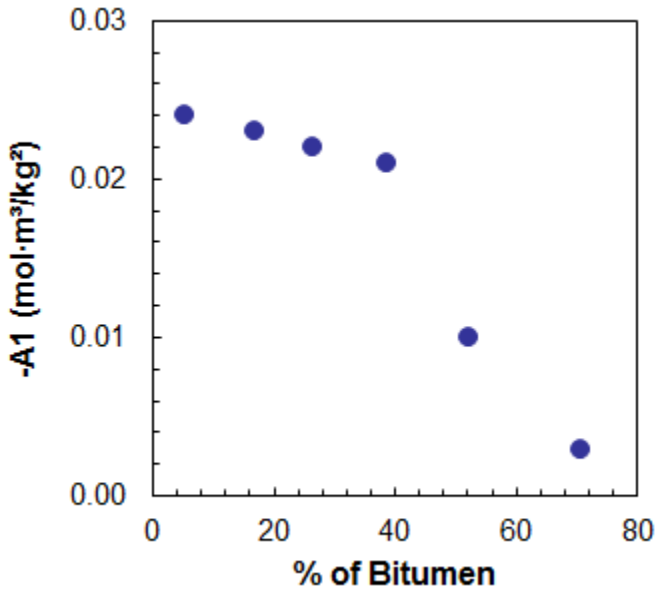

Figure 3.1. Values of the non-ideal parameter A_1 for distillation fractions from Peace River bitumen.

Given the lack of data on the ideality of the solutions, in this thesis it was assumed that the asphaltenes form ideal solutions with toluene. Also, other methods, such as SANS and SAXS, suggest that asphaltenes form large aggregates (Ravey *et al*., 1988) and it was

considered preferable to retain the higher molecular weights from the ideal assumption without more evidence to the contrary. Note that all of the asphaltene fraction data are shifted similarly with the same value of A_1. Therefore, the models and conclusions presented in the thesis are not qualitatively affected by the ideal assumption. Only the values of molecular weight and model parameters will be affected.

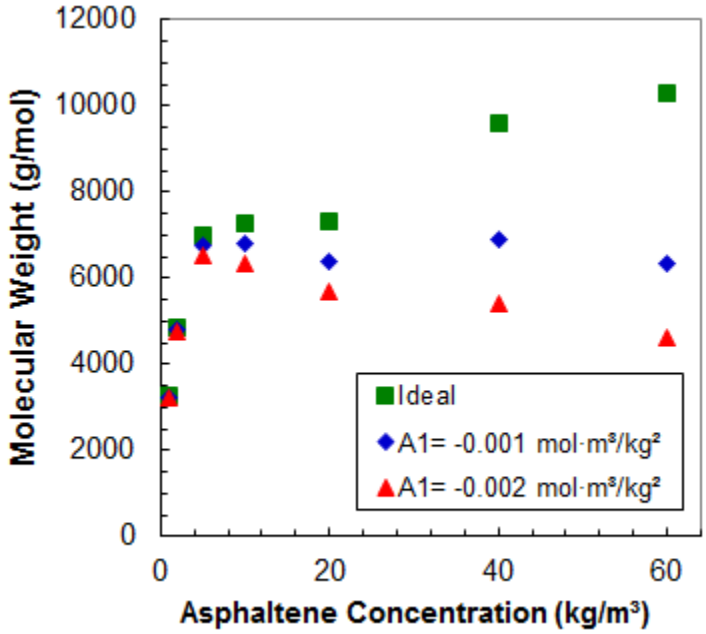

Figure 3.2. Effect of non-ideality of solution on apparent molecular weight of Peace River HT92H asphaltene fraction in toluene at 50°C.

3.2.6. Density Measurement

Asphaltene densities were calculated indirectly from the densities of mixtures of asphaltenes in toluene. At low concentration, regular solution behavior was assumed where the density of a solution of toluene and asphaltenes is given by:

$$\frac{1}{\rho_M} = \frac{1}{\rho_T} + \left(\frac{1}{\rho_A} - \frac{1}{\rho_T} \right) w_A \tag{3.5}$$

where ρ_M, ρ_T and ρ_A are the mixture, toluene and asphaltene density (kg/m³) respectively, and w_A is the asphaltene mass fraction. The density of asphaltenes can be

determined indirectly from a plot of the specific volume (the inverse of the mixture density) versus asphaltene mass fraction in solution with toluene,

$$\rho_A = \frac{1}{S + I} \tag{3.6}$$

where S and I are the slope and intercept respectively in the specific volume plot. A typical plot for the specific volume versus asphaltene mass fraction is shown for Peace River asphaltenes in Figure 3.3.

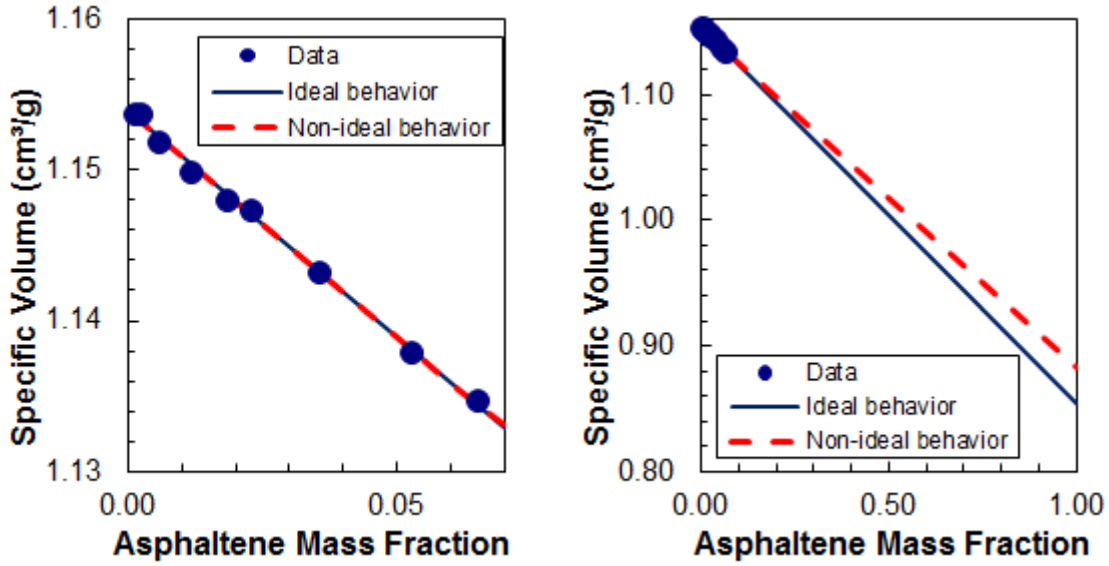

Figure 3.3. Density of Peace River whole asphaltenes in solution with toluene as asphaltene concentration changes.

Densities for the solutions of asphaltenes were measured at 21°C and atmospheric pressure with an Anton Paar DMA 46 density meter. Reverse osmosis water and air were used for the calibration. Asphaltene concentrations ranged from 0 to 6.47 wt%. The instrument precision was ±0.0005 g/cm³.

Since the asphaltene densities were calculated indirectly from solutions of toluene, there are additional uncertainties in the measurement: 1) concentration errors; 2) excess volumes of mixing. Concentration errors were assessed by repeat experiments and the repeatability of the asphaltenes densities was found to be ±0.0008 g/cm³.

Excess mixing volumes could not be determined directly because only up to approximately 7 wt% of asphaltenes could be dissolved in toluene. At these low mass fractions, the difference between a regular solution (no excess volume of mixing) and an irregular solution cannot be distinguished beyond the experimental error. Consider the following excess volume mixing rule for an irregular solution:

$$\frac{1}{\rho_M} = \frac{w_T}{\rho_T} + \frac{w_A}{\rho_A} + w_A w_T \left(\frac{1}{\rho_A} - \frac{1}{\rho_T} \right) \beta_{AT} \tag{3.4}$$

where w_T is the mass fraction of toluene and β_{AT} is a binary interaction parameter between the asphaltenes and toluene. The last term in the expression is the excess volume of mixing.

Sanchez (2012) also examined the densities of several distillation fractions from Peace River bitumen. She confirmed that the heavy distillation fractions formed irregular solutions with toluene, as shown in Figure 3.4, and found that the value of β_{AT} increased towards the heavier fractions. She extrapolated the trend of β_{AT} versus mass fraction distilled and estimated a β_{AT} of 0.015 for asphaltenes.

Figure 3.3 shows that both the excess volume mixing rule with β_{AT} = 0.015 and the regular mixing rule both fit the specific volume (inverse of density) data and are indistinguishable from each other. Yet, the irregular mixing rule extrapolates to an asphaltene density of 1132 kg/m³ while the regular solution mixing rule extrapolates to a density of 1171 kg/m³ both for Peace River asphaltenes.

Table 3.2 shows Peace River asphaltene densities calculated based on both the regular mixing rule and the excess volume mixing rule with β_{AT} = 0.015. Note that the value calculated using the regular mixing rule is approximately 40 kg/m^3 higher than the value obtained with the excess volume mixing rule. The same behavior occurs for all of the asphaltene fraction data, which are shifted similarly when the excess volume mixing rule is used instead of the regular mixing rule.

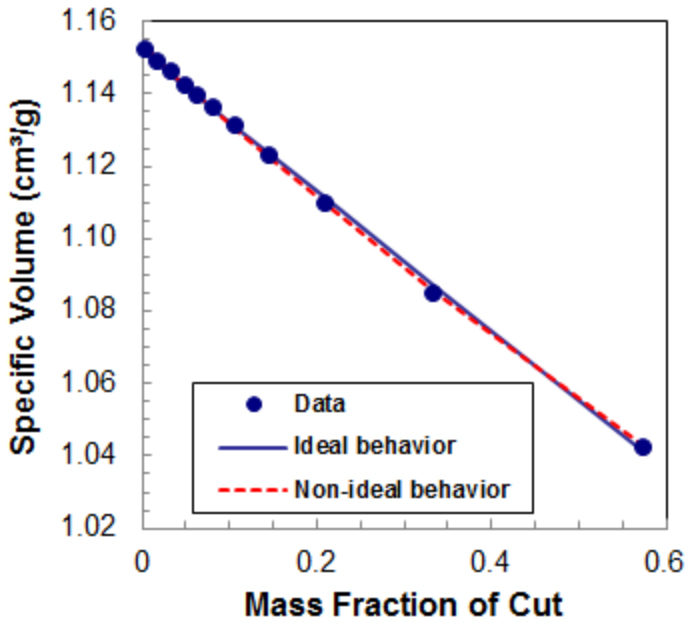

Figure 3.4. Specific volume of a Peace River residue fraction constituting the heaviest 40 wt% of the maltenes. Data from Sanchez, 2012.

Table 3.2. Density of fractions for Peace River asphaltenes using both regular and excess volume mixing rules.

Fraction	ρ_A with regular mixing rule (kg/m^3)	ρ_A with excess volume mixing rule (kg/m^3)
HT92L	1078	1044
HT77L	1138	1101
HT60L	1162	1124
Whole	1171	1132
HT92H	1184	1145
HT77H	1187	1146
HT60H	1190	1150

The value of β_{AT} for asphaltenes used in the excess volume mixing rule is a preliminary estimation that has not been confirmed yet with additional experimental data. Even though it is necessary to account for the non-ideality of the asphaltene-toluene mixtures, there is not certainty about the correct β_{AT} parameter to use and, for now, the density of asphaltenes was calculated with the regular mixing rule. These values will be used for the determination of the density correlations for all the samples. Note that the models and conclusions presented in the thesis are not qualitatively affected by mixing rule assumption. Only the values of asphaltene density and model parameters will be affected.

Chapter 4: Asphaltene Association Model

This chapter describes the derivation of the asphaltene association model used to determine the molecular weight distribution. The basic model was developed and published by Agrawala and Yarranton (2001). First, the principles of the original model are shown and then the modifications introduced to account for the non-associating material present in asphaltenes are introduced.

4.1. Single-End Termination Model

Thermal and chemical degradation studies show that asphaltenes consist of polyaromatic ring structures linked with aliphatic chains and with heteroatoms associated in functional groups, such as acids, ketones, thiophenes, pyridines and porphyrins (Strausz *et al.*, 1992). There are many ways in which each molecule can link with all the surrounding molecules, including hydrogen bonding (Moschopedis *et al.*, 1976), aromatic stacking (Larsen *et al.*, 1995), acid-base interactions (Maruska *et al.*, 1987) and van der Waals interactions (Rogel, 2000).

The strength and number of the potential links per molecule depend on the type of molecules and the nature of the site that acts as the link. Asphaltenes contain a variety of functional groups interacting in a mixture of many different chemical species and therefore links with a wide variety of strength are possible. The type of solvent and temperature of the system also affect the potential links. Strongly polar solvents and systems at high temperatures promote asphaltene-solvent interactions decreasing the probability that a given link will form. More asphaltenes will remain as separate entities but “strong” sites will still form asphaltene-asphaltene links. The opposite behavior occurs with non-polar solvents and systems at low temperatures.

4.1.1. Basic Concepts

Agrawala *et al.*, (2001) proposed a model to account for asphaltene self-association where aggregates are macromolecules of asphaltenes and resins. The association was treated like polymerization or oligomerization except that the molecules were assumed to link by van der Waals forces rather than covalent bonding. It was assumed that asphaltene association was analogous to a linear polymerization.

The asphaltenes (and resins) are then considered to be free molecules in solution with multiple functional groups that interact with other molecules to form aggregates. The asphaltenes plus resins are divided into two classes of molecules: propagators and terminators. A *propagator* is defined as a molecule with multiple active sites that is capable of linking with other similar molecules or aggregates and promoting additional association. A *terminator* is defined as a molecule with a single active site that is capable of linking with other molecules but terminates further association. This model defines any mixture in terms of its content of propagators and terminators, and the proportion of each type of molecule determines the extent of association.

This model recognizes the similar chemical nature of resins and asphaltenes. Asphaltenes are simply mixtures made up primarily of propagators while resins are mixtures made up primarily of terminators. The aggregates are, in effect, macromolecules of asphaltenes and resins as has been observed in asphaltene phase behavior and molecular weight measurements (Agrawala *et al.*, 2001; Merino-Garcia *et al.*, 2004; Merino-Garcia *et al*., 2007). Note that the model is almost certainly a gross oversimplification of the true aggregation behaviour of asphaltenes. However, it has been proven to fit the available molecular weight data of associated asphaltenes and resins in a self-consistent and physically plausible manner (Yarranton *et al*., 2007). In addition, there are insufficient data to justify constructing a more complex model.

4.1.2. Formulation of the Model

Only two reaction schemes are required for the model: propagation and termination. Unlike polymerization reactions, an initiation step is not required because association is not a free radical reaction (Agrawala *et al.*, 2001).

4.1.2.1. Propagation

Propagation reactions occur when a monomer P_1 links up with another monomer P_1 or an existing aggregate P_n (where n is the number of monomers in the aggregate). Propagator monomers can link freely with other molecules and grow in each subsequent step of the polymerization. Reactions are assumed to be first order with respect to both the propagator monomer and the aggregate molecules. The kinetics is described by the association constant, *K*, that represents the equilibrium between forward and reverse association. The association constant is assumed to be the same for all the reactions. The concentration of aggregates $[P_n]$ can be expressed as a function of the association constant and the equilibrium concentration of propagators $[P_1]$ as follows:

$$P_1 + P_1 \xleftrightarrow{K} P_2 \qquad [P_2] = K[P_1]^2 \tag{4.1}$$

$$P_1 + P_2 \xleftrightarrow{K} P_3 \qquad [P_3] = K[P_1][P_2] = K^2[P_1]^3 \tag{4.2}$$

$$P_1 + P_3 \xleftrightarrow{K} P_4 \qquad [P_4] = K[P_1][P_3] = K^3[P_1]^4 \tag{4.3}$$

The general equation for propagation is given by:

$$P_1 + P_n \xleftrightarrow{K} P_{n+1} \qquad [P_{n+1}] = K[P_1][P_n] = K^n[P_1]^{n+1} \tag{4.4}$$

4.1.2.2. Termination

This set of reactions occurs when a terminator monomer T links up with a monomer P_1 or an existing aggregate P_n, terminating the association. For this case, it is also assumed that reactions are first order with respect to both the terminator molecules and the aggregate molecules, and are characterized by an association constant K. It is also assumed that the association constant is the same for all the reactions and has the same

value as the constant from the propagation reactions. Another assumption of this model is that association stops when termination occurs at only one site of the aggregate. It was found that a model capping both ends of a linear aggregate gave similar results (Yarranton *et al.*, 2007).

The concentration of terminator aggregates $[P_nT]$ can be expressed in terms of the association constant and the equilibrium concentration of propagators $[P_1]$ as shown below:

$$P_1 + T \xleftrightarrow{K} P_1T \qquad [P_1T] = K[P_1][T] \tag{4.5}$$

$$P_2 + T \xleftrightarrow{K} P_2T \qquad [P_2T] = K[P_2][T] = K^2[P_1]^2[T] \tag{4.6}$$

$$P_3 + T \xleftrightarrow{K} P_3T \qquad [P_3T] = K[P_3][T] = K^3[P_1]^3[T] \tag{4.7}$$

The general equation for termination is given by:

$$P_n + T \xleftrightarrow{K} P_nT \qquad [P_nT] = K[P_n][T] = K^n[P_1]^n[T] \tag{4.8}$$

The assumption of equal association constant for all the reactions indicates that the probability of a monomer of any class forming a link with an aggregate of any size is the same as that of linking up with another monomer. This model does not consider aggregate-aggregate association.

4.1.2.3. Calculation of Equilibrium Composition

The set of reactions is solved simultaneously like a polymerization reaction, starting with the mass balance for both propagators and terminators. $[P_1]_0$ and $[T]_0$ are defined as the initial concentration of propagator and terminator monomers, respectively. The mass balances for the propagators and terminators are derived below.

Mass Balance of Propagator Molecules:

$$\begin{aligned}[P_1]_0 = &([P_1] + 2[P_2] + 3[P_3] + \ldots + n[P_n]) + \\ &+ ([P_1T] + 2[P_2T] + 3[P_3T] + \ldots + n[P_nT])\end{aligned} \tag{4.9}$$

Equations (4.1) through (4.8) are substituted into Equation (4.9) to obtain,

$$[P_1]_0 = \left([P_1] + 2K[P_1]^2 + 3K^2[P_1]^3 + \ldots + (n+1)K^n[P_1]^{n+1}\right) + \\ + \left(K[P_1][T] + 2K^2[P_1]^2[T] + 3K^3[P_1]^3[T] + \ldots + nK^n[P_1]^n[T]\right) \tag{4.10}$$

which can be rearranged as follows,

$$[P_1]_0 = \left(\frac{1}{K} + [T]\right)\left(K[P_1] + 2K^2[P_1]^2 + 3K^3[P_1]^3 + \ldots + (n+1)K^{n+1}[P_1]^{n+1}\right) \tag{4.11}$$

and expressed as the following summation,

$$[P_1]_0 = \left(\frac{1}{K} + [T]\right)\left(\sum_{n=1}^{\infty} nK^n[P_1]^n\right) = \left(\frac{1+K[T]}{K}\right)\left(\sum_{n=1}^{\infty} n(K[P_1])^n\right) \tag{4.12}$$

The summation has the following form:

$$\sum_{n=1}^{\infty} nx^n = \frac{x}{(1-x)^2} \tag{4.13}$$

Applying Equation 4.13 to Equation 4.12, one obtains,

$$[P_1]_0 = \left(\frac{1+K[T]}{K}\right)\frac{K[P_1]}{(1-K[P_1])^2} = \frac{[P_1](1+K[T])}{(1-K[P_1])^2} \tag{4.14}$$

which can be expressed as the following quadratic equation:

$$[P_1]_0 - (1+K(2[P_1]_0 + [T]))[P_1] + K^2[P_1]_0[P_1]^2 = 0 \tag{4.15}$$

<u>Mass Balance of Terminator Molecules:</u>

$$[T]_0 = [T] + [P_1T] + [P_2T] + [P_3T] + \ldots + [P_nT] \tag{4.16}$$

Equations (4.5) through (4.8) are substituted into Equation (4.16) to obtain,

$$[T]_0 = [T] + K[P_1][T] + K^2[P_1]^2[T] + K^3[P_1]^3[T] + \ldots + K^n[P_1]^n[T] \tag{4.17}$$

which can be rearranged as follows,

$$[T]_0 = [T]\left(1 + K[P_1] + K^2[P_1]^2 + K^3[P_1]^3 + \ldots + K^n[P_1]^n\right) \tag{4.18}$$

and expressed as the following summation,

$$[T]_0 = [T]\left(\sum_{n=0}^{\infty} K^n[P_1]^n\right) = [T]\left(\sum_{n=0}^{\infty} (K[P_1])^n\right) \tag{4.19}$$

The summation has the following form:

$$\sum_{n=0}^{\infty} x^n = \frac{1}{1-x} \tag{4.20}$$

Applying Equation 4.20 to Equation 4.19, one obtains,

$$[T]_0 = \frac{[T]}{1-K[P_1]} \tag{4.21}$$

The equilibrium concentration of terminators is given by:

$$[T] = [T]_0 (1 - K[P_1]) \tag{4.22}$$

Now, Equation 4.22 is substituted into Equation 4.15 to obtain,

$$[P_1]_0 - (1 + K(2[P_1]_0 + [T]_0))[P_1] + K^2([P_1]_0 + [T]_0)[P_1]^2 = 0 \tag{4.23}$$

Solving for $[P_1]$, the equilibrium concentration of propagators is given by,

$$[P_1] = \frac{1 + K(2[P_1]_0 + [T]_0) - \sqrt{(1 + K(2[P_1]_0 + [T]_0))^2 - 4K^2[P_1]_0([P_1]_0 + [T]_0)}}{2K^2([P_1]_0 + [T]_0)} \tag{4.24}$$

Equations 4.22 and 4.24 give the concentration of propagators $[P_1]$ and terminators $[T]$ at equilibrium. Using Equations 4.1 to 4.8, the concentration of aggregates of any size can be calculated as long as the initial concentration of monomers $[P_1]_0$ and $[T]_0$, and the association constant are defined. Since Equations 4.4 and 4.8 depend on the size of the aggregate, the maximum number of aggregates n for both propagation and termination reactions must be set high enough to include the largest molecules in the system.

4.1.2.4. Application to Asphaltene Association

The inputs for the model are the molecular weight for both terminators and propagators. These monomer molecular weights were estimated based on lightest cuts which exhibited little self-association. An initial value of the monomer molecular weight was determined by extrapolating the molecular weights of the lightest cut of each sample to zero concentration. Then, the values were adjusted to fit the data with the constraint that they could not be less than the initial monomer value or higher than 2000 g/mol.

An initial ratio of terminators to propagators $(T/P)_0$ and an association constant K are assumed and then the initial molar fraction x of each monomer in asphaltenes is calculated as follows:

$$\left(\frac{T}{P}\right)_0 = \frac{x_{T_0}}{x_{P_0}} \tag{4.25}$$

$$x_{T_0} = \frac{(T/P)_0}{1+(T/P)_0} \qquad \textit{and} \qquad x_{P_0} = 1 - x_{T_0} \tag{4.26}$$

The average molecular weight MW_{mono} of the non-aggregated system is calculated as,

$$MW_{mono} = x_{T_0} \cdot MW_T + (1 - x_{T_0}) \cdot MW_P \tag{4.27}$$

The initial mole fraction of propagators and terminators in solution depends on the mass concentration of asphaltenes C_A and the molar volume of the solvent υ_s, and is calculated as follows:

$$[P_1]_0 = \frac{1}{\left(1 + \frac{MW_{mono}}{C_A \cdot \upsilon_s}\right) \cdot (1 + (T/P)_0)} \tag{4.28}$$

$$[T]_0 = [P_1]_0 \cdot (T/P)_0 \tag{4.29}$$

The average molecular weight of the aggregate system at a given concentration is given by:

$$MW_{avg} = \sum_{n=0}^{n} \left(x_{[P_n]} \cdot MW_{[P_n]} + x_{[P_nT]} \cdot MW_{[P_nT]} \right) \tag{4.30}$$

where x and MW are the mole fraction and the molecular weight of a propagator $[P_n]$ and a terminator $[P_nT]$ aggregate, respectively. The output from the model is the molecular weight and mass fraction of propagators (P_n) and terminators (P_nT) aggregates.

The model is run with the selected fitting parameters and the calculated values of $[P_1]_0$ and $[T]_0$, and equilibrium concentrations are determined from Equations 4.22 and 4.24.

The value of $(T/P)_0$ and the association constant K are modified until the model fits the experimental average molecular weight. Since the VPO data are scattered, the matching of the molecular weight data was performed by visual inspection.

Both fitting parameters have a different effect on the calculated molecular weight. The association constant K determines the concentration at which the limiting molecular weight is reached; increasing K decreases the concentration at which the inflexion point occurs, as can be seen in the left plot of Figure 4.1. The $(T/P)_0$ ratio determines the value of the limiting molecular weight, and increasing this parameter the maximum molecular weight is reduced, as observed in Figure 4.1, right plot. This behavior is consistent with the assumptions in the association model (Agrawala *et al.*, 2001).

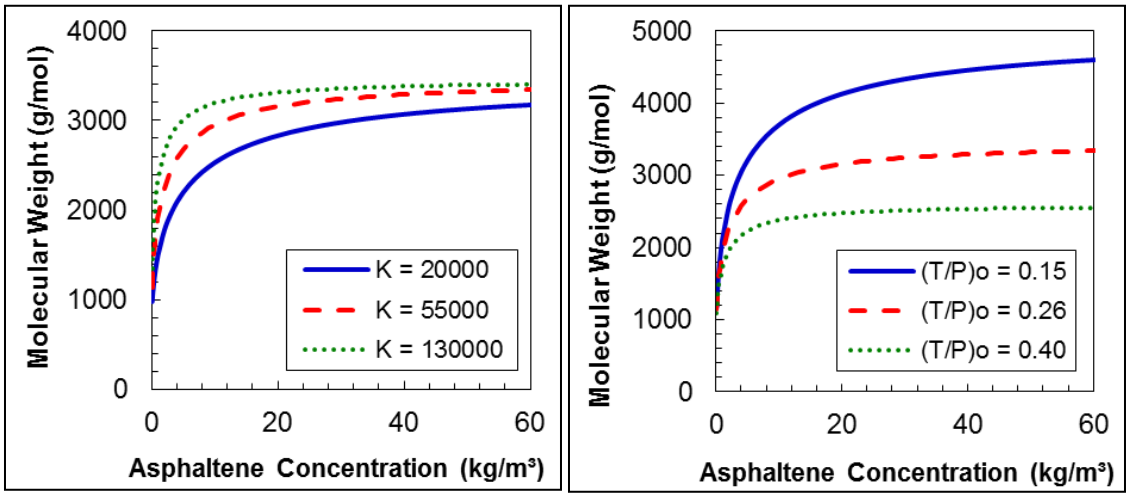

Figure 4.1. Effect of the fitting parameters on results from the association model. The plot to the left shows the effect of changing K with $(T/P)_0$ =0.26. The plot to the right shows the effect of changing $(T/P)_0$ with K=55000.

4.1.2.5. Molecular Weight Distribution

The concentration of each aggregate is determined from the solution of Equations 4.1 to 4.8. Since a distribution of monomer sizes is not accounted for, the predicted distribution is discrete. However, a continuous form is more convenient for the precipitation models. A continuous mass frequency distribution for the molecular weight of asphaltenes is

determined by sorting in ascending order the mass fraction and molecular weight data for all the aggregates and fitting those values with the least squares method to a frequency distribution with the following form:

$$cumf = A + B \cdot \exp\left(-\exp\left(\frac{C - MW}{D}\right)\right) \tag{4.31}$$

where *cumf* is the calculated cumulative mass fraction, *MW* is the aggregate molecular weight and the other terms are fitting parameters. The terms A and B modify the upper limit of the distribution and the terms C and D change the slope and the point at which the maximum value is reached (Fox, 2007). After determining the equation for the cumulative mass fraction of aggregates, the function can be divided into intervals in order to determine the molecular weight distribution.

Figure 4.2 shows a typical cumulative molecular weight distribution, in this case the results from fitting Athabasca C7-asphaltene VPO data with the Single-end termination Model and the fitting curve with the form of Equation 4.31. For this case, the error in the fitting is 0.003. In all cases, Equation 4.31 fits the discrete distributions with an error less than 0.013.

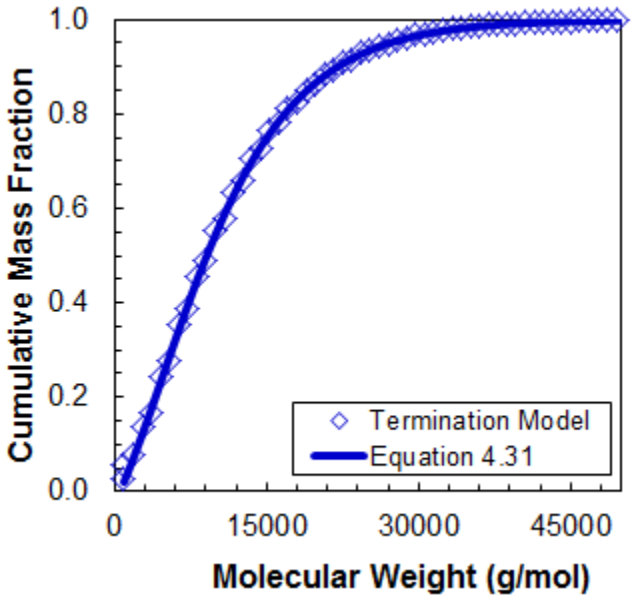

Figure 4.2. Cumulative mass frequency versus molecular weight for Athabasca C7-Asphaltenes in toluene at 50°C using the Single-end termination Model.

4.2. Termination Model Including Non-Associating Material

The single end termination model assumes that all the asphaltene (plus resin) monomers have at least one active site that promotes association with aggregates or with other monomers. Experimental results from this thesis showed that some asphaltenic material (neutrals) may be present that does not participate in the association but must be included in the model to complete the material balance. These non-associating components are defined as "*neutrals*".

The propagation and termination reactions are not affected by the presence of neutrals. However, the amount of neutrals must be accounted for when calculating the initial concentration of propagators and terminators, as follows:

$$x_{T_0} = \frac{(T/P)_0}{1+(T/P)_0} \cdot (1 - x_N) \qquad \textit{and} \qquad x_{P_0} = 1 - x_{T_0} - x_N \tag{4.32}$$

where x_N is the concentration of neutrals in the asphaltenes (plus resins). The average molecular weight MW_{mono} of the non-aggregated system is now given by:

$$MW_{mono} = x_{T_0} \cdot MW_T + (1 - x_{T_0} - x_N) \cdot MW_P + x_N \cdot MW_N \tag{4.33}$$

where MW_N is the molecular weight of neutrals, which is assumed to be the same as the molecular weight of terminator monomers.

The initial mole fraction of propagators and terminators in solution becomes:

$$[P_1]_0 = \frac{1}{\left(1 + \frac{MW_{mono}}{C_A \cdot \upsilon_s}\right)(1 + (T/P)_0)} \cdot (1 - x_N) \tag{4.34}$$

$$[T]_0 = [P_1]_0 \cdot (T/P)_0 \tag{4.35}$$

The initial mole fraction of neutrals in solution is calculated as follows:

$$[N]_0 = \frac{x_N}{\left(1 + \frac{MW_{mono}}{C_A \cdot \upsilon_s}\right)} \tag{4.36}$$

The model is run in the same way as the Single End Terminator Model but with x_N as an input or fitting parameter. The values of $[P_1]_0$, $[T]_0$, $[N]_0$ and the equilibrium concentrations are calculated. The average molecular weight is now given by:

$$MW_{avg} = (1 - x_{N,final}) \cdot \left(\sum_{n=0}^{n} \left(x_{[P_n]} \cdot MW_{[P_n]} + x_{[P_nT]} \cdot MW_{[P_nT]} \right) \right) + x_{N,final} \cdot MW_N \quad (4.37)$$

where $x_{N,final}$ is the concentration of neutrals in the aggregated system and is different than x_N. The presence of neutral material increases the concentration of the lower molecular weight material in the cumulative molecular weight distribution. However, the fitting of the discrete molecular weight distribution is done with Equation 4.31 as before.

Chapter 5: Asphaltene Precipitation Modeling

This chapter presents a previously developed model for asphaltene precipitation based on regular solution theory (Akbarzadeh *et al.*, 2005). Then, modifications made to the model in this work are described including: 1) the use of output from the single-end termination model as the molecular weight distribution input; 2) new asphaltene density and solubility parameter correlations based on new asphaltene density data.

5.1. Modified Regular Solution Theory

One of the approaches to model asphaltene precipitation is regular solution theory modified to include the entropy of mixing (Alboudwarej *et al.*, 2003; Akbarzadeh *et al.*, 2004; Akbarzadeh *et al.*, 2005). This model assumes a liquid-liquid equilibrium, between a light phase (solvent-rich phase, including all components) and a heavy dense phase (asphaltene-rich phase, including only asphaltenes and resins). Note that the calculation is identical for a solid-liquid equilibrium between a liquid and an amorphous solid where the heat of fusion is negligible. A different formulation would be required for a crystalline organic solid where the heat of fusion ranges from 50 to 250 kJ/kg (Yaws, 2003). However, the heat of fusion of asphaltenes has been shown to be very small (~22 kJ/kg for C5 Athabasca asphaltenes) and can be neglected (Bazyleva *et al*., 2011).

When two phases are at equilibrium, the fugacity of any component is identical in each phase and is given by:

$$f_i = \gamma_i x_i f_i^{\,0} \exp\left[\int_0^P \frac{\upsilon_i dP}{RT}\right] \tag{5.1}$$

where i is the i^{th} component, f is the fugacity, γ is the activity coefficient, x is the mole fraction, f^0 is the standard fugacity, υ is the molar volume, P is pressure, R is the universal gas constant and T is the absolute temperature. The equilibrium ratio of the mole fractions of a component in the light (L) and heavy (H) phases can be expressed as follows:

$$K_i^{HL} = \frac{x_i^H}{x_i^L} = \left(\frac{\gamma_i^L}{\gamma_i^H}\right)\left(\frac{f_i^{0\,\mathrm{L}}}{f_i^{0\,\mathrm{H}}}\right)\exp\left[\int_0^P \frac{\Delta\upsilon_i dP}{RT}\right] \tag{5.2}$$

where K is the equilibrium ratio and $\Delta\upsilon_i$ is the difference between the molar volume of component *i* in the light and heavy liquid phase. For a liquid-liquid equilibrium, the terms $\left(f_i^{0\,\mathrm{L}} / f_i^{0\,H}\right)$ and $\exp\left[\int_0^P \left(\Delta\upsilon_i dP/RT\right)\right]$ are unity, and Equation 5.2 reduces to:

$$K_i^{HL} = \frac{x_i^H}{x_i^L} = \left(\frac{\gamma_i^L}{\gamma_i^H}\right) \tag{5.3}$$

The activity coefficient for a component in an athermal and regular solution was expressed by Prausnitz *et al.* (1999) as follows,

$$\ln\gamma_i^L = \ln\frac{\upsilon_i^L}{\upsilon_m^L} + 1 - \frac{\upsilon_i^L}{\upsilon_m^L} + \frac{\upsilon_i^L}{RT}\sum_j^n\sum_k^n \phi_j\phi_k\left(D_{ij} - 0.5D_{jk}\right) \tag{5.4}$$

where m corresponds to the mixture, and ϕ_i is the volume fraction defined as,

$$\phi_i = \frac{x_i\upsilon_i}{\sum x_i\upsilon_i} \tag{5.5}$$

and

$$D_{jk} = \left(\delta_j - \delta_k\right)^2 + 2l_{jk}\delta_j\delta_k \tag{5.6}$$

where δ is the solubility parameter and l_{jk} is the interaction parameter between the two components *j* and *k*. For every component *j*, $l_{jj} = D_{jj} = 0$. Assuming that the interaction parameter between any of the components is zero, that is $l_{jk} = 0$, Equation 5.4 reduces to:

$$\ln\gamma_i^L = \ln\frac{\upsilon_i^L}{\upsilon_m^L} + 1 - \frac{\upsilon_i^L}{\upsilon_m^L} + \frac{\upsilon_i^L}{RT}\left(\delta_i - \delta_m\right)^2 \tag{5.7}$$

The solubility parameter of the mixture, δ_m, is calculated as follows:

$$\delta_m = \sum_i^m \phi_i\delta_i \tag{5.8}$$

Equation 5.8 is substituted into Equation 5.3 to obtain:

$$K_i^{HL} = \frac{x_i^H}{x_i^L} = \exp\left(\frac{\upsilon_i^H}{\upsilon_m^H} - \frac{\upsilon_i^L}{\upsilon_m^L} + \ln\frac{\upsilon_i^L}{\upsilon_m^L} - \ln\frac{\upsilon_i^H}{\upsilon_m^H} + \frac{\upsilon_i^L}{RT}\left(\delta_i^L - \delta_m^L\right)^2 - \frac{\upsilon_i^H}{RT}\left(\delta_i^H - \delta_m^H\right)^2 \right) \quad (5.9)$$

Experimental observations showed that the heavy phase contains primarily asphaltenes and resins. In order to promote a rapid convergence and to avoid the need for asymmetric mixing rules, it is assumed that only resins and asphaltenes partition to the heavy phase.

The phase calculations are performed as shown in Figure 5.1. First, the molar composition of the feed is input and the K values are initialized. Then, the phase amounts are calculated using the Rachford-Rice method. The light phase composition is normalized and the K values are updated. Convergence is checked and if the calculation has not converged, the phase amounts are recalculated until convergence.

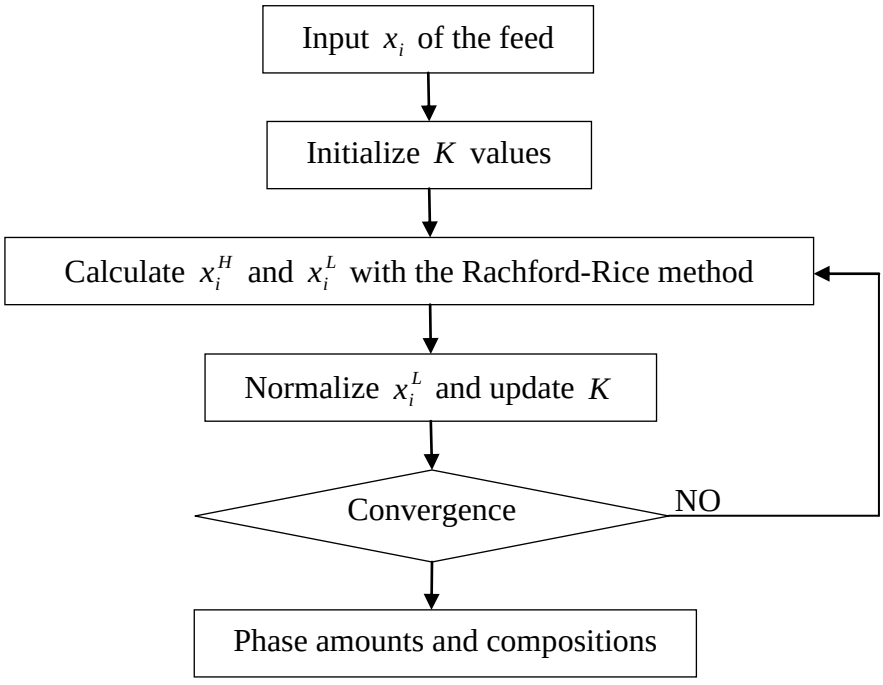

Figure 5.1. Schematic of liquid-liquid equilibrium algorithm.

5.2. Fluid Characterization

In this thesis, liquid-liquid equilibria are modeled for solutions of asphaltenes in *n*-heptane and toluene. To use the modified regular solution model, the mole fraction, density, molecular weight, and solubility parameter of each component are required. Each solvent is treated as an individual component with known properties. The asphaltenes are further divided into a set of pseudo-components representing the molecular weight distribution within the asphaltenes. The density and solubility parameter of each asphaltene pseudo-component must be determined.

5.2.1. Molecular Weight

Asphaltenes are assumed to be macromolecular aggregates of monodisperse asphaltene monomers with a distribution of aggregate sizes. Two different options to model the asphaltene molecular weight distribution are considered in this thesis. The first is to use the Gamma distribution as applied by Akbarzadeh *et al*. (2004). The second is to use the distribution predicted with the single-end termination model. Both approaches are presented below.

Gamma Distribution:

Akbarzadeh *et al.*, (2005) used a Gamma distribution function to represent the asphaltene associated molecular weight distribution because this function resembles molecular weight distributions measured with gel permeation chromatography. The Gamma distribution function (Whitson, 1983) is given by:

$$f(MW) = \frac{(MW - MW_{mono})^{\alpha-1}}{\beta^{\alpha}\Gamma(\alpha)} \exp\left(\frac{MW_{mono} - MW}{\beta}\right) \tag{5.10}$$

where MW_{mono} is the molecular weight of the monomer, MW is the average associated molecular weight for the whole asphaltenes, α is a parameter that defines the shape of the distribution, and β is given by:

$$\beta = \frac{MW_{avg} - MW_{mono}}{\alpha} \tag{5.11}$$

$\Gamma(\alpha)$ is the Gamma function defined as:

$$\Gamma(\alpha) = \int_0^\infty e^{-t} t^{\alpha-1} dt \tag{5.12}$$

The distribution is discretized into n fractions of constant step size (ΔMW) and the mass fraction of each fraction is calculated as follows:

$$x_i = \frac{\int_{MW_i}^{MW_{i+1}} f(MW)dMW}{\int_{MW_1}^{MW_n} f(MW)dMW} \tag{5.13}$$

An upper limit is also set to avoid a large number of fractions with negligible mass fraction.

In this thesis, asphaltenes were divided into 30 fractions and the maximum molecular weight was 30,000 g/mol, as recommended by Alboudwarej *et al.* (2003). The average molecular weight for asphaltenes depends on their concentration and temperature. In this thesis, the solubility tests were performed at 23°C and 10 kg/m^3 asphaltene concentration. The average molecular weight was set equal to the measured molecular weight for the whole asphaltenes at 50°C and 10 kg/m^3, corrected to 23°C as follows:

$$MW_{23°C} = MW_{50°C} \cdot \exp\left(0.0073 \cdot (50°C - 23°C)\right) \tag{5.14}$$

Equation 5.14 is based on previous observations of the change in the average molecular weight of the associated asphaltenes with temperature (Yarranton et al., 2000). A value of α close to 2 is recommended for polymer systems (Akbarzadeh, 2005) and α was adjusted to fit the shape of the experimental asphaltene precipitation curves.

<u>Single-End Termination Model Distribution:</u>

As was discussed in Chapter 4, the output from the single-end termination model is the molecular weight and mass fraction for all the aggregates and neutral material. The discrete distribution was fitted with a continuous function (Equation 4.31). The

distribution was divided into n fractions of constant step size (ΔMW) where the mass fraction of each increment is given by:

$$w_i = cumf_i - cumf_{i-1} \tag{5.15}$$

where $cumf$ is the integrated distribution function (Equation 4.31). The mass fraction and average molecular weight of each fraction are then input into the modified regular solution model. In this thesis, the asphaltenes were divided into 40 fractions and the maximum molecular weight depended on the sample used.

5.2.2. Molar Volume

The molar volume is the ratio of molecular weight to density. For the solvents, the molecular weights are known and the molar volumes were calculated using the Hankinson–Brobst–Thomson (HBT) technique (Reid *et al.*, 1989).

In the previous model (Yarranton *et al.*, 1996), asphaltene density, ρ, was correlated to molecular, MW, weight as follows:

$$\rho = 670 MW^{0.0639} \tag{5.16}$$

with the density expressed in kg/m^3 and the molecular weight in g/mol. This correlation was based on a limited set of measurements for Athabasca bitumen asphaltenes. In this thesis, the correlation of density to molecular weight will be revised based on new measurements as will be discussed in Chapter 6. The revised density correlation has the following form:

$$\rho = \rho_0 + \Delta\rho \cdot \left(1 - \exp\left(\frac{MW_0 - MW}{a}\right)\right) \tag{5.17}$$

where ρ_0, $\Delta\rho$, MW_0 and a are fitting parameters. The density is expressed in kg/m^3 and the molecular weight in g/mol.

5.2.3. Solubility Parameter

The solubility parameters for the solvents were calculated using Equation 5.15 (Hildebrand *et al.*, 1949):

$$\delta = \left(\frac{\Delta H^{vap} - RT}{v} \right)^{1/2} \tag{5.18}$$

where ΔH^{vap} is the heat of vaporization reported in the literature (Perry and Green, 1997).

Yarranton *et al.* (1996) recommended the following correlation for the solubility parameter of asphaltenes:

$$\delta = (A\rho)^{1/2} \tag{5.19}$$

where δ is the solubility parameter expressed in $MPa^{0.5}$ and *A* is approximately equal to the monomer heat of vaporization in kJ/g. The value of *A* is a function of temperature given by,

$$A(T) = -7.5 \times 10^{-4} T + 0.579 \tag{5.20}$$

where *T* is in Kelvin.

Equation 5.20 is specific for the density correlation given by Eq. 5-16 because it was obtained by fitting the model with this correlation to one set of asphaltene–*n*-heptane–toluene precipitation data at 23°C (Alboudwarej *et al.*, 2003). In this work, the density correlations are different for each sample and the correlation was modified as follows,

$$\delta = \left(A\rho \left(cMW^{d} \right) \right)^{1/2} \tag{5.21}$$

where *c* and *d* are constants adjusted to fit the predicted precipitation curve to the experimental values. The value of *A* will be revised as discussed in Chapter 6.

The following procedure is used to tune the asphaltene property parameters based on asphaltene precipitation data:

1. Enter the input parameters of the model: pressure, temperature, solvent composition, and asphaltene concentration.

2. Calculate the liquid molar volumes and solubility parameters of the *n*-alkanes
3. Enter parameters for the asphaltene molecular weight distribution (from the single-end termination model or from the Gamma distribution).
4. Calculate densities and solubility parameters of asphaltene subfractions.
5. Calculate the mole fraction of each component.
6. Set initial guesses for parameters *A*, *c* and *d*.
7. Perform liquid-liquid equilibrium calculations (Figure 5.1) and calculate the amount of precipitation.
8. Compare the model predictions with experimental data. If within tolerance, exit algorithm; otherwise return to Step 3 to adjust asphaltene molecular weight distribution or Step 6 to tune asphaltene solubility parameters.

Notice that the only adjustment to the molecular weight distribution was to tune α when the Gamma function was used. The main objective was to determine the asphaltene solubility parameters.

Chapter 6: Results and Discussion

In this chapter, asphaltene molecular weight and density distributions are reconstructed for eight crude oils based on the measured properties of asphaltene solubility fractions. Since asphaltenes self-associate, the terminator-propagator self-association model is used to interpret the measured data for the molecular weight of the aggregates. Finally, the property distributions are applied with the modified regular solution approach to model asphaltene precipitation data.

6.1. Asphaltene Fractions

Nine crude oil samples were initially considered for this study and their asphaltenes and solids contents are reported in Table 6.1. However, the Gippsland sample was subsequently eliminated from the study, as will be discussed later. The first five samples are from native oils that were not upgraded. Note, the Peace River sample was from a steam assisted gravity drainage process (SAGD) and had been stored for approximately 10 years and therefore some alteration of the crude may have occurred.

The last four samples are refinery streams that have undergone some processing and reaction. The following data were provided from Shell about the reaction conditions:

Sample	Temp.	Pressure	Extent of Reaction
27034-87	314°C	2.90 MPa	78.9%
27034-113	275°C	9.84 MPa	29.9%
26845	317°C	1.96 MPa	97.8%
27-168-178	-	-	-

The 27-168-178 sample is a reacted stream but no information was provided about its reaction conditions. No information was available for the source or type of process applied to any of the reacted samples.

Asphaltene fractions were selected based on the solubility curve of the whole asphaltenes in solutions of *n*-heptane/toluene at 23°C. For example, Figure 6.1 shows the solubility

curves for Athabasca and Peace River asphaltenes. For both cases, the onset of asphaltene precipitation occurred at approximately 40 wt% *n*-heptane and the yield approached 100% in pure n-heptane. For all the samples, the shape of the curve is similar although the exact onset of precipitation and slope of the yield versus *n*-heptane content differ.

For most of the samples, three fractions were separated, with the goal to obtain 25%, 50% and 75% of heavy material respectively. For Athabasca asphaltenes, four fractions were recovered, using HT60, HT70, HT80 and HT90 corresponding to 42%, 54%, 73% and 85% of heavy asphaltenes, respectively (Figure 6.2). In the case of Peace River asphaltenes, the heptol percentages used were HT60, HT77 and HT92, with a heavy phase content of 19%, 54% and 79%, respectively.

After fractionation of each sample, density and molecular weight were measured for all the fractions and also for the whole asphaltenes in order to characterize the light and heavy material that composes asphaltenes. This is an approach to determine how properties change among the whole sample and to build the property distribution.

Table 6.1. Asphaltene and solids content for the samples used in the thesis.

Sample	Measured Asphaltene wt%	Measured Solids wt% in Asphaltenes	Calculated Solids wt% in Crude Oil
Athabasca bitumen	16.50	7.67	1.27
Arabian crude oil	6.44	0.54	0.03
Gippsland crude oil	1.24	10.00	0.12
Cliffdale bitumen	11.76	1.82	0.21
Peace River bitumen	16.30	3.85	0.63
27-168-178	3.57	0.93	0.03
27034-87	3.62	1.26	0.05
27034-113	11.76	1.82	0.21
26845	-	1.82	-

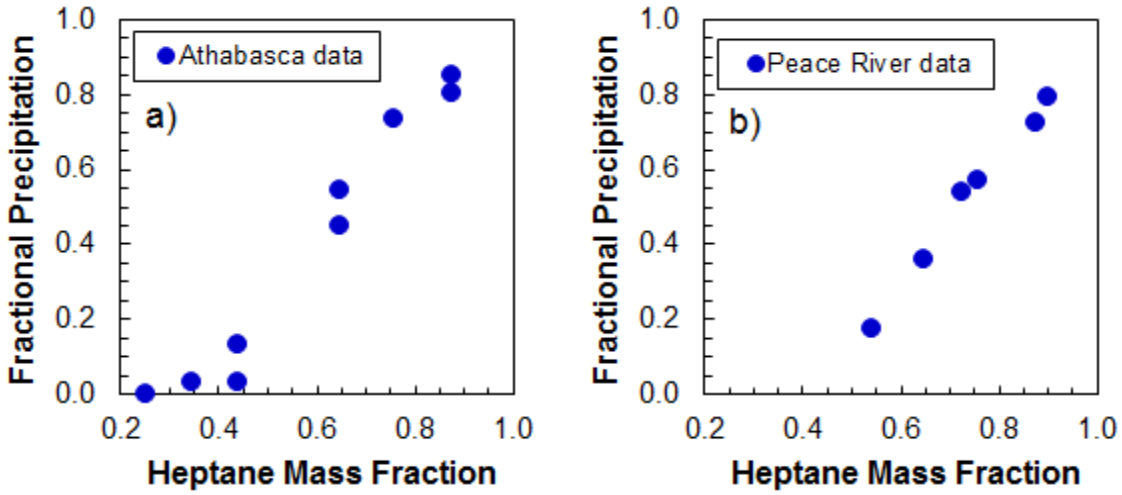

Figure 6.1. Fractional precipitation of asphaltenes from heptol mixtures: a) Athabasca, b) Peace River.

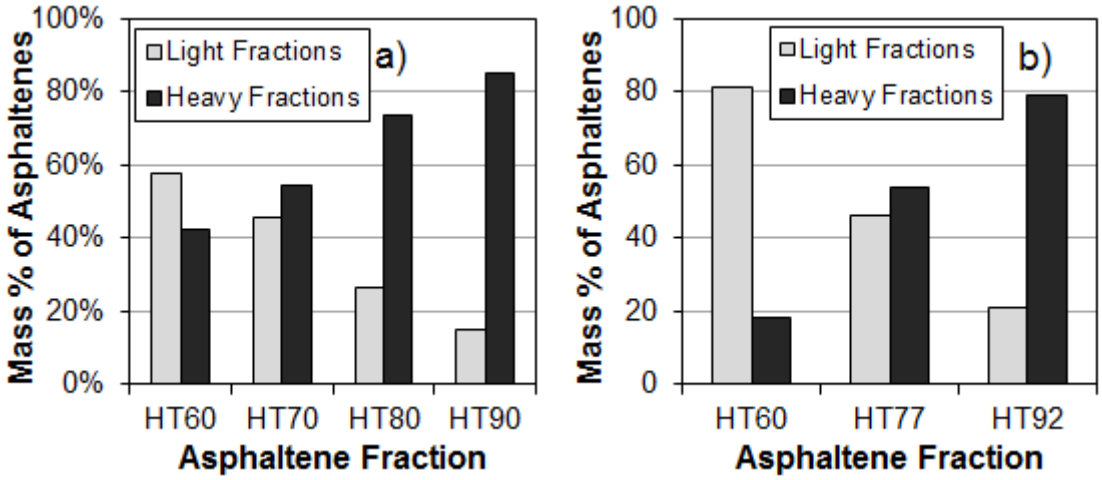

Figure 6.2. Mass percentage of heavy and light fractions for (a) Athabasca and (b) Peace River asphaltenes.

The Gippsland crude oil was significantly different from the other samples. Its asphaltene content of 1.24% was very low compared to the other samples, Table 6.1, consistent with the relatively low density of 796 kg/m³ for this oil. During the separation of the Gippsland asphaltenes, it was observed that they looked more like a wax than an asphaltene. Typical asphaltenes were fine bright black solids after solids removal, while Gippsland asphaltenes looked brown and tended to stick together creating flakes.

The properties of the Gippsland asphaltenes were also significantly different than the other samples. Figure 6.3 shows the molecular weight for the whole asphaltenes and for the light (70.1% of asphaltenes) and heavy fractions (29.9% of asphaltenes) obtained with a heptol ratio of HT62. For the whole asphaltenes, the molecular weight was very low and even the heavy fraction showed little self-association. Table 6.2 shows the density measured for the three cuts, which is also very low compared with values reported previously for asphaltenes from different sources (Akbarzadeh *et al.*, 2004). It is likely that the "asphaltenes" collected from this oil include both asphaltenes and co-precipitated wax. Therefore, the Gippsland sample was excluded from further analysis.

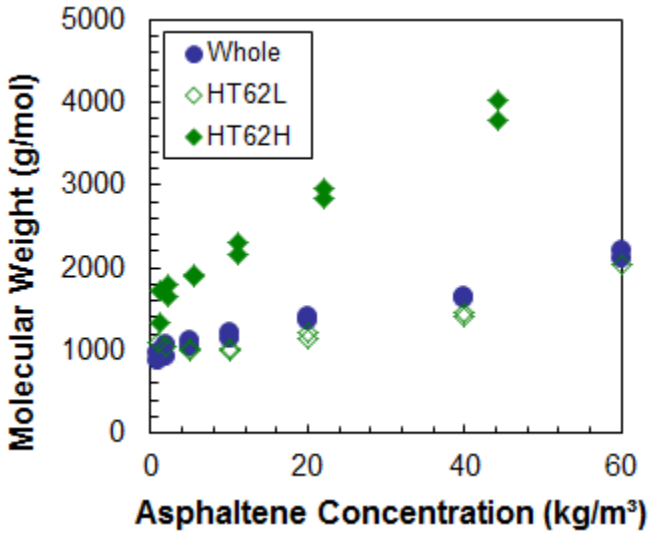

Figure 6.3. Molecular weight for Gippsland whole asphaltenes and fractions using a heptol fraction of HT62.

Table 6.2. Density for Gippsland fractions and whole asphaltenes.

Fraction	Asphaltene Mass Fraction	Density (kg/m^3)
HT62L	0.701	1061
Whole	1	1092
HT62H	0.299	1171

6.2. Measured Molecular Weight and Density Distributions

6.2.1 Molecular Weight

Figure 6.4 shows the molecular weight for Athabasca and Peace River asphaltenes and a pair of solubility fractions. The molecular weight of all but the lightest fractions increased with increasing asphaltene concentration, as expected for a self-associating material. The molecular weight of the lightest fraction increased little with concentration, suggesting that it contained little self-associating material. The molecular weight of the heaviest fraction increased significantly, indicating that it contained a high proportion of self-associating molecules or more strongly self-associating molecules. Similar behavior for molecular weight was observed for all of the other samples, as shown in Figures B.41 to B.46, Appendix B.

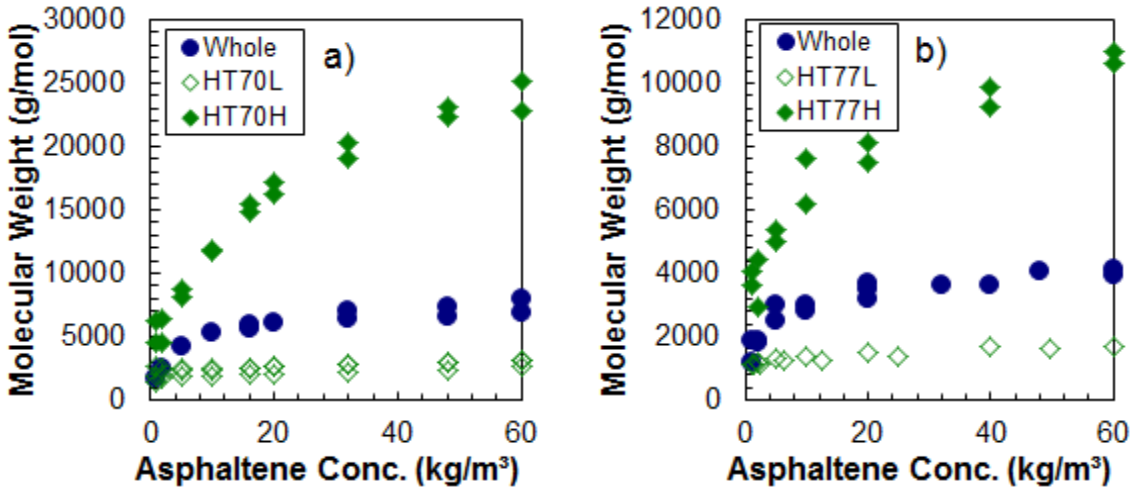

Figure 6.4. Molecular weight for (a) Athabasca and (b) Peace River whole asphaltenes and fractions precipitated using HT70 and HT77, respectively.

To simplify the comparison of samples, only the molecular weight for the lightest fraction, the whole asphaltenes, and the heaviest fraction at 60 kg/m^3 for each sample are considered here, as reported in Table 6.3. The molecular weights of the lightest fractions range between 900 and 2500 g/mol except for the Cliffdale sample with a molecular weight of 4200 g/mol. The variation in molecular weight is likely related to the

proportion of self-associating molecules in each light fraction. The variation increases for the whole asphaltenes and heavy fractions where self-association is more significant.

In Figure 6.5, the molecular weights at 60 kg/m^3 of the four samples from native oils are shown on the left and those of the four samples from reacted streams are shown on the right. Considering that we are examining self-associating materials from different sources, there is surprisingly little difference in the molecular weight distributions. Additionally, there is more variation in the molecular weights of the native asphaltenes compared with the reacted asphaltenes. The Peace River asphaltenes have a relatively low molecular weight, perhaps due to its recovery method or storage history. The Athabasca and Cliffdale asphaltenes have a higher average molecular weight than the other samples. These source oils were the most viscous of the samples indicating that they experienced more biodegradation in the reservoir. Perhaps biodegradation leaves higher molecular weight asphaltenes in the crude oil.

Table 6.3. Molecular weight at 60 kg/m^3 in toluene of whole, lightest fraction, and heaviest fraction of asphaltenes from different sources.

Sample	Whole	Lightest Fraction		Heaviest Fraction	
	MW (g/mol)	Mass Fraction of Asphaltene	MW (g/mol)	Mass Fraction of Asphaltene	MW (g/mol)
Athabasca	6800	0.15	1300	0.42	27000
Arabian	4200	0.27	2200	0.30	24000
Cliffdale	11000	0.30	4300	0.24	38000
Peace River	4000	0.21	900	0.19	12300
27-168-178	5500	0.20	1800	0.09	25000
27034-87	4700	0.16	1800	0.11	22000
27034-113	6200	0.32	2800	0.27	N/A
26845	3500	0.23	1400	0.29	25000

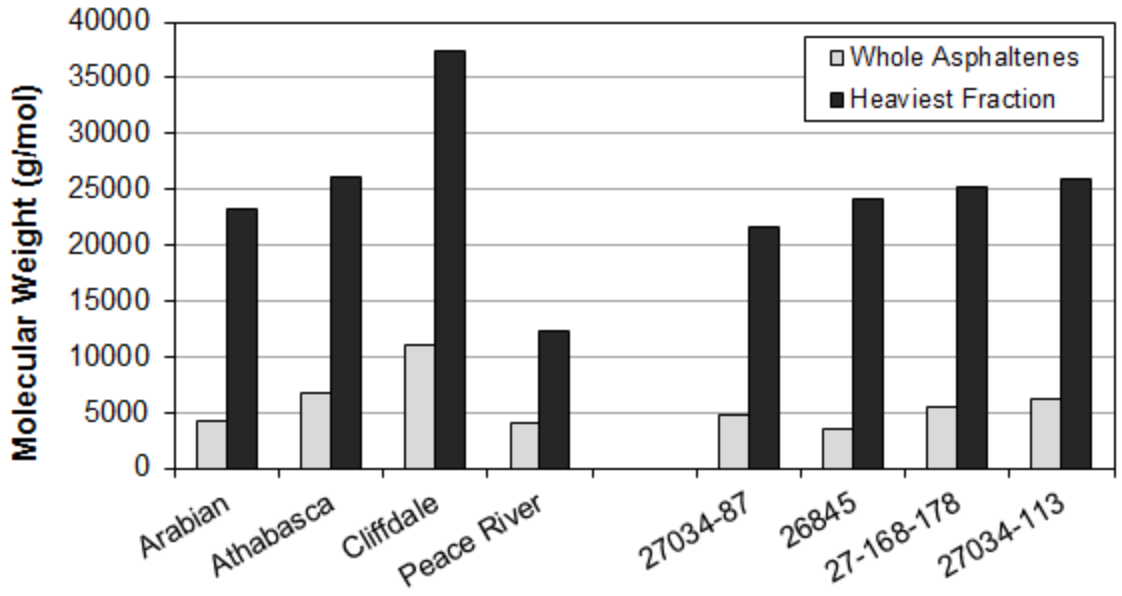

Figure 6.5. Molecular weight at 60 kg/m^3 in toluene for whole and heaviest fraction of asphaltenes from different sources.

If asphaltenes did not self-associate, their molecular weights would be additive and the molecular weight of the whole asphaltenes could be calculated from the molecular weight of its fractions as follows:

$$MW_{whole} = x_{HT\#\#L} MW_{HT\#\#L} + (1 - x_{HT\#\#L}) MW_{HT\#\#H} \tag{6.1}$$

where MW is the molecular weight data at a specific asphaltene concentration, $HT\#\#L$ and $HT\#\#H$ are the light and heavy fractions, respectively, with a heptol ratio of $HT\#\#$. Figure 6.6 shows the calculated molecular weight for the whole Athabasca asphaltenes. For all the fractions, the calculated molecular weight was significantly less than the measured value. The same behavior was observed for Cliffdale, Peace River, 26845, 27-168-178 asphaltenes. For the Arabian and 27034-87 asphaltenes, the calculated molecular weight exceeded the measured values while, for the 27034-113 asphaltenes, there was good agreement with the measured values. Since the molecular weights were additive in only one case, self-association must be accounted for when interpreting the molecular weight distributions.

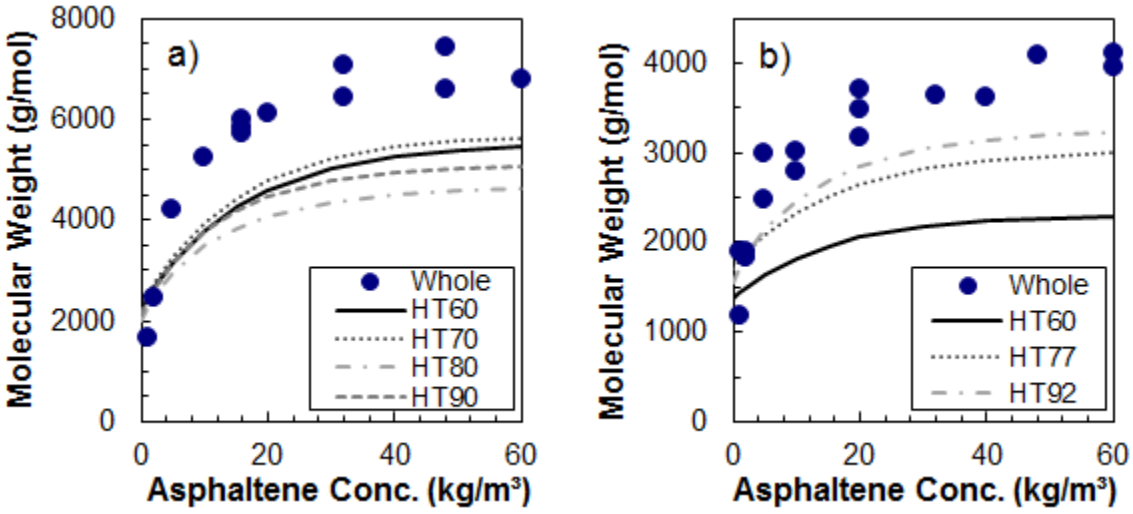

Figure 6.6. Recalculation of Athabasca (a) and Peace River (b) molecular weight assuming additive molecular weights.

When asphaltenes are divided into two solubility fractions, the lower molecular weight aggregates tend to remain soluble and report to the light fractions while the high molecular weight aggregates tend to precipitate and report to the heavy fraction, as observed in Figure 6.7. Then, when each fraction is dissolved in toluene for a molecular weight measurement, it will re-associate but not necessarily to the same distribution as it had in the original asphaltene mixture when in equilibrium with all the other asphaltene molecules and aggregates. Therefore, the measured molecular weights are not necessarily additive. Instead, a self-association model is used to fit the data to determine the number of monomers of different types of asphaltene molecule in each fraction (such as non-associating neutrals, propagators and terminators). Then, a material balance can be performed on the monomers and the molecular weight distribution calculated for any fraction or combination of fractions using the self-association model (Section 6.3). Before applying the self-association model, the density data are examined as help to assess the amount of non-associating and associating monomers in the asphaltenes.

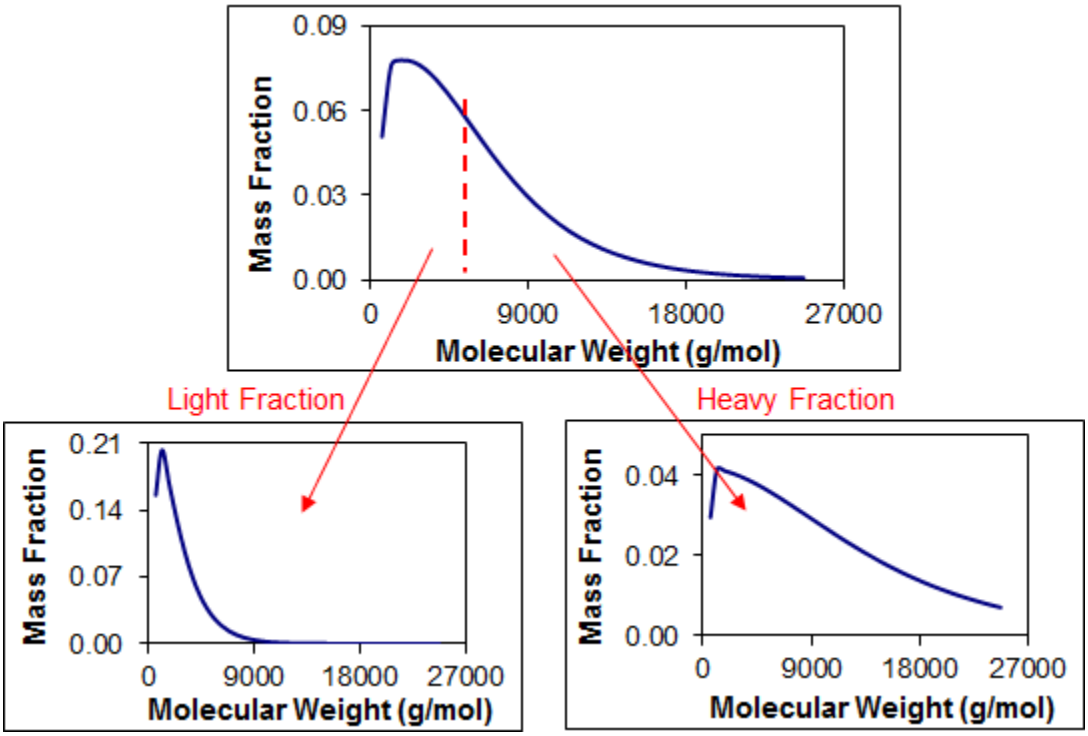

Figure 6.7. General illustration of partitioning of asphaltene aggregates into solubility fractions and self-association into new molecular weight distributions.

6.2.2 Density

Figure 6.8 compares the densities of the whole asphaltenes for the samples used in this thesis. The densities of the native stream asphaltenes were very similar with an average density of approximately 1176 kg/m³. The density of the reacted stream asphaltenes ranged from 1190 to 1245 kg/m³ with an average of 1200 kg/m³. Reacting a crude oil appears to increase the density of the asphaltene fraction and the relatively wide range in asphaltene density may reflect different extents of reaction or reaction histories. Data on the reaction history were not available and no further assessment was possible.

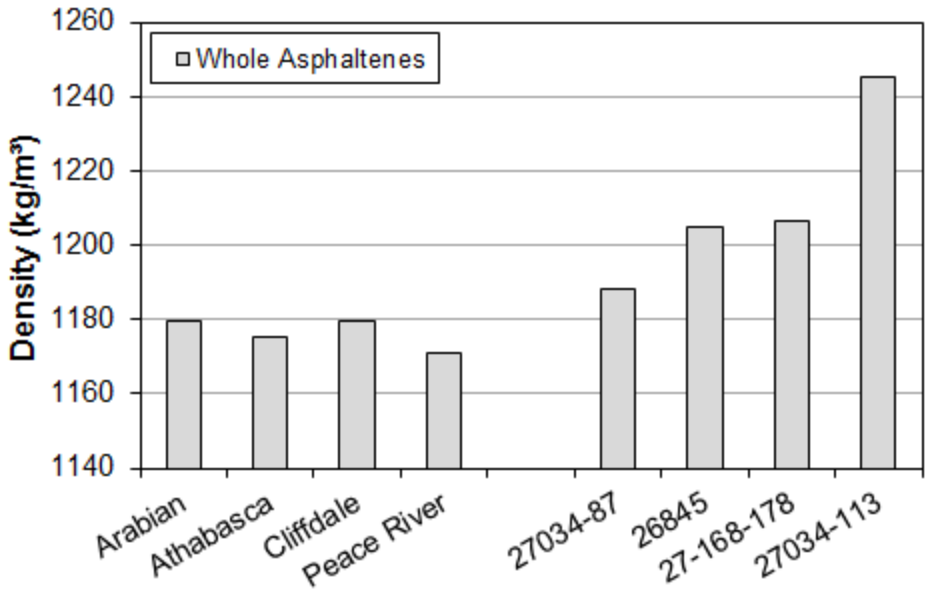

Figure 6.8. Density of the whole asphaltenes for all the samples used in this thesis.

The density distribution within the asphaltenes was determined from the density of the asphaltene solubility fractions. Figure 6.9 shows the density of the light and heavy fractions of Athabasca and Peace River asphaltenes versus the mass fraction of the whole asphaltenes. Each data point for a light cut is the average density of the components between zero and the mass fraction of that point. Each data point for a heavy cut is the average density of the components between that point and a mass fraction of one. It appears that the heaviest (and highest molecular weight) asphaltenes precipitate first and the lightest (lowest molecular weight) asphaltenes precipitate last.

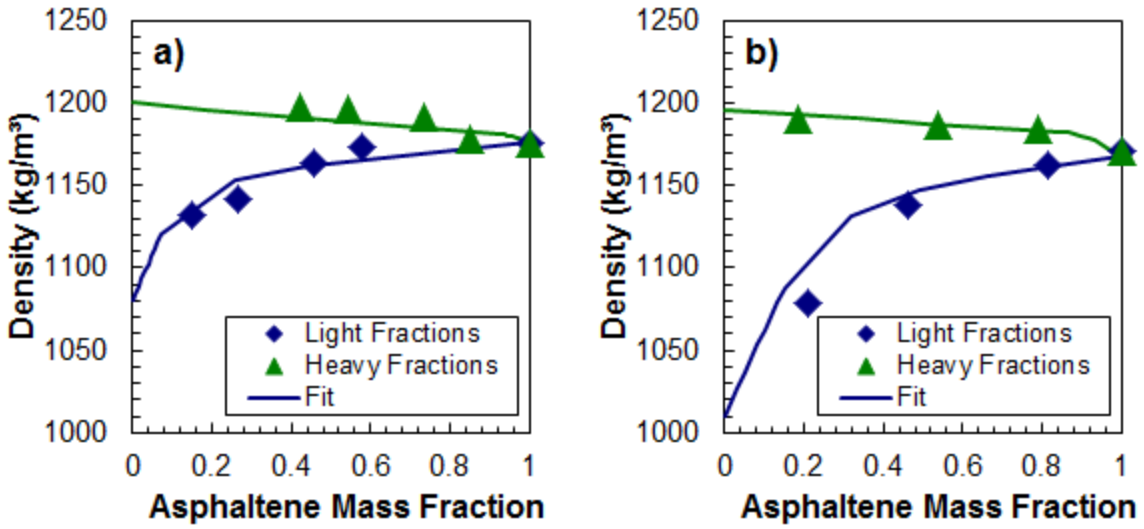

Figure 6.9. Density of Athabasca (a) and Peace River (b) asphaltene fractions. Lines are the cumulative density distribution calculated from the density distribution in Figure 6.10.

To determine the density distribution, the increment in the density from fraction to fraction is required. For the light fractions, the increment in the mass fraction w_i was determined as follows:

$$w_i = cumw_i - cumw_{i-1} \tag{6.2}$$

where $cumw_{i-1}$ represents the cumulative mass fraction of asphaltenes measured experimentally. For the first fraction, $cumw_{i-1}$ is equal to 0. Then, the average mass fraction $\overline{w}_i$ for each increment was calculated using the following equation,

$$\overline{w}_i = \frac{w_{i-1} + w_i}{2} \tag{6.3}$$

For the first fraction, w_{i-1} is equal to 0. The density for each increment was calculated as an average between the density of the fractions, as follows:

$$\rho_{incr,i} = \frac{\dfrac{w_i}{w_i + w_{i-1}}}{\dfrac{1}{\rho_i} - \dfrac{w_{i-1}}{\rho_{i-1}}} \qquad (6.4)$$

For the first fraction, $\rho_{incr,i} = \rho_i$. A similar procedure was used for the heavy fractions. Figure 6.10 shows the density distribution determined for the Athabasca and Peace River asphaltenes. Note that both light and heavy fraction results are plotted separately, but all were used to construct the density distributions.

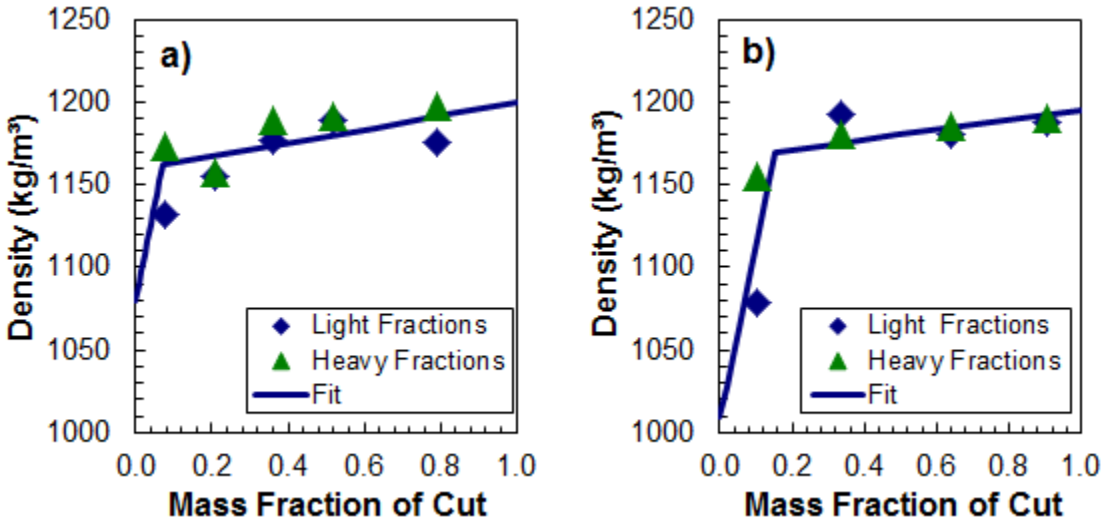

Figure 6.10. Density distribution for Athabasca (a) and Peace River (b) asphaltenes.

Figures 6.11 and 6.12 show the density distributions for the native and reacted samples, respectively. In almost every case, the density distributions of both the native and reacted asphaltenes showed two distinct trends: a steep rise in density followed by a shallow rise or plateau. The steep rise corresponded to the lightest lowest molecular weight fractions where little or no self-association was observed in the molecular weight data. The shallow rise or plateau corresponded to fractions exhibiting self-association. Therefore, it is likely that some of the asphaltenes do not self-associate and these asphaltenes are found predominantly in the most soluble fraction of the asphaltenes. Like any other molecules in the crude oil, there is a distribution of densities and therefore a relatively

steep slope versus mass fraction. Note that the lower end of this trend was similar to the density of resins; for example, the lowest density of the Peace River asphaltenes was 1078 kg/m³ compared with a resin density of 1075 kg/m³. Self-associated asphaltenes are aggregates likely formed from a number of molecules of varying density. The density of the aggregates will tend to the average density of the monomers. Therefore, the density does not change significantly across the mass fraction of self-associated asphaltenes.

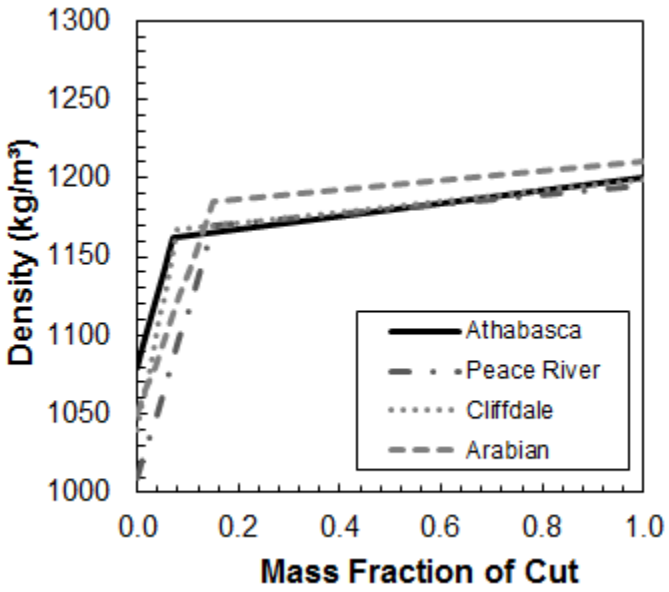

Figure 6.11. Density distributions for native samples.

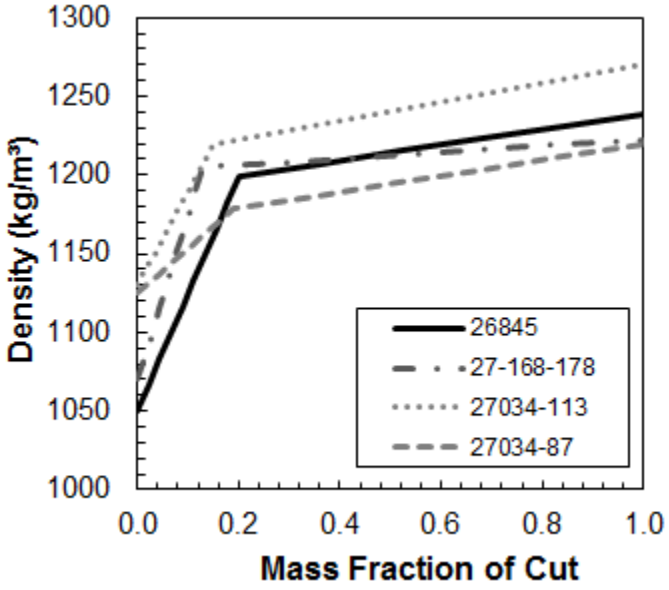

Figure 6.12. Density distributions for reacted samples.

Table 6.4 summarizes the minimum and maximum density of each sample as well as the point where the slope changes. The mass fraction where the slope changes is a preliminary measure of the mass fraction of non-associating asphaltenes in each sample. The non-associated zone ranges from 7 to 20 wt% of the asphaltenes, indicating that the majority of these asphaltenes tend to associate.

The density distributions of the native asphaltenes are very similar to each other. The maximum density for each native sample is approximately 1200 kg/m³. There are some differences in the minimum density, which may indicate some property differences but could also reflect the uncertainty in fitting the density data or slight differences in washing the asphaltenes in the preparation of the samples. The reacted samples show more variation in the aggregate densities with the maximum density ranging from 1220 to 1270 kg/m³. Such variation is not surprising because the reacted samples come from different parts of the refinery and likely have a different reaction history. Nonetheless, it is curious that their densities differ while their molecular weights are so similar.

Table 6.4. Minimum and maximum density and proposed mass fraction of non-associating material for all the asphaltene samples.

Sample	Minimum Density (kg/m^3)	Maximum Density (kg/m^3)	Mass Fraction of Non-Associating Material
Athabasca	1133	1197	7
Arabian	1122	1209	15
Cliffdale	1146	1203	8
Peace River	1078	1190	15
27-168-178	1154	1214	13
27034-87	1145	1223	19
27034-113	1193	1273	15
26845	1115	1246	20

6.2.3 Correlation of Density to Molecular Weight

When using a regular solution model for asphaltene precipitation, the two main inputs are the molecular weight and density distribution of the asphaltenes. Therefore, it is convenient to correlate density to molecular weight. A power law correlation was developed previously (Yarranton et al., 1996) based on a small dataset but can now be tested on a more extensive dataset.

Recall that molecular weights were measured as a function of asphaltene concentration in toluene at 50°C. The densities were determined from measurements at 21°C at different concentrations in toluene which were extrapolated to the asphaltene density using the regular solution mixing rule, as shown in Chapter 3. Since asphaltene molecular weight is dependent on temperature (Yarranton *et al.*, 2000), the molecular weight values were corrected to 21°C using Equation 5.14 in order to correlate density to molecular weight at the same conditions.

Figure 6.13 shows the density as a function of molecular weight for Athabasca asphaltenes. The dashed line represents the original density correlation which does not follow the experimental data accurately. Instead, the following new correlation was developed:

$$\rho = \rho_0 + \Delta\rho \cdot \left(1 - \exp\left(\frac{MW_0 - MW}{a}\right)\right) \tag{6.5}$$

where ρ_0 (kg/m³) and MW_0 (g/mol) are the density and the lowest molecular weight for an asphaltene molecule or aggregate, respectively, $\Delta\rho$ is the density difference between the lowest and highest molecular weight asphaltene, and a is a fitting parameter. The value R^2 is 0.93 for Athabasca asphaltenes, and in most of the cases is better than using a power function which gave values as low as 0.61 for 27034-87 asphaltenes.

Table 6.5 provides the fitted parameters of the density correlation (Equation 6.5) for all the samples. There is no common correlation even for the native samples partly because the correlation does not explicitly account for the mass fraction of non-associating

components. If this mass fraction was used as an input to the correlation, a common set of correlation parameters could likely be found for the native crude oils. However, since there is currently no simple method to determine this mass fraction, this approach was not pursued further.

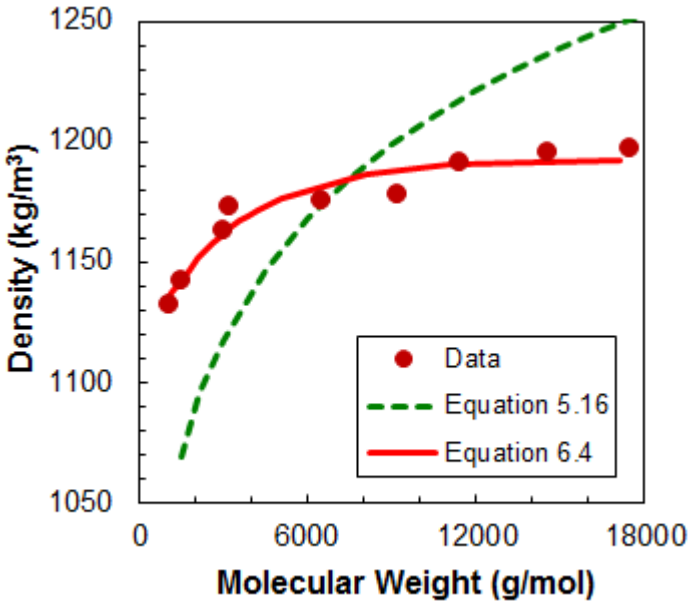

Figure 6.13. Density as a function of molecular weight for Athabasca asphaltenes.

Table 6.5. Parameters and fit coefficient for the density correlation in Equation 6.5.

Sample	ρ_0 **(kg/m³)**	$\Delta\rho$ **(kg/m³(**	MW_0 **(g/mol)**	a **(mol/g)**	R^2
Athabasca	1133	58	1007	3090	0.927
Arabian	1097	107	1983	1502	0.825
Cliffdale	1093	103	1108	4212	0.825
Peace River	1105	79	1183	669	0.975
27-168-178	1102	110	850	2064	0.959
27034-87	1065	132	455	1606	0.667
27034-113	1153	113	1014	2690	0.951
26845	1066	152	1171	559	0.887

6.3. Asphaltene Association and Single-End Termination Model

6.3.1 Modified Single-End Termination Model

The single-end termination model developed by Agrawala *et al.* (2001), as discussed in Chapter 4, was used to model the asphaltene molecular weight data. The original single-end termination model assumes that asphaltene association is similar to a linear polymerization with the presence of propagator and terminator molecules. However, all of the asphaltene samples have some non-associating "neutral" molecules. Therefore, the modified model developed in Chapter 4, which includes neutrals, is used here. Based on the molecular weight and density data, it was assumed that, during fractionation, neutrals partitioned only into the lightest asphaltene fraction.

Figure 6.14 shows the difference in the modeling of asphaltenes with or without neutrals for Athabasca whole asphaltenes. The solid line represents 5 mol% neutrals in the monomers and a $(T/P)_0$ ratio equal to 0.235, while the dashed line corresponds to a case without neutrals with $(T/P)_0$ equal to 0.32. Introducing the concept of neutrals in the asphaltene molecules improves the fitting of the experimental data, reducing the average absolute deviation (AAD) from 749 to 621 for 0 and 5 mol% neutrals, respectively.

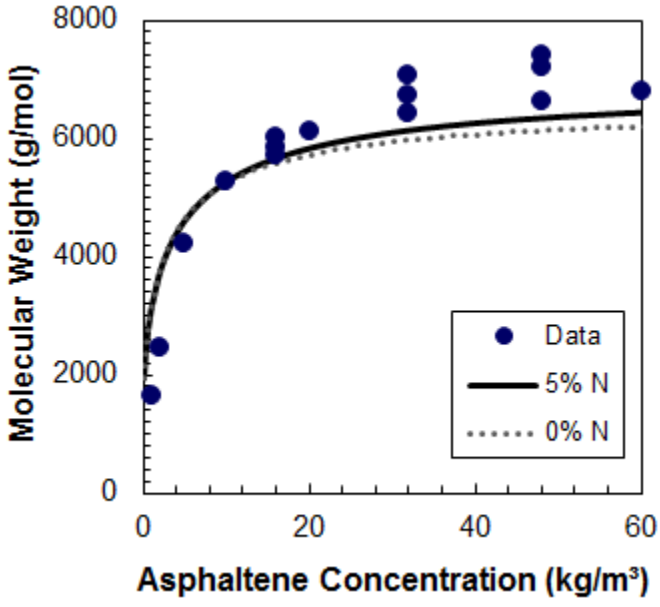

Figure 6.14. Effect of presence of neutrals on results for Athabasca whole asphaltenes.

The methodology for the implementation of the single-end termination model is shown in Figure 6.15. First, the model was run for each light and heavy fraction and the value of $(T/P)_0$ that best fit the molecular weight data for each fraction was determined. Second, the model was used to determine the optimum $(T/P)_0$ value for the whole asphaltenes, with the constraint that the molecular weight at 10 kg/m^3 was approximately the same as the measured value. Next, the initial moles of propagators and terminators were determined for each of the light and heavy fractions, and the moles in the whole asphaltenes were calculated from each corresponding pair of fractions (e.g. HT60L and HT60H) with a material balance. The $(T/P)_0$ value was calculated for the whole asphaltenes and compared with the fitted $(T/P)_0$ value. If the difference between both fitted and calculated values was less than 15%, the asphaltene molecular weight distribution was determined from the fitted amounts of neutral, propagators and terminators. Otherwise, the values of $(T/P)_0$ for all the fractions were modified until good agreement was reached.

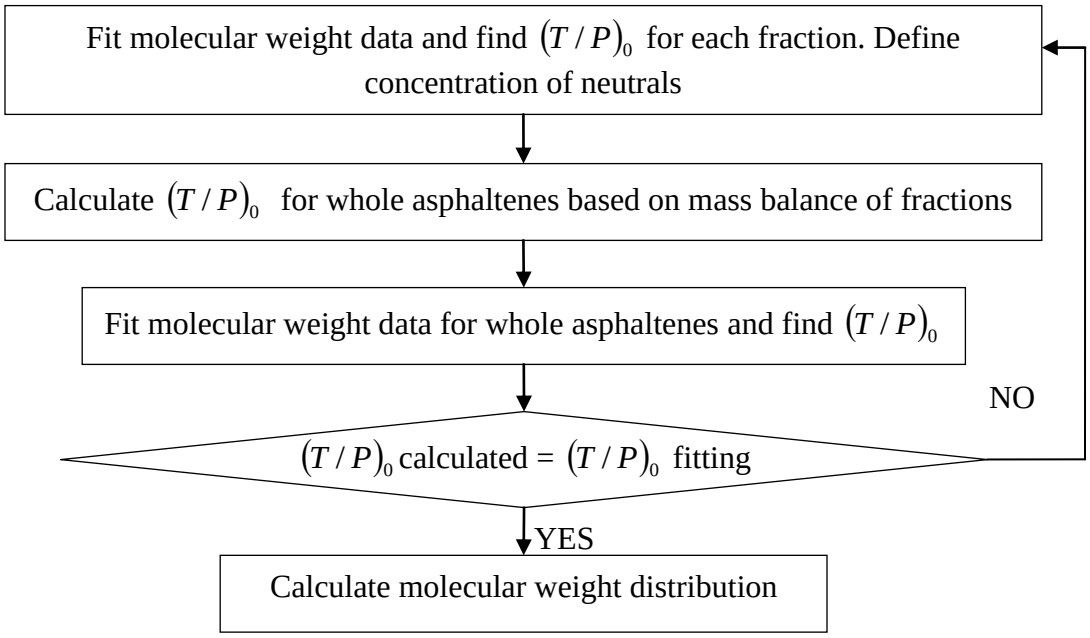

Figure 6.15. Algorithm to fit single-end termination model to molecular weight data.

Table 6.6 presents the calculated $(T/P)_0$ ratio for all Athabasca asphaltene fractions, and the fitted value for the whole asphaltenes. Note that error is approximately 10% for all the fractions. The quality of the fit is very good considering the high scatter in the molecular weight measurements and that the single-end termination model is a simplified representation of asphaltene association. For all the other samples, the error in the recalculated $(T/P)_0$ value was lower than 17%, except for Arabian asphaltenes where the error values were approximately 27%, as shown in Appendix A. The reason for the higher error for the Arabian asphaltenes is not known.

Table 6.6. Recalculation of $(T/P)_0$ for Athabasca asphaltene fractions.

Fraction	**$(T/P)_0$**	**Error**
Whole	0.235	---
HT60	0.260	10.7%
HT70	0.259	10.1%
HT80	0.259	10.2%
HT90	0.259	10.0%

Figure 6.16 shows the fitting for Athabasca light fractions and whole asphaltenes, while Figure 6.17 shows Athabasca heavy and whole asphaltenes. Similar results were obtained for the other samples, as observed in Appendix B. The model successfully represented the main features of asphaltene self-association: the increase in molecular weight with asphaltene concentration, the change in self-association from light fractions to heavy fractions, and the lack of self-association in the lightest fraction. Note that the model overestimated the molecular weight for the light fractions at low concentrations possibly because the reaction constant, *K*, was assumed to be the same for all the fractions. The model fits can be improved by changing the association constant for each fraction, as will be discussed in Section 6.3.2.

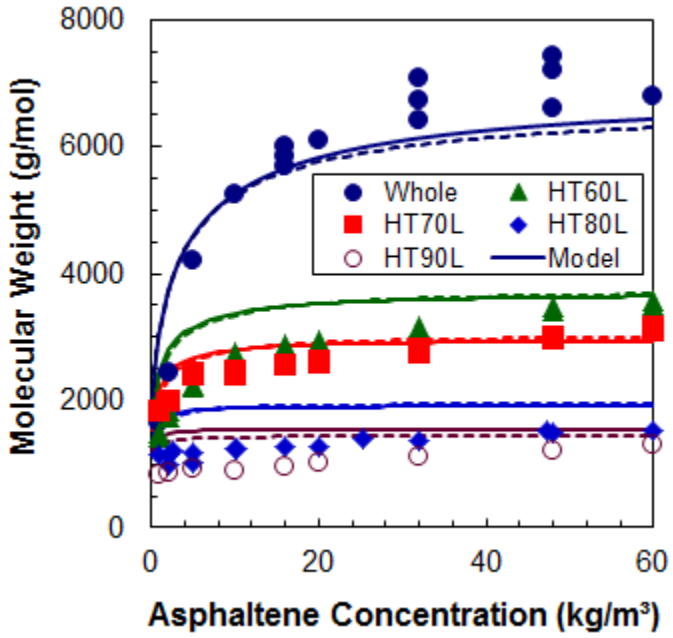

Figure 6.16. Fitting of molecular weight data using the single-end termination model for light fractions and whole Athabasca asphaltenes: solid lines – constant K; dotted lines – variable K.

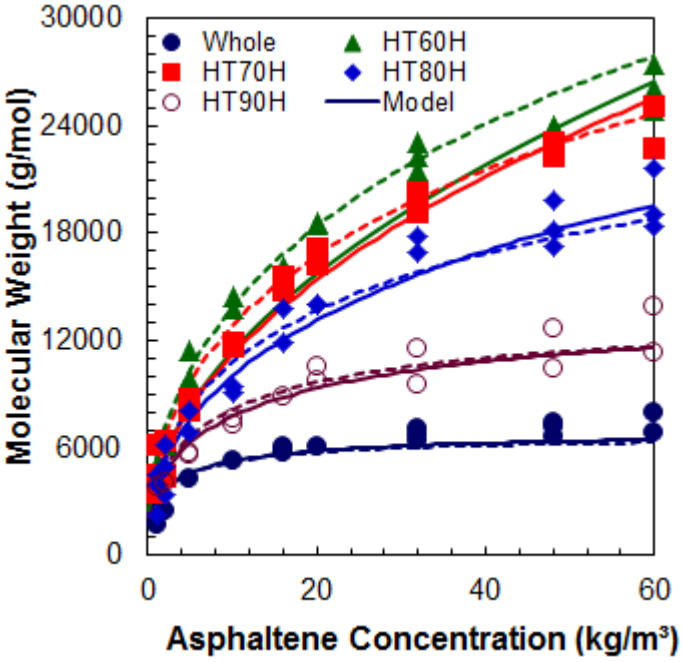

Figure 6.17. Fitting of molecular weight data using the single-end termination model for heavy fractions and whole Athabasca asphaltenes: solid lines – constant K; dotted lines – variable K.

Table 6.7 summarizes the fitting parameters and inputs of the single-end termination model for the different samples. For the native streams, the value of K was 55000 mol^{-1} while the reacted streams were modeled with K = 65000 mol^{-1}. For all the samples, the molar percentage of neutral monomers ranged between 3 and 7 mol%, and was larger for the reacted samples than for the native ones, as was observed with the density data. The mass fraction of neutrals was calculated and ranged between 2.1 and 5.6 wt%. These values are lower than the values obtained from the density distribution but confirm the presence of non-associated molecules. Note, that amount of neutrals determined from the model are a fit parameter while the amount determined from the density distributions is an experimental observation and therefore likely to be more accurate. The molecular weight of terminators and neutrals ranged from 700 to 1800 g/mol and for the propagators it was between 900 and 2000 g/mol. Note that for all cases the propagator monomer molecules are larger than the terminator molecules.

Table 6.7. Inputs and parameters of the single-end termination model for all the samples (T = Terminator, P = Propagator, N = Neutral).

Sample	**MW_T (g/mol)**	**MW_P (g/mol)**	**MW_N (g/mol)**	$(T/P)_0$	**mol% N - monomers**	K **(1/mol)**	**mass% N**
Athabasca	900	1800	900	0.235	5	55000	2.8
Arabian	1200	2000	1200	0.592	3	55000	2.1
Cliffdale	1600	1900	1600	0.135	5	55000	4.3
Peace River	700	900	700	0.26	5	55000	4.1
27-168-178	1000	1900	1000	0.418	6	65000	3.8
27034-87	900	1400	900	0.293	6	65000	4.3
27034-113	900	1200	900	0.258	7	65000	5.6
26845	800	1300	800	0.412	7	65000	5.0

6.3.2 Single End Termination Model with Variable Association Constant

Note that for all fractions, the value of the association constant, *K*, was held constant because the model was derived based on the assumption that the association constant is the same for all the association and termination reactions. However, it is likely that different molecules have different reaction constants and that the average constant may be different for each fraction. As a preliminary test, the association constant was varied using Athabasca asphaltenes as an example, with the restriction that the recalculated association constant from each fraction was equal to the association constant for the whole asphaltenes:

$$K_{whole} = x_{HT\#\#L} K_{HT\#\#L} + x_{HT\#\#H} K_{HT\#\#H} \tag{6.6}$$

where x is the molar fraction, and K is the association constant for the heavy (H), light (L) and whole fractions in a heptol ratio of $HT\#\#$. Note that the model assumption of constant K is now violated; hence, the results from this preliminary test are only qualitative.

Table 6.8. Recombined parameters Athabasca asphaltenes with the K variable scenario.

Fraction	K_L	K_H	$K_{whole,recomb}$	**Error %**	**$(T/P)_0$**	**Error**
Whole	56000	-	-	-	0.272	-
HT60	41000	110000	55742	1.3	0.296	9.0
HT70	35000	100000	54122	1.6	0.298	9.7
HT80	28000	82000	54252	1.4	0.298	9.5
HT90	24000	70000	54467	1.0	0.297	9.2

Table 6.8 shows the association constant values for all the Athabasca fractions and the recombined value. Note that the recalculated association constant for fraction is within 2% of the whole asphaltene value. The single-end termination model was run with the new constants and the results are shown on Figures 6.16 and 6.17 as dotted lines. There is a slight improvement in the fitting of the experimental data from the constant K model and the AAD error for all the fractions was reduced from 6942 to 6417 g/mol. The error in the recalculated $(T/P)_0$ is less than 9.8% for all the Athabasca fractions compared

with 10.8% for the constant *K* model. The improvement in the model fit to the data is too small to justify introducing a variable association constant to the model. Therefore, the constant *K* model is used for the remainder of the thesis. The modification of the reaction constant based on the aggregate molecular weight may be an option for future work when more data become available.

6.3.3 Molecular Weight Distribution

Once the parameters of the single-end termination model were determined and adjusted so that the mass balances for all the samples were achieved, the molecular weight distribution was determined. The output of the model was the molecular weight and mass fraction for all the associated species in the system. The cumulative mass fraction was plotted as a function of the molecular weight, and the values were fitted using the least squares method with Equation 4.31. Figure 6.18 shows the fitting of the modeled cumulative distribution for Athabasca whole asphaltenes. For this case, the error in the fitting was of 0.3% and, for all cases, the error was less than 1.3%. The parameters of the molecular weight distribution are shown in Table 6.9, along with $MW_{cumf=0}$ that corresponds to the molecular weight when $cumf = 0$.

Table 6.9. Parameters for the asphaltene molecular weight distribution at 50°C.

Sample	***A***	***B***	***C***	***D***	$MW_{av@50°C}$	$MW_{cumf=0}$	MW_{mono}	MW_{final}
Athabasca	1.191	7074	4770	-0.191	5250	492	1592	50000
Arabian	1.442	4679	1629	-0.442	3950	844	1687	30000
Cliffdale	1.2574	9079	5163	-0.257	6980	972	1851	55000
Peace River	1.296	3882	1923	-0.296	2900	410	851	25000
27-168-178	1.334	5148	2173	-0.333	4200	553	1597	35000
27034-87	1.285	5390	2727	-0.284	3950	514	1264	30000
27034-113	1.376	4147	1536	-0.376	3650	491	1122	30000
26845	1.292	5661	2798	-0.292	3020	456	1129	25000

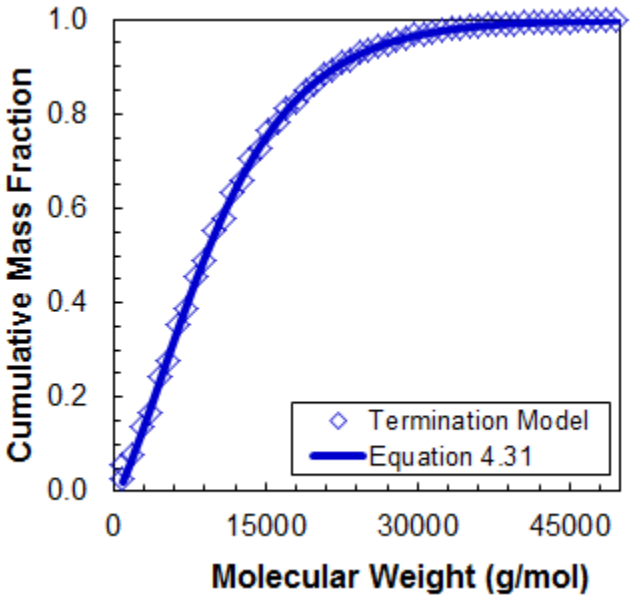

Figure 6.18. Cumulative mass fraction for Athabasca asphaltenes at 50°C.

In order to obtain the molecular weight distribution for each asphaltene sample, the cumulative distribution was discretized as discussed in Chapter 5. The cumulative distribution was calculated between the average monomer molecular weight MW_{mono} calculated using Equation 4.33 and a maximum value MW_{final} that accounted for more than 99% of the associated material, as reported in Table 6.9. Then the range of molecular weights was divided into 40 fractions of constant step size, and the distribution was calculated for each interval. The mass fraction, w_i, was calculated using Equation 5.15 and the average molecular weight, $MW_{av,i}$, for the increment, i, was calculated as follows:

$$MW_{av,i} = \frac{MW_i + MW_{i-1}}{2} \tag{6.7}$$

For the first interval, the average molecular weight was calculated as the average between the average monomer molecular weight, MW_{mono}, and the molecular weight when $cumf = 0$, $MW_{cumf=0}$. The average molecular weight of the distribution was calculated as:

$$MW_{av} = \sum_{i=1}^{40} \frac{w_i}{MW_{av,i}} \tag{6.8}$$

Table 6.9 shows the average molecular weight of the distribution calculated for all the samples, which was matched with the molecular weight measured experimentally at 10 kg/m^3 for the whole asphaltenes. Figure 6.19 shows the molecular weight distribution for Athabasca asphaltenes at 50°C.

In order to use the molecular weight distribution as an input for the regular solution model, the distribution was corrected to 23°C to account for the effect of temperature on asphaltene molecular weight. The methodology for the correction is as follows: the molecular weight of the distribution at 50°C was recalculated at 23°C using Equation 5.14, and the single-end termination model was run again changing only the $(T/P)_0$ ratio until the average molecular weight of the new distribution corresponded to the corrected value at 23°C.

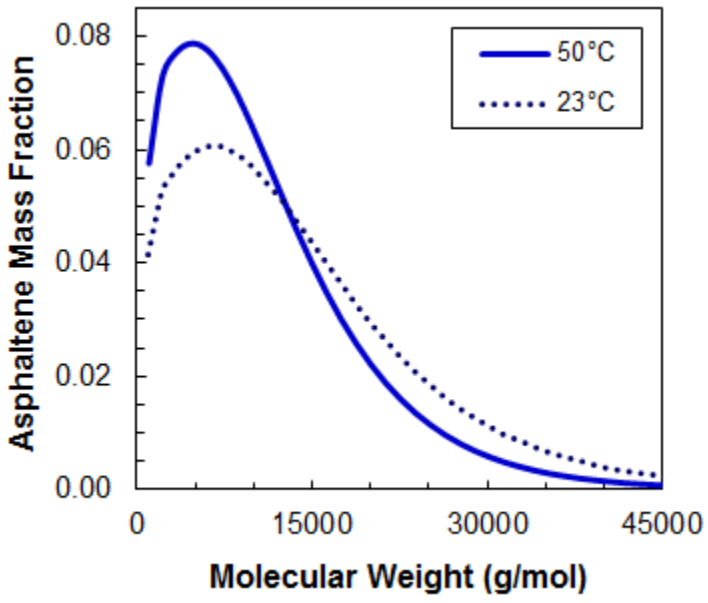

Figure 6.19. Molecular weight distribution for Athabasca asphaltenes at 23 and 50°C.

Table 6.10 shows the $(T/P)_0$ parameter used to obtain the molecular weight distribution at 23°C for each sample; the molecular weight distribution and its average molecular weight at the corrected temperature were calculated in the same way as shown previously at 50°C. Note that Equation 4.31 was also used to fit the molecular weight of the whole asphaltenes. One constraint of the distribution at 23°C was that the value of $MW_{cumf=0}$ was the same as that for the distribution at 50°C. The error in the fitting of the model results at 23°C for Athabasca asphaltenes is 0.08% and for all cases is less than 0.56%. Figure 6.19 compares the molecular weight distributions for Athabasca asphaltenes at 23°C and 50°C, and it can be seen that the distribution at a lower temperature predicts not only a lower concentration of light material, but also a higher concentration of associated material, that matches with the increasing in the average molecular weight from 5250 to 6488 g/mol for Athabasca asphaltenes. The same behaviour occurs for the other samples.

Table 6.10. Parameters for the asphaltene molecular weight distribution at 23°C.

Parameter	*A*	*B*	*C*	*D*	$MW_{av@23°C}$	$(T/P)_{0@23°C}$
Athabasca	1.164	8984	6533	-0.164	6488	0.125
Arabian	1.366	6252	2566	-0.366	4846	0.374
Cliffdale	1.208	11549	7501	-0.208	8636	0.040
Peace River	1.248	5000	2812	-0.248	3583	0.164
27-168-178	1.247	7296	4073	-0.247	5185	0.268
27034-87	1.242	6944	3937	-0.242	4880	0.182
27034-113	1.286	6680	3224	-0.285	4512	0.157
26845	1.319	5415	2355	-0.319	3731	0.271

Figures 6.20 and 6.21 show the molecular weight distributions at 23°C for native and reacted streams, respectively in mass and mole fraction basis. All the distributions have a similar shape and show that asphaltenes consist mostly of material with molecular weight lower than 15000 g/mol, with a lesser amount of aggregates ranging up to 50000 g/mol or more. As noted previously, the molecular weight distributions are similar for most samples. The Athabasca and Cliffdale samples have a broader distribution than the other samples perhaps indicating a more biodegraded oil.

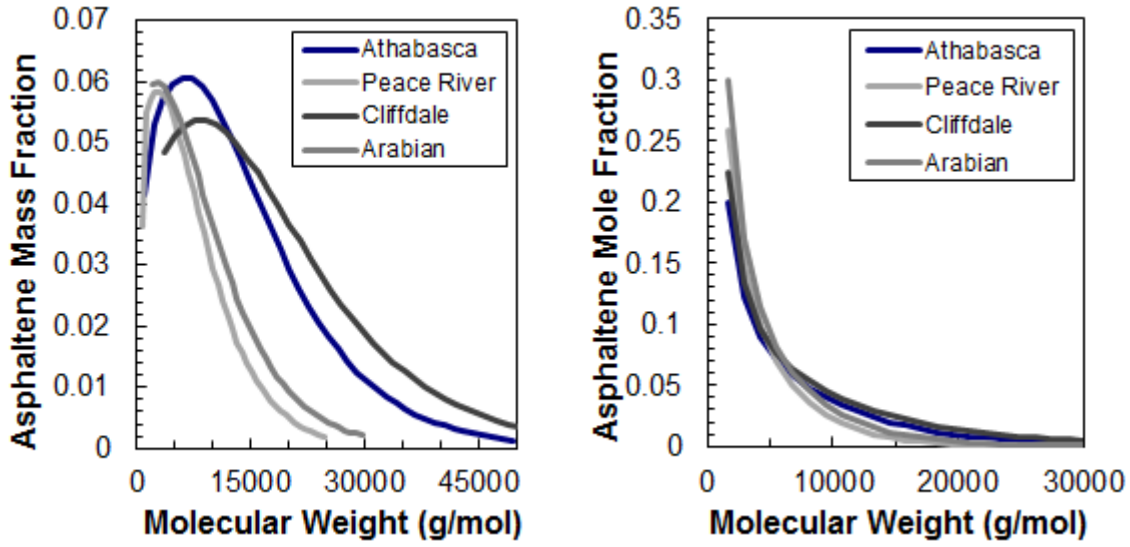

Figure 6.20. Molecular weight distribution for asphaltenes from native samples at 23°C.

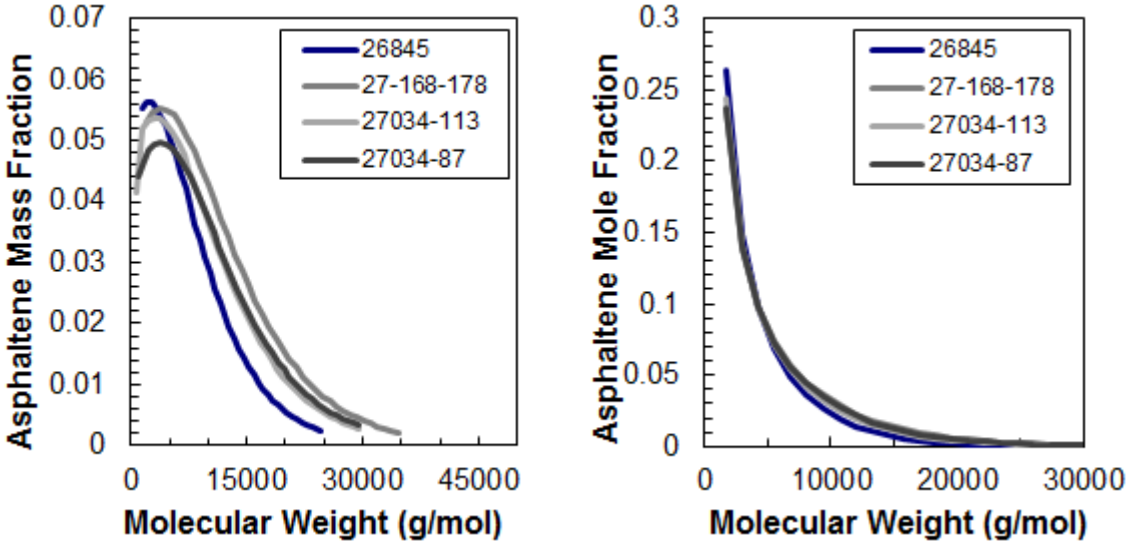

Figure 6.21. Molecular weight distribution for asphaltenes in reacted samples at 23°C.

It was assumed previously that asphaltene molecular weight distribution followed a Gamma distribution (Akbarzadeh *et al*., 2004). The Gamma distribution requires fewer parameters than the association model and is more convenient for use in simulation. The parameters of this type of distribution were determined for all asphaltene samples, as shown in Table 6.11. Note that the average molecular weight used in the distribution corresponds to the molecular weight measured for the whole asphaltenes at 10 kg/m^3 and only α was adjusted.

Figure 6.22 shows as an example the molar frequency and cumulative molecular weight distributions for both Athabasca and 27034-113 asphaltenes, where the solid lines represent the single-end termination distribution and the dashed lines correspond to the Gamma distribution. The same behavior was observed for the other samples. Note that both distributions give similar results on a mole basis, which was expected because both have the same average molecular weight. However, the Single-end distribution predicts a slightly higher number of molecules of very small size than the Gamma distribution, which may be an effect of the addition of the neutral molecules to the Single-end termination model. Therefore, the Gamma distribution is expected to give similar but not identical predictions for the precipitation of asphaltenes from the regular solution model as would the Single-end distribution.

Table 6.11. Parameters of Gamma molecular weight distribution for all samples. A monomer molecular weight of 800 g/mol and a maximum molecular weight of 30000 g/mol with 30 fractions were used in all cases.

Param.	**Athab.**	**Arabian**	**Cliffdale**	**Peace River**	**27-168 -178**	**27034-87**	**27034 -113**	**26845**
M_{avg}	5250	3920	6980	2900	4200	3950	3650	3020
α	1.05	1.04	1.5	1.05	1.6	1.35	1	1.05

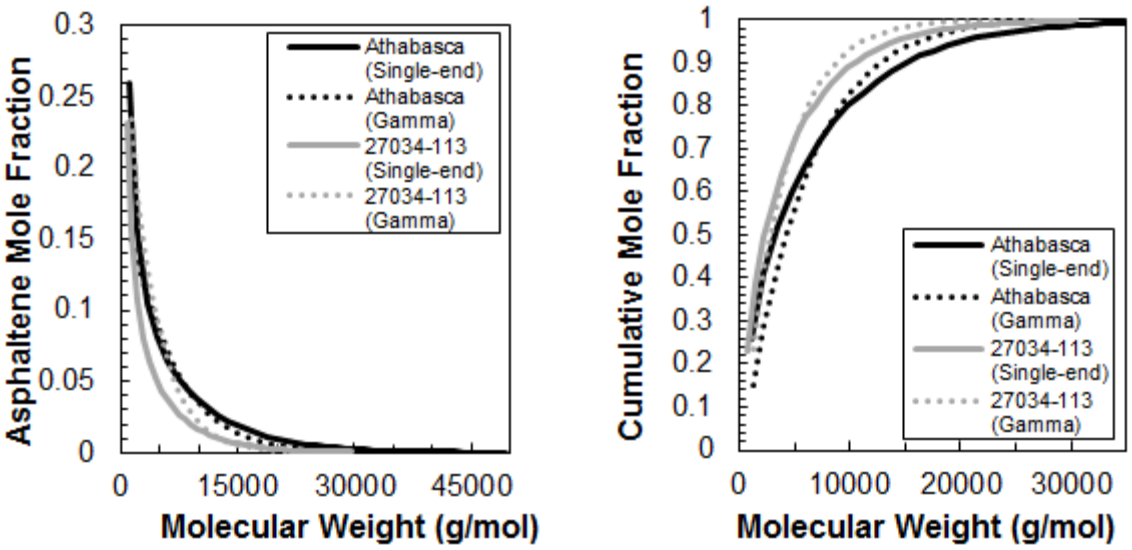

Figure 6.22. Differences between the Gamma and the single-end distributions.

6.4. Regular Solution Modeling

6.4.1 Modifications to the Model

The previously developed modified regular solution model (Alboudwarej *et al.*, 2003) was used to calculate the fractional precipitation of asphaltene samples. Some additional modifications were made in order to introduce the molecular weight and density distributions developed through this thesis.

Previously, the model was run assuming that molecular weight for asphaltenes could be described by a Gamma distribution. The inputs for the Gamma distribution are the average molecular weight, the minimum molecular weight, and the shape factor, α. The model was adapted to accept the Single-end distribution parameters (A, B, C, D, MW_{mono}, $MW_{cumf=0}$, and MW_{final}) as an input as well.

Previously, the model assumed a density distribution that followed Equation 5.16. However, this equation was not representative for most of the samples used in this thesis,

so an alternative density distribution, Equation 6.5, was used. The inputs for the new distribution were ρ_0, MW_0, $\Delta\rho$ and a.

The solubility parameter depends on the density, and due to the changes in the correlation for this property, the previous correlation (Equation 5.19) required modification as shown in Equation 5.21. Two new parameters c and d were required to account for the change in solubility parameter with the changing size and density of the asphaltene aggregates.

The methodology followed for testing the regular solution model is as follows. Initially, both Gamma and single-end molecular weight distributions were used with the old density correlation. Then, both distributions were also used with the new density correlation, and the values of c and d were modified until a good fit of the experimental results for the fractional precipitation of asphaltenes at 10 kg/m^3 was obtained.

6.4.2 Results from Previous Model

The input parameters for the Gamma distribution are provided in Table 6.11. The distribution was divided into 30 fractions of equal size, and calculated between 800 and 30,000 g/mol. The inputs for the Single-end distribution are provided in Tables 6.9 and 6.10. The distribution was divided into 40 fractions of equal interval, between MW_{mono} and MW_{final}.

Figure 6.23 shows the results from the regular solution model for Athabasca asphaltenes using Equation 5.16 for the asphaltene density, the default correlation for the solubility parameter, Equation 5.19, and the Gamma distribution (dashed line). The AAD of the predicted values was 0.035. It is not surprising that the Gamma distribution provided a good prediction in this case because the solubility parameter correlation was constructed from the same model applied to asphaltenes from similar sources.

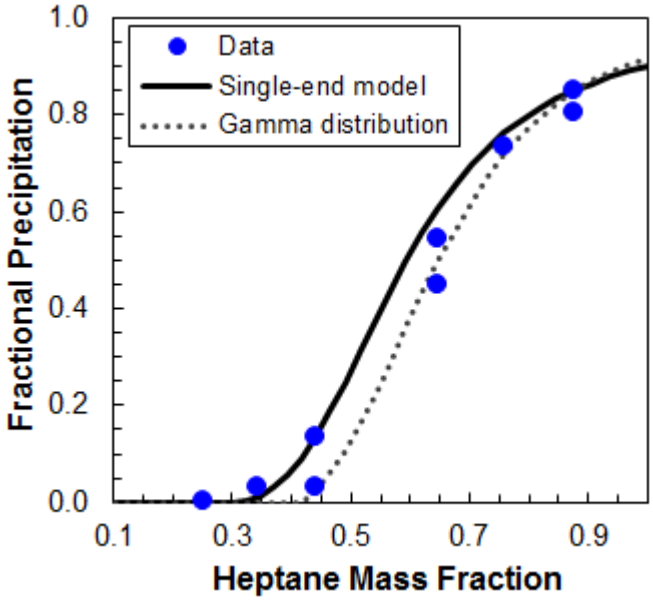

Figure 6.23. Fractional precipitation of Athabasca asphaltenes from solutions of *n*-heptane and toluene at 23°C using the old density correlation.

For some of the samples, the model underestimated the fractional precipitation by a significant percentage. The highest deviations were observed for the reacted samples; for example, an AAD of 32 wt% for 26845 asphaltenes using the Gamma distribution, Appendix A. The asphaltenes in the reacted streams have been chemically altered and therefore the solubility parameter correlation developed for native crude oils no longer applies. Hence, a modification of the *A* factor in the solubility parameter correlation for the asphaltenes, Equation 5.19, was required as follows:

$$A(T) = \left(-7.5\times10^{-4}T + 0.579\right) + A' \qquad (6.9)$$

where A' is a fitting parameter that shifts the curve to left and right.

Table 6.12 shows the value of A' required when using the Gamma distribution. Note, that of the native crude oils, only the Peace River sample required modification suggesting that this sample did indeed undergo some chemical alterations during its history. Figure 6.24 shows the effect of A' on the model and the improvement in the results for 26845 asphaltenes. The AAD decreased from 0.318 to 0.059 for this sample. It

appears that a simple constant shift in the *A* parameter is sufficient to model the results for all samples.

Table 6.12. Fitting parameter introduced in Equation 6.9 using the Gamma distribution.

Sample	*A*'
Athabasca	0
Arabian	0
Cliffdale	0
Peace River	0.0126
27-168-178	0
27034-87	0.0180
27034-113	0.0300
26845	0.0260

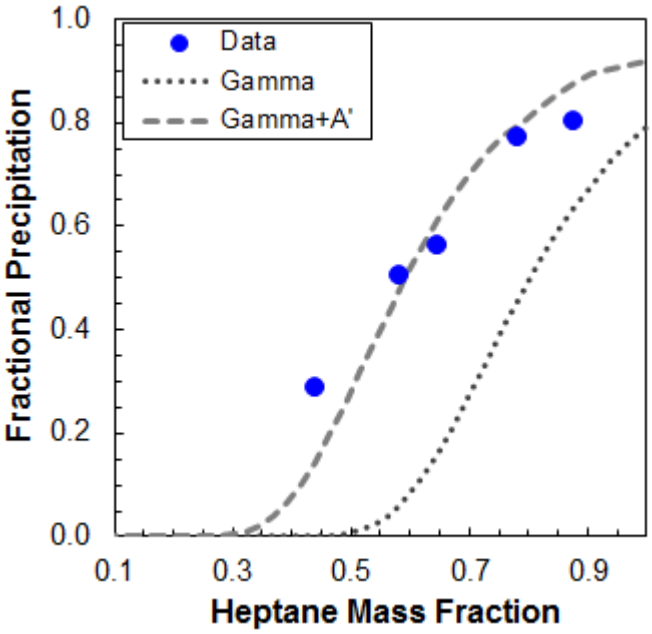

Figure 6.24. Effect of the addition of the *A*' parameter on the fractional precipitation of 26845 asphaltenes from solutions of *n*-heptane and toluene at 23°C.

6.4.3 Results from Modified Model

Figure 6.23 compares the predicted yields for Athabasca asphaltenes based on the Gamma distribution (dashed line) and the Single-end distribution (solid line). Both distributions provide good predictions at high yields but the Single-end distribution slightly over-predicts the low yield data. The AAD of the predicted values for the Single-end model was 0.047 compared with 0.035 with the Gamma distribution. Clearly, the tuning of the solubility parameter correlation is sensitive to the shape of the asphaltene molecular weight distribution. Therefore, separate correlations were used for the Gamma distribution and the Single-end distribution cases.

The next step was to evaluate the model using the fitted density distributions instead of the density correlation. Figure 6.25 shows the model fits for the yield of Athabasca asphaltenes. Equation 5.21 was used for the solubility parameter and therefore the A' parameter was not used here. The fitting parameters used in Equation 5.21 to calculate the solubility parameter were $c = 0.650$ and $d = 0.0495$ with the Gamma distribution and $c = 0.637$ and $d = 0.0495$ for the Single-end distribution. Table 6.13 summarizes the parameters c and d using both distributions for all the samples. Note that the value of d is the same in all cases; in other words, the yields could be fitted by adjusting only the value of c.

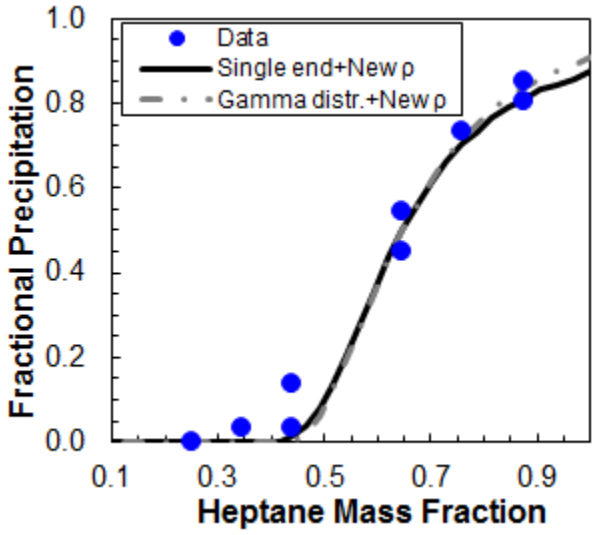

Figure 6.25. Fractional precipitation of Athabasca asphaltenes from solutions of *n*-heptane and toluene at 23°C using the new density correlation and optimum c values.

Table 6.13. Fitting parameters used to calculate the solubility parameter using the new density correlations.

Sample	Gamma Distribution		Single-end Distribution	
	c	***d***	***c***	***d***
Athabasca	0.647	0.0495	0.636	0.0495
Arabian	0.644	0.0495	0.639	0.0495
Cliffdale	0.634	0.0495	0.621	0.0495
Peace River	0.664	0.0495	0.651	0.0495
27-168-178	0.636	0.0495	0.622	0.0495
27034-87	0.672	0.0495	0.658	0.0495
27034-113	0.663	0.0495	0.651	0.0495
26845	0.668	0.0495	0.658	0.0495

Table 6.13 shows that values of *c* fall into two categories: 1) a lower set of values for the native streams including Athabasca, Arabian, and Cliffdale; 2) a higher set of values for the reacted streams including 27034-87, 27034-113 and 26845. The Peace River asphaltenes fell into the reacted stream category, consistent with previous observations. The 27-168-178 asphaltenes fell into the native stream category. Recall that no information was provided on the reaction history of this stream and it is possible that there was little or no chemical change in these asphaltenes. The following average values were determined for each category:

Native crudes	Gamma distribution	$c = 0.643$
	Single-end distribution	$c = 0.632$
Reacted streams	Gamma distribution	$c = 0.665$
	Single-end distribution	$c = 0.651$

The model results are compared with data for each sample in Figures 6.26 through 6.33. The AAD is less than 0.08 in all cases compared with an AAD less than 0.05 for the best fit case modeled with the parameters from Table 6.13. Hence, the average parameters

appear to be a reasonable approximation as long as it is known if the sample has been reacted or not.

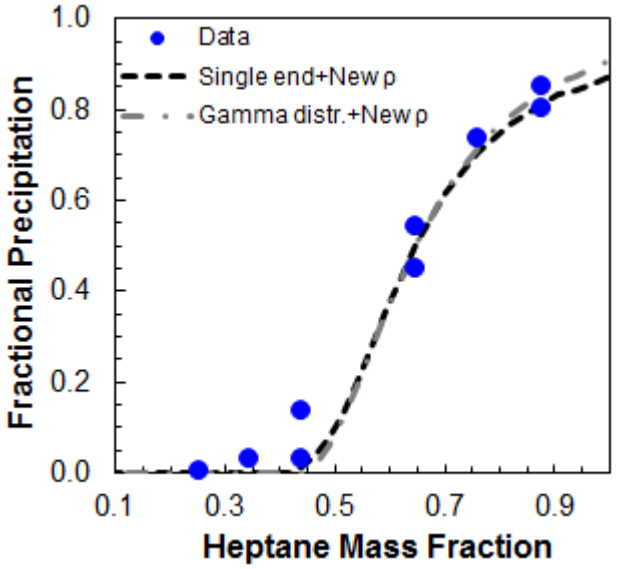

Figure 6.26. Model predictions for the fractional precipitation of Athabasca asphaltenes from solutions of *n*-heptane and toluene at 23°C using the generalized c parameters (single-end: c =0.632; Gamma: c =0.643).

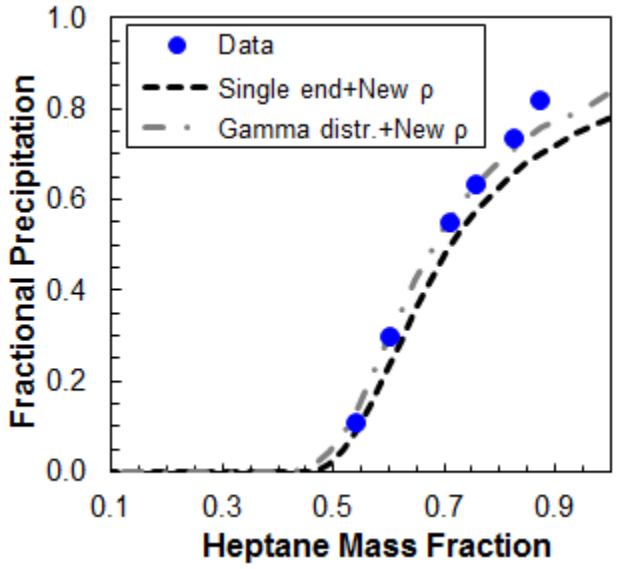

Figure 6.27. Model predictions for the fractional precipitation of Arabian asphaltenes from solutions of *n*-heptane and toluene at 23°C using the generalized c parameters (single-end: c =0.632; Gamma: c =0.643).

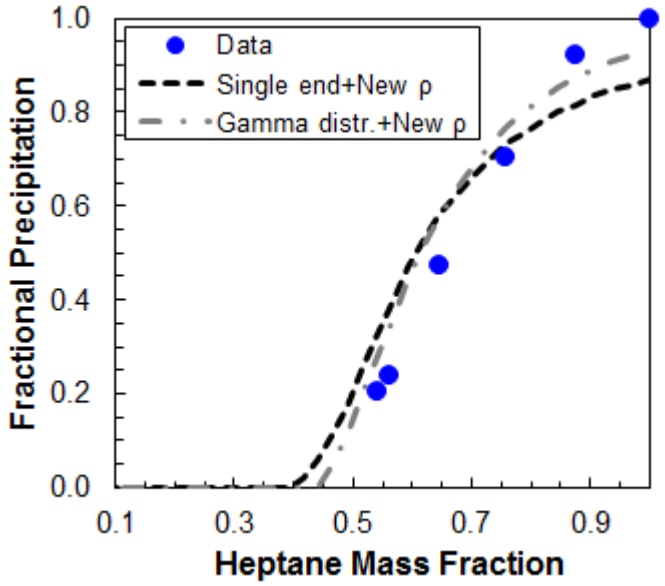

Figure 6.28. Model predictions for the fractional precipitation of Cliffdale asphaltenes from solutions of *n*-heptane and toluene at 23°C using the generalized c parameters (single-end: c =0.632; Gamma: c =0.643).

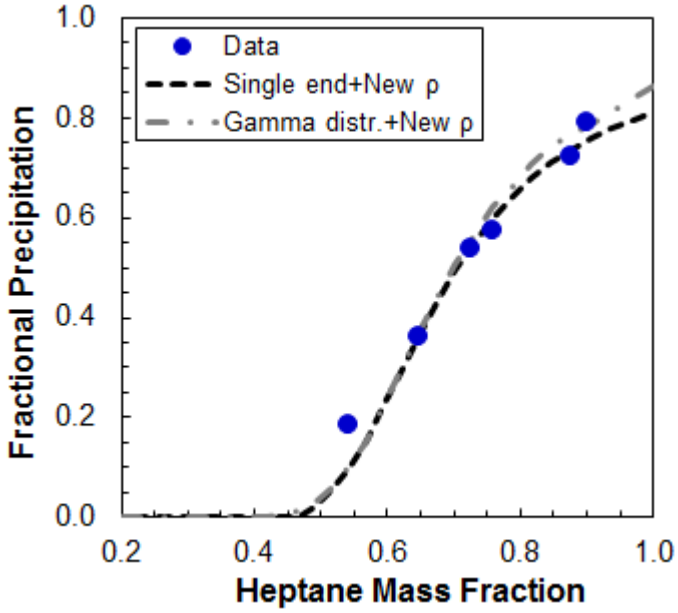

Figure 6.29. Model predictions for the fractional precipitation of Peace River asphaltenes from solutions of *n*-heptane and toluene at 23°C using the generalized c parameters (single-end: c =0.651; Gamma: c =0.665).

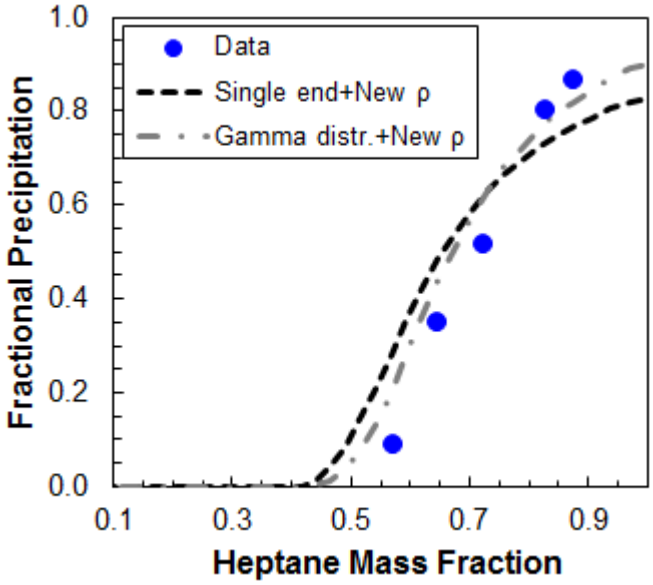

Figure 6.30. Model predictions for the fractional precipitation of 27-168-178 asphaltenes from solutions of *n*-heptane and toluene at 23°C using the generalized c parameters (single-end: c =0.632; Gamma: c =0.643).

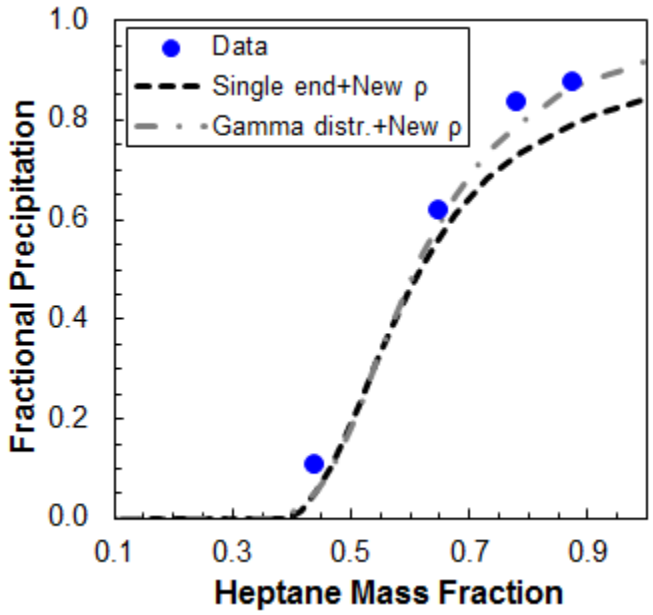

Figure 6.31. Model predictions for the fractional precipitation of 27034-87 asphaltenes from solutions of *n*-heptane and toluene at 23°C using the generalized c parameters (single-end: c =0.651; Gamma: c =0.665).

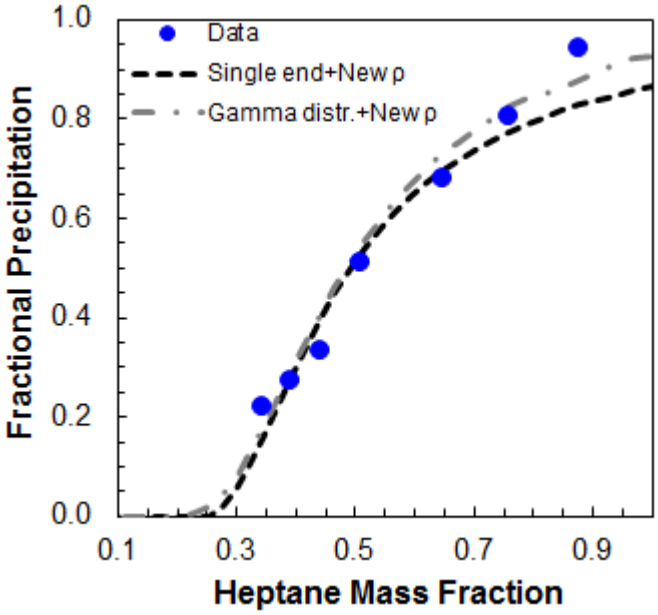

Figure 6.32. Model predictions for the fractional precipitation of 27034-113 asphaltenes from solutions of n-heptane and toluene at 23°C using the generalized c parameters (single-end: c =0.651; Gamma: c =0.665).

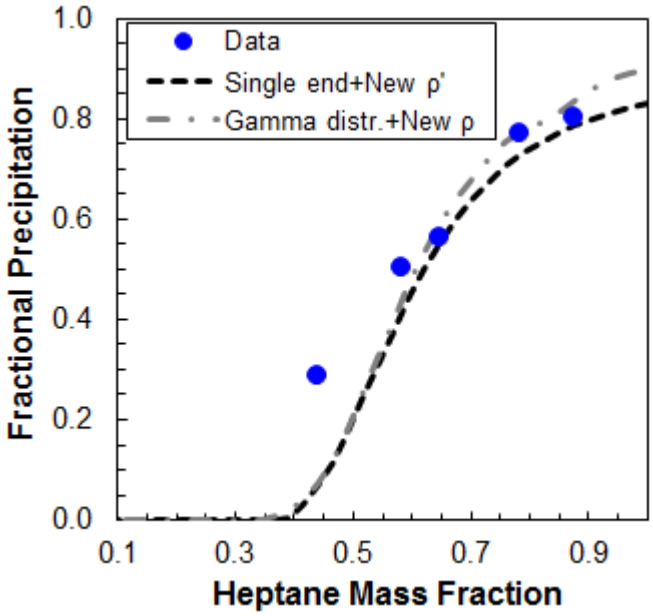

Figure 6.33. Model predictions for the fractional precipitation of 26845 asphaltenes from solutions of *n*-heptane and toluene at 23°C using the generalized c parameters (single-end: c =0.651; Gamma: c =0.665).

Figures 6.26 to 6.33 show that the model with a Gamma distribution can fit the entire yield curve with small deviation. When the Single-end termination model is used, the precipitation yield at high concentrations of *n*-heptane was under-predicted. It is the most soluble material that affects this part of the yield curve. It is possible that the solubility parameter distribution of the neutrals must be accounted for. The Gamma distribution may compensate for this error because the shape of the distribution was adjusted to fit the data.

The use of specific property distributions for each sample improved the model, particularly for the reacted samples, because the use of an additional parameter A' was not required. The effect of reacting the streams also became more apparent with distinct solubility parameter correlations for reacted and native samples. Interestingly, the Peace River sample, which was suspected to have undergone some chemical alteration, required the reacted stream parameters to model the yield data. The SAGD process may modify asphaltene properties. Overall, the results demonstrate that the regular solution approach can be extended to asphaltenes from reacted streams, although it may be necessary to measure the density distribution or at least the average density of the asphaltenes.

Chapter 7: Conclusions and Recommendations

Properties such as molecular weight and density were measured for nine different native and reacted asphaltene samples, and their respective fractions. Property distributions were established and used as inputs into a previously developed regular solution model. One sample, the Gippsland oil, was eliminated from further consideration because the precipitate from this oil appeared to include a significant amount of wax.

Experimental Conclusions

In almost every case, the apparent molecular weight increased as asphaltene concentration increased. This trend is characteristic of a self-association. The increase was most significant for the heavier, least soluble fractions. On the other hand, the molecular weight for light fractions was approximately constant indicating that these cuts contained little or no self-associating components. It appears that the largest aggregates are the least soluble part of the asphaltenes. It also appears that asphaltenes contains some non-associating "neutral" species that are among the most soluble components in the asphaltenes.

In every case, the density increased sharply from the most soluble asphaltenes to intermediate cuts but changed little from the intermediate cuts to the least soluble cuts. It is likely that self-association forces properties like density towards an average value. Hence, density increases through the neutral asphaltenes just as it does through the aromatic/resin continuum but becomes almost constant through the aggregated asphaltenes. The amount of neutral material in each fraction is in qualitative agreement with the molecular weight data.

The property differences between the native and reacted asphaltenes were relatively small. The molecular weight distributions of the reacted samples were not significantly different than the distributions of native samples. The density of the reacted samples (average of 1200 kg/m^3) was higher than the native asphaltenes (average of 1180 kg/m^3). The reacted samples appeared to have less neutral asphaltenes (average of 10 wt%) than

the native samples (average of 18 wt%). These differences confirm that the reactions have altered the properties of the asphaltenes but more details on the reaction history are required to warrant further investigation.

The densities of the cuts from each asphaltene sample were correlated to molecular weight. The shape of the correlation was different than the previously established correlation used in regular solution modeling of asphaltene precipitation. Therefore, the correlations used in this model were updated.

Modeling Conclusions

Self-association phenomena observed for asphaltenes were included into the molecular weight distribution by using the Single-end Termination model. This model required some minor changes in order to include the non-associating "neutral" material present in asphaltenes. The model successfully fit the molecular weight data for the light and heavy fractions, and the whole asphaltenes for each sample. The molecular weight distribution for the whole asphaltenes was reconstructed from a mass balance of the monomer material in the heavy and light fractions, which was then input into the model. This very simple model was able to capture all of the observed self-association behaviour of the asphaltenes.

The asphaltene molecular weight distribution for each sample was determined as an output of the Single-end termination model. It was observed that there are slight differences between the calculated distribution and the Gamma distribution, previously used to represent the asphaltene molecular weight distribution. The Single-end distribution has a higher concentration of material with low molecular weight and is wider than the Gamma distribution.

The Modified Regular Solution model was used to predict asphaltene fractional precipitation in solutions of *n*-heptane and toluene at 23°C. The previously developed model predicted the yields of native asphaltenes without any modifications. However, some modifications were required for its use with reacted streams. The model was first

adapted to use the measured density distributions and a new solubility parameter correlation was developed. A single correlation was sufficient to model the yields from the native crude oils. The solubility parameter of the reacted asphaltenes appeared to be altered by the reaction and a different correlation was required. Interestingly, the same correlation was found to be adequate for all of the reacted asphaltene samples.

The predictions from the Modified Regular Solution model were found to be sensitive to the shape of the asphaltene molecular weight distribution and a different set of solubility correlation parameters were required when using the Gamma versus the Single-end molecular weight distributions. The model fit the onset of asphaltene precipitation well with either distribution; however, the Gamma distribution predicted the yields at high *n*-heptane content with slightly more accuracy than the single-end distribution. Nevertheless, both cases provided acceptable fits of asphaltene onsets and yields. The Single-end distribution has a better experimental basis but is difficult to determine in practice. Therefore, when using the regular solution modeling approach, it is necessary to fix the type of molecular weight distribution to be used as an input and then select the appropriate solubility parameter correlation. Overall, it was demonstrated that the regular solution modeling approach could be extended to reacted asphaltenes.

Recommendations

When determining the density of asphaltene cuts, it was assumed that asphaltenes and toluene formed regular solutions; that is, there was no excess volume of mixing. Density data for maltene fractions indicated that there may be non-zero excess volumes and therefore interaction parameters should be included in the density calculations. However, the excess volumes cannot be established for asphaltenes because the density cannot be measured at sufficiently high concentrations due to the low solubility of asphaltenes in toluene. It is recommended to evaluate the excess volumes of maltene fractions and the most soluble asphaltenes to establish a trend in the excess volumes that could be used to estimate excess volumes for the less soluble asphaltenes. A similar methodology could be used to establish if there are non-idealities in the molecular weight measurements and then to compensate for any non-ideal behaviour.

The yield curves predicted with the regular solution model with the Single-end distribution under-predicted the yields at high *n*-heptane content. A power-law relationship between the solubility parameter and the molecular weight of the asphaltene aggregates was assumed. It is recommended to test different functional forms for the solubility parameter correlation to improve the fit to the yield data.

The Single-end Termination model could be improved by introducing an association constant that is a function of the size of the aggregates, nature of the monomers, or other parameters. For example, the asphaltene molecules could be represented as species with two reaction sites. A distribution of reaction constants could be assigned to these sites using a Monte Carlo approach. Species with two sites with low reaction constants would be "neutrals", those with two sites with high reaction constants would be "propagators" and so on. Self-association could be then modeled with a collision simulation applied to a finite number of species.

There was insufficient data on the reaction history of the asphaltenes to relate property changes to reaction conditions. It is recommended to obtain samples with a known history and that have undergone more severe reaction conditions. Such samples would allow a more rigorous testing and development of the solubility parameter correlations. It may then also be possible to correlate the solubility parameter to reaction indicators such as the H/C ratio.

References

Agrawala, M. *Measurement and Modeling of Asphaltene Association*. Department of Chemical and Petroleum Engineering. University of Calgary. Calgary, Canada. 2001.

Agrawala, M.; Yarranton, H. W. *An Asphaltene Association Model Analogous to Linear Polymerization.* Industrial and Engineering Chemistry Research. 40, 4664-4672, 2001.

Akbarzadeh, K.; Dhillon, A.; Svrcek, W. Y.; Yarranton, H. W. *Methodology for the Characterization and Modeling of Asphaltene Precipitation from Heavy Oils Diluted with n-Alkanes.* Energy and Fuels. 18, 1434-1441, 2004.

Akbarzadeh, K.; Alboudwarej, H.; Svrcek, W. Y.; Yarranton, H. W. *A Generalized Regular Solution Model for Asphaltene Precipitation from n-Alkane Diluted Heavy Oils and Bitumens.* Fluid Phase Equilibria. 232, 159-170, 2005.

Alboudwarej, H.; Akbarzadeh, K.; Beck, I.; Svrcek, W. Y.; Yarranton, H. W. *Regular Solution Model for Asphaltene Precipitation from Bitumens and Solvents.* AIChE Journal. 49 (11), 2948-2956, 2003.

Altgelt, K. H.; Boduszynski, M. M. *Composition and Analysis of Heavy Petroleum Fractions*. Marcel Dekker, Inc. New York, New York. 1994.

Ancheyta, J.; Trejo, F.; Rana, M. S. *Asphaltenes: Chemical Transformation during Hydroprocessing of Heavy Oils.* CRC Press Taylor and Francis Group. Boca Raton, Florida. 2009.

Andersen, S. I. *Association of Petroleum Asphaltenes and the Effect on Solution Properties.* Handbook of Surface and Colloid Chemistry, Third Edition. Birdi, K. S. Ed. CRC Press Taylor and Francis Group. Boca Raton, Florida. 2008.

Andersen, S. I.; Speight, J. G. *Thermodynamic Models for Asphaltene Solubility and Precipitation.* Journal of Petroleum Science and Engineering. 22, 53-66, 1999.

Bazyleva, A.; Fulem, M.; Becerra, M.; Zhao, B.; Shaw, J. M. *Phase Behavior of Athabasca Bitumen.* Journal of Chemical and Engineering Data. 56, 3242-3253, 2011.

Buch, L.; Groenzin, H.; Buenrostro-Gonzalez, E.; Andersen, S. I.; Lira-Galeana, C.; Mullins, O. C. *Molecular Size of Asphaltene Fractions Obtained from Residuum Hydrotreatment*. Fuel. 82, 1075-1084, 2003.

Fan, T.; Buckley, J. S. *Rapid and Accurate SARA Analysis of Medium Gravity Crude Oils.* Energy and Fuels. 16, 1571-1575, 2002.

Flory, P. J. *Principles of Polymer Chemistry.* Cornel University Press. Ithaca, New York. 1953.

Fossen, M.; Sjoblom, J.; Kallevik, H.; Jakobsson, J. *A New Procedure for Direct Precipitation and Fractionation of Asphaltenes from Crude Oil.* Journal of Dispersion Science and Technology. 28, 193-197, 2007.

Fox, W. A. *Effect of Resins on Asphaltene Self-Association and Solubility*. Department of Chemical and Petroleum Engineering. University of Calgary. Calgary, Canada. 2007.

Friberg, S. E. *Micellization.* Asphaltenes, Heavy Oils and Petroleochemics. Mullins, O.C.; Sheu, E.Y.; Hammami, A.; Marshall, A.G. Eds. Springer. 2007.

Fussell, L. T. *A Technique for Calculating Multiphase Equilibria.* SPE Journal. 203-208. 1979.

Groenzis, H.; Mullins, O. C. *Asphaltene Molecular Size and Weight by Time-Resolved Fluorescence Depolarization.* Asphaltenes, Heavy Oils and

Petroleochemics. Mullins, O.C.; Sheu, E.Y.; Hammami, A.; Marshall, A.G. Eds. Springer. 2007.

Gupta, A. K. *A model for asphaltene flocculation using an equation of state.* Department of Chemical and Petroleum Engineering. University of Calgary. Calgary, Canada. 1986.

Hammami, A.; Ratulowski, J. *Precipitation and Deposition of Asphaltenes in Production Systems: A Flow Assurance Overview.* Asphaltenes, Heavy Oils and Petroleochemics. Mullins, O.C.; Sheu, E.Y.; Hammami, A.; Marshall, A.G. Eds. Springer. 2007.

Hildebrand, J. H.; Scott, R. L. *The Solubility of Non-Electrolytes.* Third Edition. Reinhold Publishing Corp. New York. 1949.

Hildebrand, J. H.; Scott, R. L. *Regular Solutions.* Prentice Hall. Englewood Cliffs, New Jersey. 1962.

Hirschberg, A.; DeJong, L. N. J.; Schipper, B. A.; Meijer, J. G. *Influence of Temperature and Pressure on Asphaltene Flocculation.* SPE Journal. 283-293, 1984.

Huggins, M. L. *Solutions of Long Chain Compounds.* The Journal of Chemical Physics. 9 (5), 440, 1941.

Kaminski, T. J.; Fogler, H. S.; Wolf, N.; Wattana, P.; Mairal, A. *Classification of Asphaltenes via Fractionation and the Effect of Heteroatom Content on Dissolution Kinetics.* Energy and Fuels. 14, 25-30, 2000.

Kawanaka, S.; Park, S.J.; Mansoori, G.A. *Organic Deposition from Reservoir Fluids: A Thermodynamic Predictive Technique.* SPE Reservoir Engineering. 185-192, 1991.

Kuznicki, T.; Masliyah J. H.; Bhattacharjee, S. *Molecular Dynamics Study of Model Molecules Resembling Asphaltene-like Structures in Aqueous Organic Solvent Systems.* Energy and Fuels. 22, 2379-2389, 2008.

Larsen, J. W.; Shang, L. *Determination of Bitumen Molecular Weight Distributions Using ^{252}Cf Plasma Desorption Mass Spectrometry*. Energy and Fuels. 9, 760-764, 1995.

Leontaritis, K. J. *Asphaltene Deposition: A Comprehensive Description of Problem Manifestations and Modeling Approaches.* SPE Production Operations Symposium. Oklahoma City, Oklahoma. SPE 18892, March 1989.

Leontaritis, K. J.; Mansoori, G. A. *Asphaltene Flocculation During Oil Production and Processing: A Thermodynamic Colloidal Model.* SPE International Symposium on Oilfield Chemistry. San Antonio, Texas. SPE 16258, January 1987.

Li, Z.; Firoozabadi, A. *Modeling Asphaltene Precipitation by n-Alkanes from Heavy Oils and Bitumens Using Cubic-Plus-Association Equation of State.* Energy and Fuels. 24, 1106-1113, 2010.

Martin, R. B. *Comparisons of Indefinite Self-Association Models.* Chemical Reviews. 3043-3064, 1996.

Maruska, H. P.; Rao, B. M. L. *The Role of Polar Species in the Aggregation of Asphaltenes.* Fuel Science & Technology International. 5, 119, 1987.

McLean, J. D.; Kilpatrick, P. K. *Effects of Asphaltene Solvency on Stability of Water-in-Crude-Oil Emulsions.* Journal of Colloid and Interface Science. 189, 242–253, 1997.

Merino-Garcia, D.; Murgich, J.; Andersen, S. I. *Asphaltene Self-Association: Modeling and Effect of Fractionation with a Polar Solvent.* Petroleum Science and technology. 22 (7, 8), 735–758, 2004.

Merino-Garcia, D.; Andersen, S. I. *Application of Isothermal Titration Calorimetry in the Investigation of Asphaltene Association.* Asphaltenes, Heavy Oils and Petroleochemics. Mullins, O.C.; Sheu, E.Y.; Hammami, A.; Marshall, A.G. Eds. Springer. 2007.

Mitchell, D.L.; Speight, J.G. *The solubility of asphaltenes in hydrocarbon solvents.* Fuel. 52, 149-152, 1973.

Moschopedis, S. E.; Fryer, J. F.; Speight, J. G. *Investigation of Asphaltene Molecular Weights.* Fuel. 55, 227-232, 1976.

Moschopedis, S. E.; Speight, J. G. *Oxygen Functions in Asphaltenes.* Fuel. 55, 334-336, 1976.

Murgich, J.; Merino-Garcia, D.; Andersen, S. I.; del Rio-Garcia, J. M.; Lira-Galeana, C. *Molecular Mechanics and Microcalorimetric Investigations of the Effects of Molecular Water on the Aggregation of Asphaltenes in Solutions.* Langmuir. 18, 9080-9086, 2002.

Peramanu, S.; Pruden, B. B.; Rahimi, P. *Molecular Weight and Specific Gravity Distributions for Athabasca and Cold Lake Bitumens and Their Saturate, Aromatic, Resin, and Asphaltene Fractions*. Industrial and Engineering Chemistry Research. 38, 3121-3130, 1999.

Perry, R. H.; Green, D. *Perry's Chemical Engineers' Handbook.* Seventh Edition. McGraw-Hill. New York. 1997.

Pfeiffer, J. P.; Saal, R. N. J. *Asphaltic Bitumens and Colloid System.* Journal of Physical Chemistry. 44, 139-149, 1940.

Prausnitz, J. M.; Lichtenthaler, R. N.; Azevedo, E. G. D. *Molecular Thermodynamics of Fluid Phase Equilibria.* Third Edition. Prentice Hall PTR. Upper Saddle River, New Jewrsey. 1999.

Ravey, J.C.; Ducouret, G.; Espinat, D. *Asphaltene macrostructure by small angle neutron.* Fuel. 67, 1560-1567, 1988.

Reid, R.C.; Prausnitz, J. M.; Poling, B. E. *The Properties of Gases and Liquids.* Fourth Edition. McGraw-Hill. New York. 1989.

Rogel, E. *Simulation of Interactions in Asphaltene Aggregates*. Energy and Fuels. 14, 567, 2000.

Sabbagh, O.; Akbarzadeh, K.; Badamchi-Zadeh, A.; Svrcek, A. W.; Yarranton, H. W. *Applying the PR-EoS to Asphaltene Precipitation from n-Alkane Diluted Heavy Oils and Bitumens.* Energy and Fuels. 20, 625-634, 2006.

Sanchez, M.C., Personal Communication, Calgary, 2012.

Scott, R. L. *The Thermodynamics of High-Polymer Solutions: II. The Solubility and Fractionation of a Polymer of Heterogeneous Distribution.* The Journal of Chemical Physics. 178-187, 1945.

Scott, R. L.; Magat, M. *The Thermodynamics of High-Polymer Solutions: I. The Free Energy of Mixing of Solvents and Polymers of Heterogeneous Distribution.* The Journal of Chemical Physics. 172-177. 1945.

Sheremata, J. M.; Gray, M. R.; Dettman, H. D.; McCaffrey W. C. *Quantitative Molecular Representation and Sequential Optimization of Athabasca Asphaltenes.* Energy and Fuels. 18, 1377-1384, 2004.

Speight, J. G. *Chemical and Physical Studies of Petroleum Asphaltenes.* Developments in Petroleum Science, Volume 40, Part A, Yen, T.F.; Chilingarian, G.V. Eds. Elsevier. Amsterdam. 7-65. 1994.

Speight, J. G. *Handbook of Petroleum Analysis.* John Wiley & Sons Inc. Hoboken, New Jersey. 2001.

Speight, J. G. *The Chemistry and Technology of Petroleum.* Fourth Edition. CRC Press Taylor & Francis Group. Boca Raton, Florida. 2007.

Speight, J.G.; Moschopedis, S.E. *Chemistry of Asphaltenes.* Advances in Chemistry Series No. 195. Bunger, J.W.; Li, N.C. Eds. American Chemical Society. Washington, DC. 1982.

Spiecker, P. M.; Gawrys, K. L.; Kilpatrick, P. K. *Aggregation and solubility behavior of asphaltenes and their subfractions.* Journal of Colloid and Interface Science. 267, 178-193, 2003.

Strausz, O.P.; Mojelsky, T.W.; Lown, E.M. *The Molecular Structure of Aspha1tene: An Unfolding Story*. Fuel. 71, 1355-1363, 1992.

Ting, P. D.; Hirasaki, G. J.; Chapman, W. G. *Modeling of Asphaltene Phase Behavior with the SAFT Equation of State.* Petroleum Science and Technology. 21, 647-661, 2003.

Tojima, M.; Suhara, S.; Imamura, M.; Furuta, A. *Effect of Heavy Asphaltene on Stability of Residual Oil.* Catalysis Today. 43, 347-351, 1998.

Whitson, C. H. *Characterizing Hydrocarbon Plus Fractions.* SPE Journal. 23 (4), 683-694, 1983.

Wiehe, I. A. *Process Chemistry of Petroleum Macromolecules*. CRC Press Taylor and Francis Group. Boca Raton, Florida. 2008.

Yarranton, H. W.; Masliyah, J. H. *Molar Mass Distribution and Solubility Modeling of Asphaltenes.* AIChE Journal. 42. 3533-3543, 1996.

Yarranton, H. W.; Alboudwarej, H.; Jakher, R. *Investigation of Asphaltene Association with Vapor Pressure osmometry and Interfacial Tension Measurements.* Industrial and Engineering Chemistry Research. 39, 2916-2924, 2000.

Yarranton, H. W.; Fox, W. A.; Svrcek, W. Y. *Effect of Resins on Asphaltene Self-Association and Solubility.* The Canadian Journal of Chemical Engineering. 85, 635-642, 2007.

Yaws, C. L. *Yaws' Handbook of Thermodynamic and Physical Properties of Chemical Compounds.* Knovel. New York. 2003.

Yen, T. F.; Erdman, J. G.; Pollack, S. S. *Investigation of the Structure of Petroleum Asphaltenes by X-Ray Diffraction.* Analytical Chemistry. 33, 1587-1594, 1961.

Appendix A: Data and Error Summary

Tables A.1 to A.8 show the error analyses for the experimental data from the solubility curve. The average of the data, μ, was calculated as follows:

$$\mu = \frac{\sum_{i=1}^{n} y_i}{n} \tag{A.1}$$

where y_i is the experimental value and n is the number of data points.

The standard deviation is calculated as:

$$\sigma = \sqrt{\frac{\sum_{i=1}^{n} (y_i - \mu)^2}{n-1}} \tag{A.2}$$

Tables A.9 to A.16 show the coefficient of determination, R^2, for the density expression as a function of the asphaltene molecular weight. R^2 expresses how well a curve fits the data and is defined as:

$$R^2 = 1 - \frac{SSE}{SST} \tag{A.3}$$

where *SSE* is the residual sum of squares and is defined as:

$$SSE = \sum_{i=1}^{n} (y_i - f(x)_i)^2 \tag{A.4}$$

where $f(x)_i$ is the value from the curve. *SST* is the total sum of squares, and is defined as:

$$SST = \sum_{i=1}^{n} (y_i - \bar{y})^2 \tag{A.5}$$

and $\bar{y}$ is calculated as:

$$\bar{y} = \frac{1}{n} \sum_{i=1}^{n} y_i \tag{A.6}$$

Tables A.17 to A.82 show the average absolute deviation (AAD) between the molecular weight data and the results from the single-end termination model. The AAD is the average of the variability and is defined as:

$$AAD = \frac{1}{n}\sum_{i=1}^{n}\left|y_i^* - y_i\right| \tag{A.7}$$

where y_i^* is the predicted value from the model.

The absolute relative deviation (ARD) for the calculation of the recombined $(T/P)_0$ parameter in the Single-end termination model is shown in Tables A.83 to A.90 and is defined as:

$$ARD = \left|\frac{y_i^* - y_i}{y_i}\right| \tag{A.6}$$

The average absolute deviation is also calculated for the fractional precipitation of asphaltenes calculated using the Regular solution model, and is reported in Tables A.91 to A.106.

The confidence interval and error was calculated in the same way for density, asphaltene solubility, asphaltene fractionation and molecular weight measurements. The following calculation shows the calculation of the confidence using a 90% confidence interval and assuming a normal distribution ($\alpha/2 = 0.05$). The interval is defined as:

$$y - \frac{z\cdot\sigma}{\sqrt{n}} < \mu < y + \frac{z\cdot\sigma}{\sqrt{n}} \tag{A.7}$$

with $z = 1.645$. Table A.107 shows the results of the calculation of the asphaltene solubility interval for Peace River asphaltenes.

Table A.1. Error analysis for Athabasca asphaltene solubility measurements in *n*-heptane/toluene mixtures at 21°C.

Heptol Percentage (v/v)	n	μ (wt/wt)	σ (wt/wt)
40	2	0.032	0.000
50	2	0.136	0.006
60	14	0.422	0.018
70	11	0.544	0.019
80	7	0.735	0.014
90	12	0.851	0.009

Table A.2. Error analysis for Arabian asphaltene solubility measurements in *n*-heptane/toluene mixtures at 21°C.

Heptol Percentage (v/v)	n	μ (wt/wt)	σ (wt/wt)
60	1	0.108	-
66	10	0.296	0.017
76	6	0.547	0.006
80	1	0.631	-
86	10	0.734	0.006
90	1	0.814	-

Table A.3. Error analysis for Cliffdale asphaltene solubility measurements in *n*-heptane/toluene mixtures at 21°C.

Heptol Percentage (v/v)	n	μ (wt/wt)	σ (wt/wt)
60	1	0.206	-
62	10	0.240	0.012
70	7	0.475	0.015
80	11	0.704	0.013
90	1	0.923	-

Table A.4. Error analysis for Peace River asphaltene solubility measurements in *n*-heptane/toluene mixtures at 21°C.

Heptol Percentage (v/v)	n	μ (wt/wt)	σ (wt/wt)
60	8	0.185	0.011
70	2	0.361	0.031
77	14	0.538	0.008
80	2	0.573	0.012
90	2	0.723	0.015
92	9	0.791	0.011

Table A.5. Error analysis for 27-168-178 asphaltene solubility measurements in *n*-heptane/toluene mixtures at 21°C.

Heptol Percentage (v/v)	n	μ (wt/wt)	σ (wt/wt)
63	5	0.091	0.003
70	1	0.352	-
77	8	0.514	0.017
86	11	0.804	0.007
90	1	0.865	-

Table A.6. Error analysis for 27034-87 asphaltene solubility measurements in *n*-heptane/toluene mixtures at 21°C.

Heptol Percentage (v/v)	n	μ (wt/wt)	σ (wt/wt)
50	10	0.108	0.009
70	9	0.620	0.011
82	12	0.837	0.010
90	1	0.877	-

Table A.7. Error analysis for 27034-113 asphaltene solubility measurements in *n*-heptane/toluene mixtures at 21°C.

Heptol Percentage (v/v)	n	μ (wt/wt)	σ (wt/wt)
40	1	0.221	-
45	9	0.271	0.044
50	1	0.332	-
57	6	0.510	0.010
70	6	0.682	0.003
80	1	0.807	-
90	1	0.944	-

Table A.8. Error analysis for 26845 asphaltene solubility measurements in *n*-heptane/toluene mixtures at 21°C.

Heptol Percentage (v/v)	n	μ (wt/wt)	σ (wt/wt)
50	12	0.290	0.290
64	4	0.503	0.503
70	1	0.564	-
82	12	0.772	0.772
90	1	0.802	-

Table A.9. Calculation of R^2 for the curve of Athabasca asphaltene density as a function of molecular weight at 21°C using Equation 5.17.

Fraction	Molecular Weight at 21°C (g/mol)	Asphaltene density (kg/m^3)	Calculated ρ with Equation 5.17 (kg/m^3)
HT90L	1107	1132	1135
HT80L	1548	1142	1143
HT70L	3019	1163	1162
HT60L	3227	1173	1164
Whole	6505	1175	1183
HT90H	9195	1178	1188
HT80H	11460	1191	1191
HT70H	14579	1196	1192
HT60H	17474	1197	1192

$\bar{y}$	1172
SST	4160
SSE	303
R^2	0.927

Table A.10. Calculation of R^2 for the curve of Arabian asphaltene density as a function of molecular weight at 21°C using Equation 5.17.

Fraction	Molecular Weight at 21°C (g/mol)	Asphaltene density (kg/m^3)	Calculated ρ with Equation 5.17 (kg/m^3)
HT86L	2736	1122	1139
HT76L	2980	1172	1149
HT66L	4109	1178	1178
Whole	4852	1180	1188
HT86H	11234	1202	1204
HT76H	15986	1206	1204
HT66H	20307	1209	1204

$\bar{y}$	1181
SST	5365
SSE	936
R^2	0.825

Table A.11. Calculation of R^2 for the curve of Cliffdale asphaltene density as a function of molecular weight at 21°C using Equation 5.17.

Fraction	Molecular Weight at 21°C (g/mol)	Asphaltene density (kg/m^3)	Calculated ρ with Equation 5.17 (kg/m^3)
HT80L	4486	1147	1150
HT70L	4806	1153	1153
HT62L	6451	1174	1167
Whole	8634	1180	1179
HT80H	12912	1182	1190
HT70H	18801	1191	1195
HT62H	27049	1202	1196

$\bar{y}$	1176
SST	2396
SSE	165
R^2	0.825

Table A.12. Calculation of R^2 for the curve of Peace River asphaltene density as a function of molecular weight at 21°C using Equation 5.17.

Fraction	Molecular Weight at 21°C (g/mol)	Asphaltene density (kg/m^3)	Calculated ρ with Equation 5.17 (kg/m^3)
HT92L	989	1078	1078
HT77L	1615	1138	1143
HT60L	1846	1162	1155
Whole	3591	1171	1182
HT92H	8261	1184	1184
HT77H	8568	1187	1184
HT60H	9645	1190	1184

$\bar{y}$	1159
SST	9455
SSE	240
R^2	0.975

Table A.13. Calculation of R^2 for the curve of 27-168-178 asphaltene density as a function of molecular weight at 21°C using Equation 5.17.

Fraction	Molecular Weight at 21°C (g/mol)	Asphaltene density (kg/m^3)	Calculated ρ with Equation 5.17 (kg/m^3)
HT86L	2029	1154	1151
HT77L	2908	1163	1172
HT63L	4052	1194	1190
Whole	5786	1206	1203
HT86H	9029	1208	1211
HT77H	13744	1210	1213
HT63H	28164	1214	1213

$\bar{y}$	1193
SST	3544
SSE	144
R^2	0.959

Table A.14. Calculation of R^2 for the curve of 27034-87 asphaltene density as a function of molecular weight at 21°C using Equation 5.17.

Fraction	Molecular Weight at 21°C (g/mol)	Asphaltene density (kg/m^3)	Calculated ρ with Equation 5.17 (kg/m^3)
HT82L	1969	1145	1146
HT70L	2797	1168	1166
HT50L	3756	1179	1180
Whole	4884	1188	1189
HT82H	11200	1177	1197
HT70H	12160	1191	1197
HT50H	12551	1223	1197

$\bar{y}$	1182
SST	3439
SSE	1144
R^2	0.667

Table A.15. Calculation of R^2 for the curve of 27034-113 asphaltene density as a function of molecular weight at 21°C using Equation 5.17.

Fraction	Molecular Weight at 21°C (g/mol)	Asphaltene density (kg/m^3)	Calculated ρ with Equation 5.17 (kg/m^3)
HT70L	2167	1193	1192
HT57L	2743	1203	1207
HT45L	3968	1226	1228
Whole	4509	1245	1235
HT70H	8397	1250	1259
HT57H	10862	1260	1263
HT45H	17313	1273	1266

$\bar{y}$	1236
SST	5195
SSE	256
R^2	0.951

Table A.16. Calculation of R^2 for the curve of 26845 asphaltene density as a function of molecular weight at 21°C using Equation 5.17.

Fraction	Molecular Weight at 21°C (g/mol)	Asphaltene density (kg/m^3)	Calculated ρ with Equation 5.17 (kg/m^3)
HT82L	1409	1115	1118
HT64L	1751	1172	1164
HT50L	2488	1196	1204
Whole	3733	1205	1216
HT82H	8408	1209	1218
HT64H	9903	1213	1218
HT50H	23152	1246	1218

$\bar{y}$	1194
SST	10075
SSE	1143
R^2	0.887

Table A.17. Advanced average deviation for Whole Athabasca asphaltene molecular weight data using the Single-end termination model. K=55000, $(T/P)_0$=0.235.

Asphaltene Concentration (kg/m^3)	Asphaltene Molecular Weight (g/mol)		AAD
	Experimental	Calculated	
1	1661	3130	1469
2	2451	3724	1273
5	4217	4606	389
10	5261	5263	2
16	5705	5661	43
16	6007	5661	346
16	5832	5661	171
20	6113	5830	283
32	7072	6136	936
32	6734	6136	598
32	6425	6137	289
48	6614	6344	269
48	7422	6344	1078
48	7201	6344	857
60	6808	6438	370
60	8001	6438	1563
		Total AAD	621

Table A.18. Advanced average deviation for HT60L Athabasca asphaltene molecular weight data using the Single-end termination model. K=55000, $(T/P)_0$=0.51.

Asphaltene Concentration (kg/m^3)	Asphaltene Molecular Weight (g/mol)		AAD
	Experimental	Calculated	
1	1485	2479	994
1	1419	2479	1060
2	1756	2791	1035
2	1848	2791	943
5	2266	3165	899
5	2208	3165	957
10	2767	3380	613
10	2570	3380	810
10	2492	3380	888
16	2897	3485	588
16	2699	3485	786
20	2834	3525	691
20	2799	3525	726
20	2962	3525	563
32	3176	3590	414
32	3114	3590	476
48	3493	3628	136
48	3435	3628	193
60	3577	3645	68
60	3529	3645	116
		Total AAD	648

Table A.19. Advanced average deviation for HT60H Athabasca asphaltene molecular weight data using the Single-end termination model. K=55000, $(T/P)_0$=0.0.0005.

Asphaltene Concentration (kg/m^3)	Asphaltene Molecular Weight (g/mol)		AAD
	Experimental	Calculated	
1	5050	4340	710
1	4040	4340	300
2	6184	5679	504
2	6184	5679	504
5	9836	8373	1463
5	11391	8373	3018
10	14428	11424	3004
10	13835	11424	2411
16	15947	14186	1761
16	16160	14186	1974
20	18646	15742	2904
20	18532	15742	2790
32	21498	19644	1854
32	23085	19644	3441
32	22289	19644	2645
48	23960	23822	138
48	23960	23822	138
60	27503	26500	1003
60	24836	26500	1664
60	26158	26500	342
		Total AAD	1629

Table A.20. Advanced average deviation for HT70L Athabasca asphaltene molecular weight data using the Single-end termination model. K=55000, $(T/P)_0$=0.69.

Asphaltene Concentration (kg/m^3)	Asphaltene Molecular Weight (g/mol)		AAD
	Experimental	Calculated	
1	1440	2213	773
1	1859	2213	354
2	1764	2435	670
2	2000	2435	435
5	2409	2677	268
5	2436	2677	241
10	2418	2802	384
10	2465	2802	337
16	2570	2860	289
16	2579	2860	281
20	2615	2881	265
20	2637	2881	244
32	2743	2914	171
32	2818	2914	96
48	3021	2933	88
48	2971	2933	37
60	3108	2941	167
60	3159	2941	218
		Total AAD	295

Table A.21. Advanced average deviation for HT70H Athabasca asphaltene molecular weight data using the Single-end termination model. K=55000, $(T/P)_0$=0.0055.

Asphaltene Concentration (kg/m^3)	Asphaltene Molecular Weight (g/mol)		AAD
	Experimental	Calculated	
1	3500	4314	813
1	4522	4314	209
1	6184	4314	1870
2	4369	5635	1265
2	6379	5635	744
2	4489	5635	1146
5	8707	8276	431
5	8058	8276	218
10	11699	11244	454
10	11882	11244	638
16	14780	13910	871
16	15538	13910	1629
20	16203	15402	801
20	17167	15402	1764
32	20242	19116	1126
32	19124	19116	8
48	22341	23047	707
48	23049	23047	1
60	25110	25544	434
60	22725	25544	2820
		Total AAD	897

Table A.22. Advanced average deviation for HT80L Athabasca asphaltene molecular weight data using the Single-end termination model. K=55000, $(T/P)_0$=1.36.

Asphaltene Concentration (kg/m^3)	Asphaltene Molecular Weight (g/mol)		AAD
	Experimental	Calculated	
1	1165	1680	514
2	995	1768	772
2	1146	1768	622
2.5	1228	1808	580
5	1192	1847	655
5	1025	1847	822
10	1247	1882	635
10.1	1256	1882	626
16	1289	1896	608
20	1284	1901	618
25.3	1391	1905	515
32	1378	1909	531
47.3	1526	1913	387
48	1482	1913	431
60	1525	1915	390
		Total AAD	580

Table A.23. Advanced average deviation for HT80H Athabasca asphaltene molecular weight data using the Single-end termination model. K=55000, $(T/P)_0$=0.043.

Asphaltene Concentration (kg/m^3)	Asphaltene Molecular Weight (g/mol)		AAD
	Experimental	Calculated	
1	2200	4129	1929
1	3935	4129	194
1	4456	4129	327
2	6121	5321	800
2	3373	5321	1947
2	4967	5321	354
5	8101	7605	497
5	6810	7605	795
10	9068	10020	952
10	9469	10020	551
16	13733	12056	1678
16	10113	12056	1942
16	11853	12056	203
20	13963	13143	820
20	14060	13143	917
32	17791	15692	2099
32	16921	15692	1229
48	18180	18158	22
48	17246	18158	911
48	19841	18158	1684
60	21668	19608	2060
60	18426	19608	1182
60	19056	19608	552
		Total AAD	1028

Table A.24. Advanced average deviation for HT90L Athabasca asphaltene molecular weight data using the Single-end termination model. K=55000, $(T/P)_0$=1.82.

Asphaltene Concentration (kg/m^3)	Asphaltene Molecular Weight (g/mol)		AAD
	Experimental	Calculated	
1	841	1431	590
2	876	1481	605
5	931	1525	594
10	896	1542	647
16	976	1550	574
20	1037	1552	515
32	1105	1556	451
48	1224	1558	334
60	1304	1559	255
		Total AAD	507

Table A.25. Advanced average deviation for HT80L Athabasca asphaltene molecular weight data using the Single-end termination model. K=55000, $(T/P)_0$=0.135.

Asphaltene Concentration (kg/m^3)	Asphaltene Molecular Weight (g/mol)		AAD
	Experimental	Calculated	
1	3835	3740	96
2	4095	4675	581
5	5590	6293	703
5	5761	6293	532
10	7572	7765	193
10	7301	7765	464
16	8895	8829	66
20	9727	9336	391
20	10562	9336	1226
32	9542	10370	829
32	11515	10370	1145
48	12669	11189	1480
48	10474	11189	715
60	13909	11598	2311
60	11284	11598	315
		Total AAD	736

Table A.26. Summary of AAD for Athabasca asphaltene molecular weight. Results obtained using the single-end termination model with parameters showed in Tables A.17 to A.25.

Fraction	AAD (g/mol)
HT90L	507
HT80L	580
HT70L	295
HT60L	648
Whole	621
HT90H	736
HT80H	1028
HT70H	897
HT60H	1629
AAD	771

Table A.27. Advanced average deviation for whole Arabian asphaltene molecular weight data using the Single-end termination model. K=55000, $(T/P)_0$=0.592.

Asphaltene Concentration (kg/m^3)	Asphaltene Molecular Weight (g/mol)		AAD
	Experimental	Calculated	
1	3063	2845	218
1	3522	2845	677
2	3636	3214	422
5	4026	3662	364
5	3660	3662	2
10	3844	3919	75
10	4003	3919	83
20	4072	4093	21
20	3938	4093	155
40	3914	4198	284
40	4200	4198	2
60	4240	4236	4
60	4180	4236	56
		Total AAD	182

Table A.28. Advanced average deviation for HT66L Arabian asphaltene molecular weight data using the Single-end termination model. K=55000, $(T/P)_0$=0.69.

Asphaltene Concentration (kg/m^3)	Asphaltene Molecular Weight (g/mol)		AAD
	Experimental	Calculated	
1	2172	2682	511
1	2721	2682	38
2	2553	2989	436
2	3247	2989	258
10	3725	3537	188
20	3934	3662	272
20	3703	3662	41
40	3802	3735	67
40	3804	3735	69
60	3925	3761	164
60	3934	3761	173
		Total AAD	201

Table A.29. Advanced average deviation for HT66H Arabian asphaltene molecular weight data using the Single-end termination model. K=55000, $(T/P)_0$=0.0052.

Asphaltene Concentration (kg/m^3)	Asphaltene Molecular Weight (g/mol)		AAD
	Experimental	Calculated	
1	10612	4586	6026
2	10215	4586	5629
3	14030	7031	6999
3	11144	7031	4113
6	12819	9444	3375
6	11518	9444	2074
12	16423	12845	3577
24	20189	17611	2579
24	18503	17611	893
47	23949	24008	58
49	22581	24475	1894
		Total AAD	3383

Table A.30. Advanced average deviation for HT76L Arabian asphaltene molecular weight data using the Single-end termination model. K=55000, $(T/P)_0$=1.37.

Asphaltene Concentration (kg/m^3)	Asphaltene Molecular Weight (g/mol)		AAD
	Experimental	Calculated	
1	1264	2126	862
1	1264	2126	862
2	1672	2261	588
2	1610	2261	651
5	1871	2388	517
10	2184	2445	261
20	2425	2478	53
40	2505	2496	9
40	2767	2496	271
60	2766	2502	264
60	2847	2502	345
		Total AAD	426

Table A.31. Advanced average deviation for HT76H Arabian asphaltene molecular weight data using the Single-end termination model. K=55000, $(T/P)_0$=0.024.

Asphaltene Concentration (kg/m^3)	Asphaltene Molecular Weight (g/mol)		AAD
	Experimental	Calculated	
1	6873	4495	2378
5	13168	8387	4780
5	11007	8387	2620
10	13106	11210	1897
10	12751	11210	1541
20	16479	15027	1452
20	15232	15027	205
40	18600	20074	1474
40	20164	20074	90
60	21986	23678	1692
60	23614	23678	64
		Total AAD	1654

Table A.32. Advanced average deviation for HT86L Arabian asphaltene molecular weight data using the Single-end termination model. K=55000, $(T/P)_0$=2.4.

Asphaltene Concentration (kg/m^3)	Asphaltene Molecular Weight (g/mol)		AAD
	Experimental	Calculated	
1	1491	1766	275
1	1623	1766	142
2	1824	1828	4
2	1708	1828	120
5	2033	1880	153
5	2174	1880	294
10	2179	1901	278
10	2245	1901	344
20	2129	1913	216
20	2031	1913	118
40	2149	1919	230
40	2178	1919	259
60	2117	1921	196
60	2185	1921	263
		Total AAD	207

Table A.33. Advanced average deviation for HT86H Arabian asphaltene molecular weight data using the Single-end termination model. K=55000, $(T/P)_0$=0.14.

Asphaltene Concentration (kg/m^3)	Asphaltene Molecular Weight (g/mol)		AAD
	Experimental	Calculated	
1	2846	4015	1169
2	5693	5002	691
5	7699	6722	977
10	8387	8301	86
10	9784	8301	1484
20	10797	10002	794
20	9362	10002	641
40	10735	11643	909
40	11656	11643	13
60	11138	12494	1356
60	12665	12494	171
		Total AAD	754

Table A.34. Summary of AAD for Arabian asphaltene molecular weight. Results obtained using the single-end termination model with parameters showed in Tables A.27 to A.33.

Fraction	AAD (g/mol)
HT86L	207
HT76L	426
HT66L	201
Whole	182
HT86H	754
HT76H	1654
HT66H	3383
AAD	972

Table A.35. Advanced average deviation for whole Cliffdale asphaltene molecular weight data using the Single-end termination model. K=55000, $(T/P)_0$=0.135.

Asphaltene Concentration (kg/m^3)	Asphaltene Molecular Weight (g/mol)		AAD
	Experimental	Calculated	
1	1500	3689	2189
1	2726	3689	963
2	2899	4490	1591
5	4922	5806	884
5	5231	5806	575
10	6869	6935	66
10	7095	6935	160
20	7962	8077	115
20	9477	8077	1400
40	9725	9115	610
40	10661	9115	1546
60	10896	9631	1265
60	11141	9631	1510
		Total AAD	990

Table A.36. Advanced average deviation for HT62L Cliffdale asphaltene molecular weight data using the Single-end termination model. K=55000, $(T/P)_0$=0.205.

Asphaltene Concentration (kg/m^3)	Asphaltene Molecular Weight (g/mol)		AAD
	Experimental	Calculated	
1	2497	3453	956
1	2842	3453	611
2	3745	4113	368
2	3265	4113	848
10	5546	5915	369
20	6296	6634	338
20	5729	6634	905
40	6958	7212	254
40	7128	7212	84
60	7950	7470	480
60	7617	7470	147
		Total AAD	487

Table A.37. Advanced average deviation for HT62H Cliffdale asphaltene molecular weight data using the Single-end termination model. K=55000, $(T/P)_0$=0.0001.

Asphaltene Concentration (kg/m^3)	Asphaltene Molecular Weight (g/mol)		AAD
	Experimental	Calculated	
1	8277	4463	3814
1	9078	4463	4615
2	8857	5827	3030
6	16505	9287	7218
12	21875	12699	9176
24	31714	17531	14183
47	38081	24114	13967
49	36586	24599	11987
		Total AAD	8499

Table A.38. Advanced average deviation for HT70L Cliffdale asphaltene molecular weight data using the Single-end termination model. K=55000, $(T/P)_0$=0.33.

Asphaltene Concentration (kg/m^3)	Asphaltene Molecular Weight (g/mol)		AAD
	Experimental	Calculated	
1	1718	3120	1402
1	2599	3120	521
2	3163	3601	438
2	2599	3601	1002
5	3607	4267	660
10	3960	4723	763
20	4764	5084	320
40	5124	5334	210
40	4926	5334	408
60	5534	5435	99
60	5672	5435	237
		Total AAD	551

Table A.39. Advanced average deviation for HT70H Cliffdale asphaltene molecular weight data using the Single-end termination model. K=55000, $(T/P)_0$=0.0001.

Asphaltene Concentration (kg/m^3)	Asphaltene Molecular Weight (g/mol)		AAD
	Experimental	Calculated	
1	2234	4463	2229
5	10791	8571	2220
5	10611	8571	2040
10	15341	11683	3658
10	15068	11683	3385
20	24844	16093	8751
20	23256	16093	7163
40	33819	22329	11490
40	31151	22329	8822
60	37783	27102	10681
60	38780	27102	11678
		Total AAD	6556

Table A.40. Advanced average deviation for HT80L Cliffdale asphaltene molecular weight data using the Single-end termination model. K=55000, $(T/P)_0$=0.56.

Asphaltene Concentration (kg/m^3)	Asphaltene Molecular Weight (g/mol)		AAD
	Experimental	Calculated	
1	2500	2666	166
1	2681	2666	15
2	3042	2949	93
2	2974	2949	25
5	3361	3293	68
5	3089	3293	204
10	3493	3492	1
10	3762	3492	270
20	3628	3629	1
20	3832	3629	203
40	4020	3712	308
40	4170	3712	458
60	4368	3743	625
60	4263	3743	520
		Total AAD	211

Table A.41. Advanced average deviation for HT80H Cliffdale asphaltene molecular weight data using the Single-end termination model. K=55000, $(T/P)_0$=0.02.

Asphaltene Concentration (kg/m^3)	Asphaltene Molecular Weight (g/mol)		AAD
	Experimental	Calculated	
1	3046	4380	1334
2	3460	5677	2217
5	7318	8232	914
10	9095	11041	1946
10	11790	11041	749
20	16536	14866	1670
20	13691	14866	1175
40	18387	19974	1587
40	21896	19974	1922
60	23911	23661	250
60	22016	23661	1645
		Total AAD	1401

Table A.42. Summary of AAD for Cliffdale asphaltene molecular weight. Results obtained using the single-end termination model with parameters showed in Tables A.35 to A.41.

Fraction	AAD (g/mol)
HT80L	211
HT70L	551
HT62L	487
Whole	990
HT80H	1401
HT70H	6556
HT62H	8499
AAD	2671

Table A.43. Advanced average deviation for Whole Peace River asphaltene molecular weight data using the Single-end termination model. K=55000, $(T/P)_0$=0.26.

Asphaltene Concentration (kg/m^3)	Asphaltene Molecular Weight (g/mol)		AAD
	Experimental	Calculated	
1	1894	1913	19
1	1174	1913	739
2	1843	2243	401
2	1902	2243	342
5	2474	2676	202
5	2993	2676	318
10	3016	2951	64
10	2793	2951	158
16	3797	3098	699
20	3707	3156	551
20	3173	3156	18
20	3484	3156	328
32	3638	3253	385
40	3627	3289	337
48	4093	3315	779
60	3953	3341	612
60	4105	3341	765
		Total AAD	395

Table A.44. Advanced average deviation for HT60L Peace River asphaltene molecular weight data using the Single-end termination model. K=55000, $(T/P)_0$=0.38.

Asphaltene Concentration (kg/m^3)	Asphaltene Molecular Weight (g/mol)		AAD
	Experimental	Calculated	
1	1443	1720	277
2	1313	1958	645
2	1372	1958	586
5	1603	2235	632
5	1595	2235	640
10	1368	2389	1021
10	1617	2389	772
20	1798	2492	693
20	1647	2492	845
40	1718	2553	834
40	1921	2553	632
60	2047	2575	528
60	1986	2575	589
		Total AAD	669

Table A.45. Advanced average deviation for HT60H Peace River asphaltene molecular weight data using the Single-end termination model. K=55000, $(T/P)_0$=0.045.

Asphaltene Concentration (kg/m^3)	Asphaltene Molecular Weight (g/mol)		AAD
	Experimental	Calculated	
1	2416	2654	239
1	3110	2654	456
2	3372	3468	96
2	2825	3468	643
5	4250	4981	732
6	3323	5351	2028
10	3894	6522	2628
12	4102	6989	2887
20	8083	8427	344
30	11835	9694	2141
60	12275	12027	247
		Total AAD	1131

Table A.46. Advanced average deviation for HT77L Peace River asphaltene molecular weight data using the Single-end termination model. K=55000, $(T/P)_0$=0.76.

Asphaltene Concentration (kg/m^3)	Asphaltene Molecular Weight (g/mol)		AAD
	Experimental	Calculated	
1	1122	1342	219
1	1110	1342	232
2	1155	1445	289
2	1200	1445	244
5	1299	1541	242
6	1241	1555	314
10	1385	1585	200
12	1227	1593	366
20	1483	1610	127
25	1368	1615	247
40	1702	1623	79
49	1603	1626	23
60	1711	1628	84
74	1685	1630	56
		Total AAD	194

Table A.47. Advanced average deviation for HT77H Peace River asphaltene molecular weight data using the Single-end termination model. K=55000, $(T/P)_0$=0.057.

Asphaltene Concentration (kg/m^3)	Asphaltene Molecular Weight (g/mol)		AAD
	Experimental	Calculated	
1	3633	2614	1019
1	4047	2614	1433
2	4464	3395	1070
2	2938	3395	457
5	4978	4819	159
5	5389	4819	569
10	7649	6231	1419
10	6208	6231	22
20	7519	7913	394
20	8128	7913	215
40	9238	9773	536
40	9897	9773	124
60	11017	10875	142
60	10650	10875	225
		Total AAD	556

Table A.48. Advanced average deviation for HT92L Peace River asphaltene molecular weight data using the Single-end termination model. K=55000, $(T/P)_0$=4.

Asphaltene Concentration (kg/m^3)	Asphaltene Molecular Weight (g/mol)		AAD
	Experimental	Calculated	
1	753	845	92
2	693	856	163
2	867	856	11
4	795	863	67
5	757	864	107
10	862	867	5
10	738	867	129
20	755	868	113
21	907	868	39
40	848	869	21
42	937	869	67
60	900	869	31
		Total AAD	70

Table A.49. Advanced average deviation for HT92H Peace River asphaltene molecular weight data using the Single-end termination model. K=55000, $(T/P)_0$=0.062.

Asphaltene Concentration (kg/m^3)	Asphaltene Molecular Weight (g/mol)		AAD
	Experimental	Calculated	
1	2298	2597	299
1	3256	2597	659
2	4407	3365	1042
2	4862	3365	1497
5	3977	4755	778
5	6980	4755	2225
10	7293	6115	1178
10	6068	6115	47
20	6664	7713	1049
20	7339	7713	374
40	9579	9444	135
40	9198	9444	246
60	11040	10447	592
60	10299	10447	148
		Total AAD	734

Table A.50. Summary of AAD for Peace River asphaltene molecular weight. Results obtained using the single-end termination model with parameters showed in Tables A.43 to A.49.

Fraction	AAD (g/mol)
HT92L	70
HT77L	194
HT60L	669
Whole	395
HT92H	734
HT77H	556
HT60H	1131
AAD	536

Table A.51. Advanced average deviation for whole 27-168-178 asphaltene molecular weight data using the Single-end termination model. K=55000, $(T/P)_0$=0.418.

Asphaltene Concentration (kg/m^3)	Asphaltene Molecular Weight (g/mol)		AAD
	Experimental	Calculated	
1	3166	2922	244
2	3583	3344	239
2	3730	3344	387
5	4028	3875	153
5	3720	3875	155
10	4679	4196	483
20	5182	4423	759
20	4577	4423	153
40	5029	4565	463
40	5463	4565	897
60	5685	4619	1066
60	5401	4619	783
		Total AAD	482

Table A.52. Advanced average deviation for HT63L 27-168-178 asphaltene molecular weight data using the Single-end termination model. K=55000, $(T/P)_0$=0.532.

Asphaltene Concentration (kg/m^3)	Asphaltene Molecular Weight (g/mol)		AAD
	Experimental	Calculated	
1	1464	2708	1244
1	1918	2708	791
2	2153	3044	892
5	2986	3438	452
10	3277	3656	379
20	3430	3800	371
20	4014	3800	213
40	3857	3886	29
40	3755	3886	131
60	3974	3917	57
60	4211	3917	294
		Total AAD	441

Table A.53. Advanced average deviation for HT63H 27-168-178 asphaltene molecular weight data using the Single-end termination model. K=55000, $(T/P)_0$=0.001.

Asphaltene Concentration (kg/m^3)	Asphaltene Molecular Weight (g/mol)		AAD
	Experimental	Calculated	
1	9219	4742	4477
3	12907	7375	5531
6	13352	9981	3371
11	22776	13135	9642
23	26251	18511	7740
46	25184	25700	516
		Total AAD	5213

Table A.54. Advanced average deviation for HT77L 27-168-178 asphaltene molecular weight data using the Single-end termination model. K=55000, $(T/P)_0$=1.01.

Asphaltene Concentration (kg/m^3)	Asphaltene Molecular Weight (g/mol)		AAD
	Experimental	Calculated	
1	2002	2085	83
1	1918	2085	168
2	1774	2232	458
5	2247	2373	126
5	2308	2373	65
10	2480	2437	43
10	2223	2437	214
20	2312	2474	163
20	2666	2474	192
40	2579	2494	85
40	2533	2494	39
60	2663	2501	162
60	2711	2501	210
		Total AAD	154

Table A.55. Advanced average deviation for HT77H 27-168-178 asphaltene molecular weight data using the Single-end termination model. K=55000, $(T/P)_0$=0.08.

Asphaltene Concentration (kg/m^3)	Asphaltene Molecular Weight (g/mol)		AAD
	Experimental	Calculated	
1	5237	4324	913
2	7073	5513	1560
2	8252	5513	2739
5	9262	7685	1577
10	11115	9831	1284
20	12578	12372	206
20	12267	12372	105
40	15299	15155	144
40	14962	15155	193
60	16689	16787	97
60	15909	16787	878
		Total AAD	882

Table A.56. Advanced average deviation for HT86L 27-168-178 asphaltene molecular weight data using the Single-end termination model. K=55000, $(T/P)_0$=2.2.

Asphaltene Concentration (kg/m^3)	Asphaltene Molecular Weight (g/mol)		AAD
	Experimental	Calculated	
1	1611	1492	119
1	1631	1492	138
2	1543	1535	8
2	1686	1535	151
5	1654	1570	85
5	1539	1570	31
10	1618	1584	35
10	1664	1584	80
20	1743	1591	152
20	1703	1591	112
40	1753	1595	158
40	1725	1595	130
60	1780	1596	184
60	1815	1596	219
		Total AAD	114

Table A.57. Advanced average deviation for HT86H 27-168-178 asphaltene molecular weight data using the Single-end termination model. K=55000, $(T/P)_0$=0.184.

Asphaltene Concentration (kg/m^3)	Asphaltene Molecular Weight (g/mol)		AAD
	Experimental	Calculated	
1	4951	3882	1070
1	4005	3882	123
2	6051	4785	1267
2	5920	4785	1135
5	6423	6250	172
5	5972	6250	279
10	7400	7469	69
10	7204	7469	265
20	8153	8638	484
20	8431	8638	207
40	9223	9615	392
40	9700	9615	85
60	10055	10063	8
60	10250	10063	188
		Total AAD	410

Table A.58. Summary of AAD for 27-168-178 asphaltene molecular weight. Results obtained using the single-end termination model with parameters showed in Tables A.51 to A.57.

Fraction	AAD (g/mol)
HT86L	114
HT77L	154
HT63L	441
Whole	482
HT86H	410
HT77H	882
HT63H	5213
AAD	1099

Table A.59. Advanced average deviation for whole 27034-87 asphaltene molecular weight data using the Single-end termination model. K=55000, $(T/P)_0$=0.293.

Asphaltene Concentration (kg/m^3)	Asphaltene Molecular Weight (g/mol)		AAD
	Experimental	Calculated	
1	2245	2596	352
2	2263	2596	763
5	3458	3591	133
10	4178	3954	225
10	3722	3954	232
16	4343	4148	195
20	4352	4225	127
20	4330	4225	105
32	4909	4354	554
40	4558	4402	156
48	4918	4436	481
60	4661	4471	190
60	4746	4471	275
		Total AAD	291

Table A.60. Advanced average deviation for HT50L 27034-87 asphaltene molecular weight data using the Single-end termination model. K=55000, $(T/P)_0$=0.39.

Asphaltene Concentration (kg/m^3)	Asphaltene Molecular Weight (g/mol)		AAD
	Experimental	Calculated	
1	2111	2398	287
1	2415	2398	17
2	2537	2737	200
5	3050	3148	98
5	2937	3148	211
10	3037	3386	349
20	3343	3550	207
40	3231	3650	419
40	3367	3650	283
60	3163	3687	524
60	3249	3687	438
		Total AAD	276

Table A.61. Advanced average deviation for HT50H 27034-87 asphaltene molecular weight data using the Single-end termination model. K=55000, $(T/P)_0$=0.008.

Asphaltene Concentration (kg/m^3)	Asphaltene Molecular Weight (g/mol)		AAD
	Experimental	Calculated	
2	7575	5145	2430
4	9760	6916	2844
8	10150	9398	752
17	11130	13209	2080
34	18151	18098	53
50	21535	21541	6
		Total AAD	1361

Table A.62. Advanced average deviation for HT70L 27034-87 asphaltene molecular weight data using the Single-end termination model. K=55000, $(T/P)_0$=0.81.

Asphaltene Concentration (kg/m^3)	Asphaltene Molecular Weight (g/mol)		AAD
	Experimental	Calculated	
1	1887	1774	113
1	2068	1774	294
2	1967	1905	62
2	2026	1905	121
5	2105	2032	74
5	2163	2032	131
10	2344	2090	254
10	2180	2090	90
20	2362	2124	239
20	2405	2124	281
40	2520	2142	378
40	2372	2142	230
60	2510	2148	362
60	2603	2148	455
		Total AAD	220

Table A.63. Advanced average deviation for HT70H 27034-87 asphaltene molecular weight data using the Single-end termination model. K=55000, $(T/P)_0$=0.048.

Asphaltene Concentration (kg/m^3)	Asphaltene Molecular Weight (g/mol)		AAD
	Experimental	Calculated	
1	5920	3700	2220
2	7021	4805	2216
5	8481	6874	1606
5	6989	6874	114
10	7924	9001	1077
10	9834	9001	833
20	12077	11658	419
40	15643	14795	848
40	14764	14795	32
60	16468	16784	316
60	16820	16784	36
		Total AAD	883

Table A.64. Advanced average deviation for HT82L 27034-87 asphaltene molecular weight data using the Single-end termination model. K=55000, $(T/P)_0$=6.

Asphaltene Concentration (kg/m^3)	Asphaltene Molecular Weight (g/mol)		AAD
	Experimental	Calculated	
1	1203	1040	162
2	1568	1050	518
5	1672	1056	615
10	1592	1059	534
20	1714	1060	654
40	1730	1061	669
60	1940	1061	879
		Total AAD	576

Table A.65. Advanced average deviation for HT82H 27034-87 asphaltene molecular weight data using the Single-end termination model. K=55000, $(T/P)_0$=0.0.074.

Asphaltene Concentration (kg/m^3)	Asphaltene Molecular Weight (g/mol)		AAD
	Experimental	Calculated	
1	5697	3586	2111
1	5297	3586	1711
2	5344	4605	738
2	4949	4605	344
5	7741	6448	1293
5	7624	6448	1176
10	9261	8245	1016
10	8854	8245	609
20	11546	10341	1204
20	10014	10341	327
40	12425	12591	167
40	13493	12591	902
60	13839	13884	45
60	13418	13884	466
		Total AAD	865

Table A.66. Summary of AAD for 27034-87 asphaltene molecular weight. Results obtained using the single-end termination model with parameters showed in Tables A.59 to A.65.

Fraction	AAD (g/mol)
HT82L	576
HT70L	220
HT50L	276
Whole	291
HT82H	865
HT70H	883
HT50H	1361
AAD	639

Table A.67. Advanced average deviation for whole 27034-113 asphaltene molecular weight data using the Single-end termination model. K=55000, $(T/P)_0$=0.258.

Asphaltene Concentration (kg/m^3)	Asphaltene Molecular Weight (g/mol)		AAD
	Experimental	Calculated	
1	1967	2388	421
1	2791	2388	403
2	2892	2788	104
2	2400	2788	387
5	3000	3315	314
5	3352	3315	38
10	3733	3655	77
10	3560	3655	95
20	4428	3913	516
20	4679	3913	766
40	5301	4083	1218
40	5421	4083	1338
60	6048	4149	1899
60	6484	4149	2335
		Total AAD	708

Table A.68. Advanced average deviation for HT45L 27034-113 asphaltene molecular weight data using the Single-end termination model. K=55000, $(T/P)_0$=0.34.

Asphaltene Concentration (kg/m^3)	Asphaltene Molecular Weight (g/mol)		AAD
	Experimental	Calculated	
1	2132	2171	39
2	2357	2473	117
6	2517	2903	386
7	2587	2953	366
11	3094	3079	15
13	3323	3119	204
22	3758	3219	539
26	3954	3244	710
40	4298	3296	1003
52	4388	3319	1069
60	4197	3330	867
79	5028	3347	1681
		Total AAD	583

Table A.69. Advanced average deviation for HT45H 27034-113 asphaltene molecular weight data using the Single-end termination model. K=55000, $(T/P)_0$=0.0005.

Asphaltene Concentration (kg/m^3)	Asphaltene Molecular Weight (g/mol)		AAD
	Experimental	Calculated	
1	3970	3581	389
2	6488	4772	1717
6	10392	7151	3240
11	14001	10286	3716
22	18410	14266	4144
		Total AAD	2641

Table A.70. Advanced average deviation for HT57L 27034-113 asphaltene molecular weight data using the Single-end termination model. K=55000, $(T/P)_0$=0.54.

Asphaltene Concentration (kg/m^3)	Asphaltene Molecular Weight (g/mol)		AAD
	Experimental	Calculated	
1	1765	1840	75
2	2308	2020	288
5	1869	2209	340
10	2218	2305	86
20	2695	2364	332
40	2904	2397	507
40	3315	2397	918
60	3298	2409	889
60	3159	2409	750
		Total AAD	465

Table A.71. Advanced average deviation for HT57H 27034-113 asphaltene molecular weight data using the Single-end termination model. K=55000, $(T/P)_0$=0.032.

Asphaltene Concentration (kg/m^3)	Asphaltene Molecular Weight (g/mol)		AAD
	Experimental	Calculated	
1	2400	3436	1036
1	3158	3436	278
2	3582	4509	926
2	3637	4509	872
5	6594	6552	42
5	7399	6552	847
10	9057	8709	349
10	8511	8709	197
20	10691	11499	808
20	12436	11499	937
40	16109	14965	1144
40	14613	14965	352
60	16477	17279	802
60	18206	17279	927
		Total AAD	680

Table A.72. Advanced average deviation for HT70L 27034-113 asphaltene molecular weight data using the Single-end termination model. K=55000, $(T/P)_0$=1.

Asphaltene Concentration (kg/m^3)	Asphaltene Molecular Weight (g/mol)		AAD
	Experimental	Calculated	
1	1143	1477	334
1	1177	1477	301
2	1352	1558	206
2	1364	1558	195
5	1545	1631	87
5	1430	1631	201
10	1680	1663	17
10	1825	1663	162
20	2110	1681	429
20	1971	1681	290
40	2280	1690	590
40	2494	1690	804
60	2758	1693	1065
60	2971	1693	1278
		Total AAD	426

Table A.73. Advanced average deviation for HT70H 27034-113 asphaltene molecular weight data using the Single-end termination model. K=55000, $(T/P)_0$=0.051.

Asphaltene Concentration (kg/m^3)	Asphaltene Molecular Weight (g/mol)		AAD
	Experimental	Calculated	
1	2424	3355	931
1	3038	3355	317
2	3454	4363	909
2	2791	4363	1572
5	4498	6229	1731
5	4301	6229	1928
10	6877	8119	1241
10	6704	8119	1414
20	9544	10434	891
20	9837	10434	597
40	13009	13097	87
40	13134	13097	37
60	15001	14738	264
60	16218	14738	1480
		Total AAD	957

Table A.74. Summary of AAD for 27034-113 asphaltene molecular weight. Results obtained using the single-end termination model with parameters showed in Tables A.67 to A.73.

Fraction	AAD (g/mol)
HT70L	426
HT57L	465
HT45L	583
Whole	708
HT70H	957
HT57H	680
HT45H	2641
AAD	923

Table A.75. Advanced average deviation for whole 26845 asphaltene molecular weight data using the Single-end termination model. K=55000, $(T/P)_0$=0.412.

Asphaltene Concentration (kg/m^3)	Asphaltene Molecular Weight (g/mol)		AAD
	Experimental	Calculated	
2	2912	2487	426
5	2796	2828	33
5	2954	2828	125
10	2950	3019	69
10	3087	3019	68
20	3297	3146	151
20	3103	3146	43
40	3781	3221	560
40	3447	3221	226
60	3654	3249	405
60	3361	3249	112
		Total AAD	201

Table A.76. Advanced average deviation for HT50L 26845 asphaltene molecular weight data using the Single-end termination model. K=55000, $(T/P)_0$=0.67.

Asphaltene Concentration (kg/m^3)	Asphaltene Molecular Weight (g/mol)		AAD
	Experimental	Calculated	
2	1751	1997	246
5	1888	2163	274
10	1807	2241	434
10	2218	2241	24
20	2113	2288	175
40	2455	2314	141
40	2500	2314	186
60	2715	2323	392
60	2633	2323	310
		Total AAD	243

Table A.77. Advanced average deviation for HT50H 26845 asphaltene molecular weight data using the Single-end termination model. K=55000, $(T/P)_0$=0.0001.

Asphaltene Concentration (kg/m^3)	Asphaltene Molecular Weight (g/mol)		AAD
	Experimental	Calculated	
1	11347	3760	7586
1	9390	3760	5630
5	13092	7480	5613
5	14183	7480	6704
10	17569	10284	7285
10	19877	10284	9594
20	20475	14251	6224
40	24756	19846	4910
40	23325	19846	3479
		Total AAD	6336

Table A.78. Advanced average deviation for HT64L 26845 asphaltene molecular weight data using the Single-end termination model. K=55000, $(T/P)_0$=1.25.

Asphaltene Concentration (kg/m^3)	Asphaltene Molecular Weight (g/mol)		AAD
	Experimental	Calculated	
1	1060	1446	386
2	1348	1517	168
2	1252	1517	265
5	1307	1576	270
5	1539	1576	38
10	1474	1601	127
10	1358	1601	243
20	1472	1614	142
20	1538	1614	76
40	1785	1621	164
40	1596	1621	26
60	1899	1624	275
		Total AAD	182

Table A.79. Advanced average deviation for HT64H 26845 asphaltene molecular weight data using the Single-end termination model. K=55000, $(T/P)_0$=0.038.

Asphaltene Concentration (kg/m^3)	Asphaltene Molecular Weight (g/mol)		AAD
	Experimental	Calculated	
1	4005	3574	431
1	4005	3574	431
2	4539	4668	130
2	4322	4668	346
5	5382	6742	1361
5	6363	6742	380
10	8302	8909	607
10	7714	8909	1195
20	10785	11678	893
20	11092	11678	585
40	15517	15053	463
40	15277	15053	224
60	17818	17265	553
60	15299	17265	1967
		Total AAD	683

Table A.80. Advanced average deviation for HT82L 26845 asphaltene molecular weight data using the Single-end termination model. K=55000, $(T/P)_0$=3.9.

Asphaltene Concentration (kg/m^3)	Asphaltene Molecular Weight (g/mol)		AAD
	Experimental	Calculated	
1	799	1009	210
1	627	1009	382
2	955	1022	67
2	1083	1022	60
5	1064	1032	32
5	1028	1032	4
10	1154	1036	119
10	1124	1036	89
20	1208	1037	171
20	1195	1037	157
40	1301	1038	263
40	1320	1038	282
60	1414	1039	376
60	1428	1039	389
		Total AAD	186

Table A.81. Advanced average deviation for HT82H 26845 asphaltene molecular weight data using the Single-end termination model. K=55000, $(T/P)_0$=0.119.

Asphaltene Concentration (kg/m^3)	Asphaltene Molecular Weight (g/mol)		AAD
	Experimental	Calculated	
1	6484	3234	3250
5	7055	5512	1543
5	5721	5512	209
20	8784	8076	709
20	8033	8076	43
40	8914	9263	350
40	9286	9263	23
60	9439	9849	410
60	10061	9849	212
		Total AAD	750

Table A.82. Summary of AAD for 26845 asphaltene molecular weight. Results obtained using the single-end termination model with parameters showed in Tables A.75 to A.81.

Fraction	AAD (g/mol)
HT82L	186
HT64L	182
HT50L	243
Whole	201
HT82H	750
HT64H	683
HT50H	6336
AAD	1226

Table A.83. Recalculation of $(T/P)_0$ for Athabasca asphaltene fractions.

Fraction	$(T/P)_0$	ARD (%)
Whole	0.235	---
HT60	0.260	10.7
HT70	0.259	10.1
HT80	0.259	10.2
HT90	0.259	10.0

Table A.84. Recalculation of $(T/P)_0$ for Arabian asphaltene fractions.

Fraction	$(T/P)_0$	ARD (%)
Whole	0.592	---
HT66	0.430	27.4
HT76	0.435	26.6
HT86	0.432	27.1

Table A.85. Recalculation of $(T/P)_0$ for Cliffdale asphaltene fractions.

Fraction	$(T/P)_0$	ARD (%)
Whole	0.135	---
HT62	0.147	9.1
HT70	0.146	8.3
HT80	0.127	5.8

Table A.86. Recalculation of $(T/P)_0$ for Peace River asphaltene fractions.

Fraction	$(T/P)_0$	ARD (%)
Whole	0.26	---
HT60	0.303	16.5
HT77	0.295	13.6
HT92	0.264	1.5

Table A.87. Recalculation of $(T/P)_0$ for 27-168-178 asphaltene fractions.

Fraction	$(T/P)_0$	ARD (%)
Whole	0.418	---
HT63	0.469	12.3
HT77	0.426	2.0
HT86	0.368	12.0

Table A.88. Recalculation of $(T/P)_0$ for 27034-87 asphaltene fractions.

Fraction	$(T/P)_0$	ARD (%)
Whole	0.293	---
HT50	0.338	15.3
HT70	0.253	13.5
HT82	0.252	13.9

Table A.89. Recalculation of $(T/P)_0$ for 27034-113 asphaltene fractions.

Fraction	$(T/P)_0$	ARD (%)
Whole	0.258	---
HT45	0.226	12.4
HT57	0.227	12.2
HT70	0.227	12.1

Table A.90. Recalculation of $(T/P)_0$ for 26845 asphaltene fractions.

Fraction	$(T/P)_0$	ARD (%)
Whole	0.412	---
HT50	0.412	0.0
HT64	0.449	9.0
HT82	0.377	8.6

Table A.91. AAD for predicted Athabasca asphaltene solubility in *n*-heptane/toluene mixtures at 21°C using both the Gamma and the Single-end distributions and the density correlation from Equation 5.16.

Heptol % (v/v)	Asphaltene Fractional Precipitation (wt/wt)				
	Experimental	Gamma Distribution	AAD	Single-end Distribution	AAD
30	0.003	0.000	0.003	0.000	0.003
40	0.032	0.000	0.032	0.013	0.020
50	0.136	0.024	0.112	0.135	0.001
50	0.033	0.024	0.009	0.135	0.102
70	0.449	0.500	0.051	0.608	0.160
70	0.544	0.500	0.044	0.608	0.065
80	0.735	0.720	0.015	0.764	0.029
90	0.851	0.845	0.002	0.849	0.002
90	0.804	0.845	0.046	0.849	0.045
		Average	0.035	**Average**	0.047

Table A.92. AAD for predicted Athabasca asphaltene solubility in *n*-heptane/toluene mixtures at 21°C using both the Gamma and the Single-end distributions and parameters from Table 6.5 for the density correlation.

Heptol % (v/v)	Asphaltene Fractional Precipitation (wt/wt)				
	Experimental	Gamma Distribution	AAD	Single-end Distribution	AAD
30	0.003	0.000	0.003	0.000	0.003
40	0.032	0.000	0.032	0.000	0.032
50	0.136	0.006	0.130	0.030	0.109
50	0.033	0.006	0.027	0.030	0.003
70	0.449	0.545	0.096	0.546	0.097
70	0.544	0.545	0.001	0.546	0.002
80	0.735	0.740	0.005	0.725	0.010
90	0.851	0.852	0.001	0.826	0.026
90	0.804	0.852	0.048	0.826	0.022
		Average	0.038	**Average**	0.033

Table A.93. AAD for predicted Arabian asphaltene solubility in *n*-heptane/toluene mixtures at 21°C using both the Gamma and the Single-end distributions and the density correlation from Equation 5.16.

Heptol % (v/v)	Asphaltene Fractional Precipitation (wt/wt)				
	Experimental	Gamma Distribution	AAD	Single-end Distribution	AAD
60	0.108	0.097	0.011	0.158	0.051
66	0.296	0.198	0.098	0.269	0.028
76	0.547	0.458	0.090	0.501	0.046
80	0.631	0.580	0.051	0.599	0.032
86	0.734	0.681	0.052	0.680	0.053
90	0.814	0.762	0.052	0.745	0.069
		Average	0.059	**Average**	0.046

Table A.94. AAD for predicted Arabian asphaltene solubility in *n*-heptane/toluene mixtures at 21°C using both the Gamma and the Single-end distributions and parameters from Table 6.5 for the density correlation.

Heptol % (v/v)	Asphaltene Fractional Precipitation (wt/wt)				
	Experimental	Gamma Distribution	AAD	Single-end Distribution	AAD
60	0.108	0.149	0.042	0.163	0.055
66	0.296	0.291	0.005	0.299	0.003
76	0.547	0.551	0.004	0.540	0.007
80	0.631	0.641	0.010	0.621	0.010
86	0.734	0.704	0.029	0.681	0.052
90	0.814	0.762	0.052	0.729	0.086
		Average	0.024	**Average**	0.036

Table A.95. AAD for predicted Cliffdale asphaltene solubility in *n*-heptane/toluene mixtures at 21°C using both the Gamma and the Single-end distributions and the density correlation from Equation 5.16.

Heptol % (v/v)	Asphaltene Fractional Precipitation (wt/wt)				
	Experimental	Gamma Distribution	AAD	Single-end Distribution	AAD
60	0.206	0.310	0.104	0.483	0.277
62	0.240	0.392	0.153	0.541	0.301
70	0.474	0.621	0.146	0.686	0.211
80	0.704	0.821	0.117	0.808	0.103
90	0.923	0.918	0.005	0.879	0.044
		Average	0.105	**Average**	0.187

Table A.96. AAD for predicted Cliffdale asphaltene solubility in *n*-heptane/toluene mixtures at 21°C using both the Gamma and the Single-end distributions and parameters from Table 6.5 for the density correlation.

Heptol % (v/v)	Asphaltene Fractional Precipitation (wt/wt)				
	Experimental	Gamma Distribution	AAD	Single-end Distribution	AAD
60	0.206	0.151	0.055	0.182	0.024
62	0.240	0.235	0.005	0.257	0.017
70	0.475	0.480	0.005	0.477	0.002
80	0.704	0.711	0.007	0.673	0.031
90	0.923	0.842	0.081	0.786	0.137
		Average	0.031	**Average**	0.042

Table A.97. AAD for predicted Peace River asphaltene solubility in *n*-heptane/toluene mixtures at 21°C using the Gamma, Gamma+A' and Single-end distributions and the density correlation from Equation 5.16.

Heptol % (v/v)	Asphaltene Fractional Precipitation (wt/wt)						
	Experim.	Gamma	AAD	Gamma +A'	AAD	Single-end	AAD
60	0.185	0.019	0.167	0.127	0.058	0.086	0.099
70	0.361	0.138	0.223	0.358	0.003	0.290	0.071
77	0.538	0.312	0.226	0.540	0.001	0.463	0.075
80	0.573	0.377	0.196	0.596	0.024	0.515	0.058
90	0.723	0.613	0.110	0.763	0.040	0.681	0.042
92	0.791	0.658	0.133	0.790	0.002	0.712	0.079
		Average	0.176	**Average**	0.021	**Average**	0.071

Table A.98. AAD for predicted Peace River asphaltene solubility in *n*-heptane/toluene mixtures at 21°C using both the Gamma and the Single-end distributions and parameters from Table 6.5 for the density correlation.

Heptol % (v/v)	Asphaltene Fractional Precipitation (wt/wt)				
	Experimental	Gamma Distribution	AAD	Single-end Distribution	AAD
60	0.185	0.092	0.093	0.099	0.086
70	0.361	0.356	0.005	0.361	0.000
77	0.538	0.558	0.020	0.549	0.011
80	0.573	0.613	0.040	0.598	0.025
90	0.723	0.763	0.040	0.736	0.013
92	0.791	0.784	0.007	0.759	0.032
		Average	0.034	**Average**	0.028

Table A.99. AAD for predicted 27-168-178 asphaltene solubility in *n*-heptane/toluene mixtures at 21°C using both the Gamma and the Single-end distributions and the density correlation from Equation 5.16.

Heptol % (v/v)	Asphaltene Fractional Precipitation (wt/wt)				
	Experimental	Gamma Distribution	AAD	Single-end Distribution	AAD
63	0.091	0.093	0.002	0.297	0.206
70	0.352	0.280	0.072	0.476	0.125
77	0.514	0.511	0.003	0.624	0.110
86	0.804	0.704	0.100	0.732	0.072
90	0.865	0.797	0.068	0.783	0.081
		Average	0.049	**Average**	0.119

Table A.100. AAD for predicted 27-168-178 asphaltene solubility in *n*-heptane/toluene mixtures at 21°C using both the Gamma and the Single-end distributions and parameters from Table 6.5 for the density correlation.

Heptol % (v/v)	Asphaltene Fractional Precipitation (wt/wt)				
	Experimental	Gamma Distribution	AAD	Single-end Distribution	AAD
63	0.091	0.119	0.028	0.159	0.068
70	0.352	0.347	0.005	0.374	0.023
77	0.514	0.565	0.051	0.556	0.042
86	0.804	0.716	0.088	0.676	0.128
90	0.865	0.792	0.073	0.732	0.133
		Average	0.049	**Average**	0.078

Table A.101. AAD for predicted 27034-87 asphaltene solubility in *n*-heptane/toluene mixtures at 21°C using the Gamma, Gamma+A' and Single-end distributions and the density correlation from Equation 5.16.

Heptol % (v/v)	Asphaltene Fractional Precipitation (wt/wt)						
	Experim.	Gamma	AAD	Gamma +A'	AAD	Single-end	AAD
50	0.108	0.001	0.107	0.116	0.008	0.027	0.081
70	0.620	0.274	0.346	0.636	0.016	0.442	0.178
82	0.837	0.620	0.217	0.841	0.005	0.674	0.163
90	0.877	0.768	0.109	0.902	0.025	0.761	0.116
		Average	0.195	**Average**	0.013	**Average**	0.134

Table A.102. AAD for predicted 27034-87 asphaltene solubility in *n*-heptane/toluene mixtures at 21°C using both the Gamma and the Single-end distributions and parameters from Table 6.5 for the density correlation.

Heptol % (v/v)	Asphaltene Fractional Precipitation (wt/wt)				
	Experimental	Gamma Distribution	AAD	Single-end Distribution	AAD
50	0.108	0.104	0.005	0.114	0.006
70	0.620	0.654	0.035	0.615	0.005
82	0.837	0.825	0.012	0.760	0.078
90	0.877	0.882	0.005	0.809	0.068
		Average	0.014	**Average**	0.039

Table A.103. AAD for predicted 27034-113 asphaltene solubility in *n*-heptane/toluene mixtures at 21°C using the Gamma, Gamma+A' and Single-end distributions and the density correlation from Equation 5.16.

Heptol % (v/v)	Asphaltene Fractional Precipitation (wt/wt)						
	Experim.	Gamma	AAD	Gamma +A'	AAD	Single-end	AAD
40	0.221	0.000	0.221	0.118	0.104	0.000	0.221
45	0.271	0.000	0.271	0.220	0.052	0.000	0.271
50	0.332	0.003	0.329	0.341	0.009	0.023	0.309
57	0.510	0.025	0.484	0.467	0.043	0.086	0.423
70	0.682	0.287	0.395	0.754	0.071	0.414	0.268
80	0.807	0.541	0.266	0.857	0.050	0.613	0.194
90	0.944	0.733	0.211	0.924	0.020	0.745	0.199
		Average	0.311	**Average**	0.050	**Average**	0.270

Table A.104. AAD for predicted 27034-113 asphaltene solubility in *n*-heptane/toluene mixtures at 21°C using both the Gamma and the Single-end distributions and parameters from Table 6.5 for the density correlation.

Heptol % (v/v)	Asphaltene Fractional Precipitation (wt/wt)				
	Experimental	Gamma Distribution	AAD	Single-end Distribution	AAD
40	0.221	0.156	0.065	0.155	0.067
45	0.271	0.273	0.002	0.279	0.007
50	0.332	0.390	0.058	0.398	0.066
57	0.510	0.493	0.016	0.498	0.012
70	0.682	0.724	0.042	0.695	0.013
80	0.807	0.819	0.012	0.774	0.033
90	0.944	0.872	0.073	0.828	0.116
		Average	0.038	**Average**	0.045

Table A.105. AAD for predicted 26845 asphaltene solubility in *n*-heptane/toluene mixtures at 21°C using the Gamma, Gamma+A' and Single-end distributions and the density correlation from Equation 5.16.

Heptol % (v/v)	Asphaltene Fractional Precipitation (wt/wt)						
	Experim.	Gamma	AAD	Gamma +A'	AAD	Single-end	AAD
50	0.290	0.000	0.289	0.146	0.144	0.000	0.290
64	0.503	0.074	0.430	0.504	0.000	0.194	0.309
70	0.564	0.160	0.404	0.613	0.049	0.306	0.258
82	0.772	0.469	0.303	0.799	0.028	0.570	0.202
90	0.802	0.637	0.164	0.877	0.076	0.682	0.119
		Average	0.318	**Average**	0.059	**Average**	0.236

Table A.106. AAD for predicted 26845 asphaltene solubility in *n*-heptane/toluene mixtures at 21°C using both the Gamma and the Single-end distributions and parameters from Table 6.5 for the density correlation.

Heptol % (v/v)	Asphaltene Fractional Precipitation (wt/wt)				
	Experimental	Gamma Distribution	AAD	Single-end Distribution	AAD
50	0.290	0.096	0.193	0.126	0.163
64	0.503	0.500	0.003	0.508	0.005
70	0.564	0.616	0.052	0.607	0.043
82	0.772	0.784	0.012	0.755	0.016
90	0.802	0.845	0.043	0.803	0.001
		Average	0.061	**Average**	0.046

Table A.107. Confidence interval for Peace River asphaltene solubility measurements in *n*-heptane/toluene mixtures at 21°C.

Heptol Percentage (v/v)	n	μ (wt/wt)	σ (wt/wt)	% Confidence
60	8	0.185	0.011	0.6
70	2	0.361	0.031	3.6
77	14	0.538	0.008	0.4
80	2	0.573	0.012	1.4
90	2	0.723	0.015	1.7
92	9	0.791	0.011	0.6

Appendix B: Additional Figures

Figures B.1 to B.8 show the fractional precipitation of asphaltenes in solutions of *n*-heptane and toluene at 23°C for the eight samples used in this thesis.

Figures B.9 to B.16 represent the fractions obtained for each of the samples and the respective asphaltene percentage in each phase.

Figures B.17 to B.24 show the recombined molecular weight for asphaltenes assuming ideal behavior.

Figures B.25 to B.32 show the density data and distribution for each one of the eight samples used in the thesis.

Figures B.33 to B.40 represent the correlation between asphaltene density and molecular and compare results with previous correlation.

Figures B.41 to B.48 show results from the Single-end termination model for the light and heavy fractions of each sample.

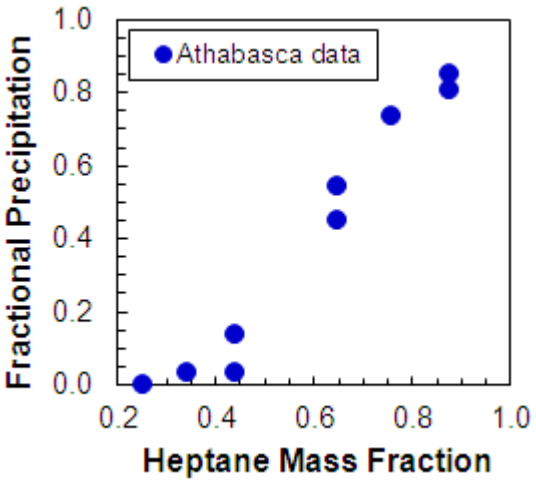

Figure B.1. Fractional precipitation of Athabasca asphaltenes from solutions of *n*-heptane and toluene at 23°C.

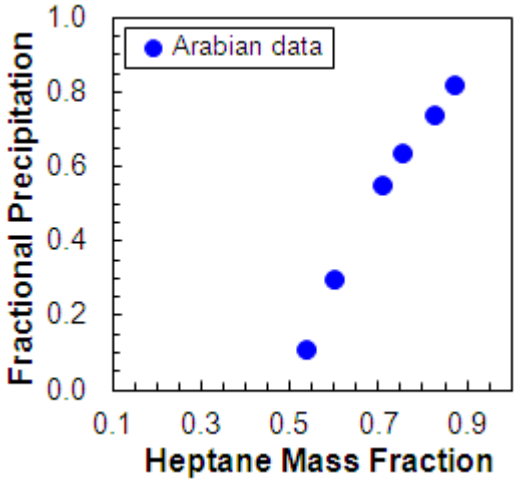

Figure B.2. Fractional precipitation of Arabian asphaltenes from solutions of *n*-heptane and toluene at 23°C.

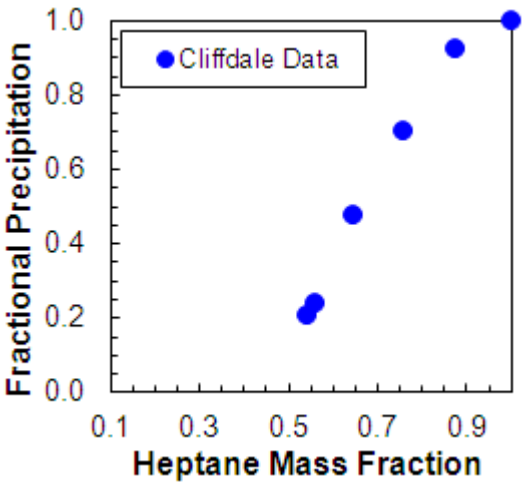

Figure B.3. Fractional precipitation of Cliffdale asphaltenes from solutions of *n*-heptane and toluene at 23°C.

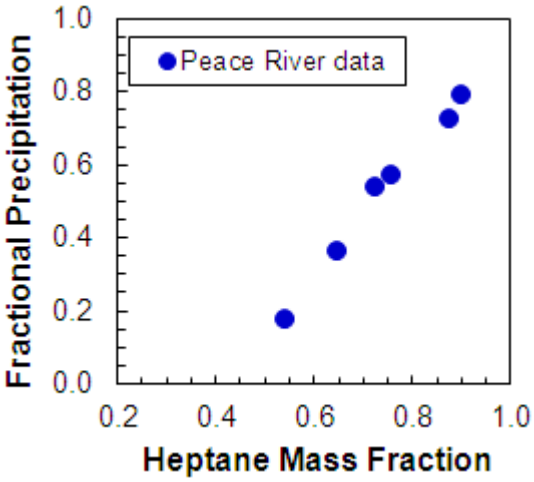

Figure B.4. Fractional precipitation of Peace River asphaltenes from solutions of *n*-heptane and toluene at 23°C.

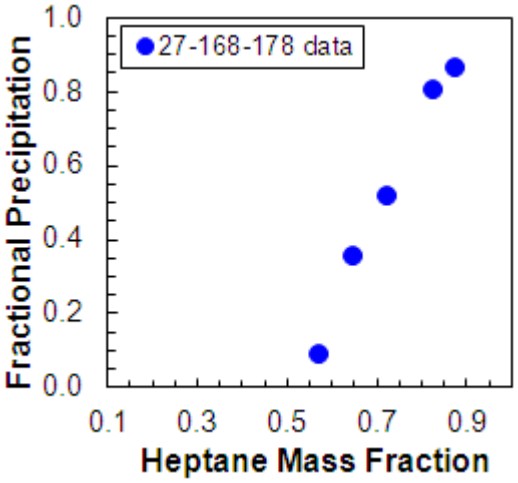

Figure B.5. Fractional precipitation of 27-168-178 asphaltenes from solutions of *n*-heptane and toluene at 23°C.

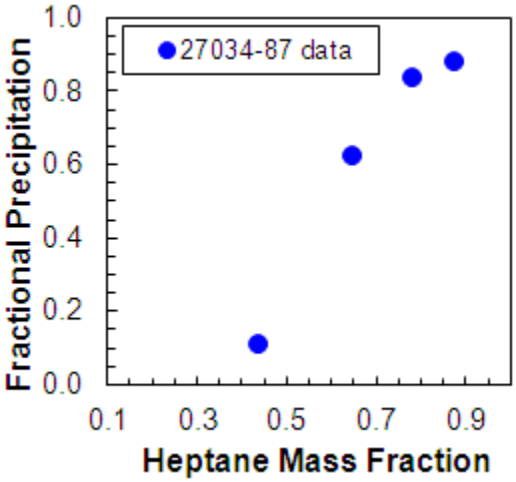

Figure B.6. Fractional precipitation of 27034-87 asphaltenes from solutions of *n*-heptane and toluene at 23°C.

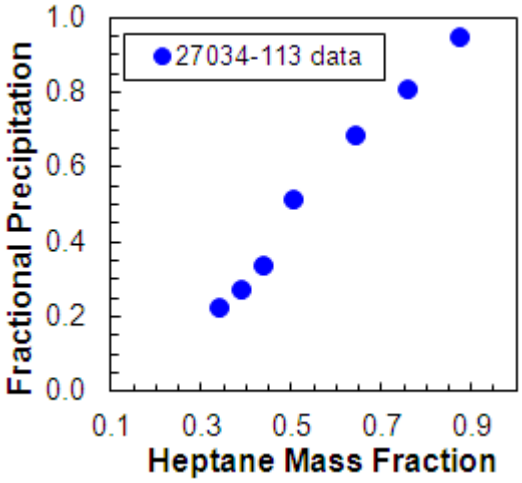

Figure B.7. Fractional precipitation of 27034-113 asphaltenes from solutions of *n*-heptane and toluene at 23°C.

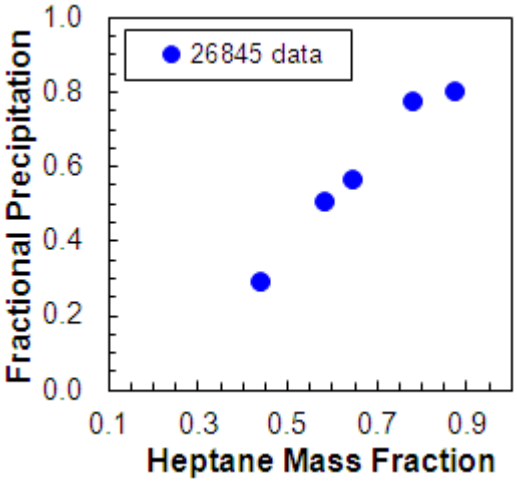

Figure B.8. Fractional precipitation of 26845 asphaltenes from solutions of *n*-heptane and toluene at 23°C.

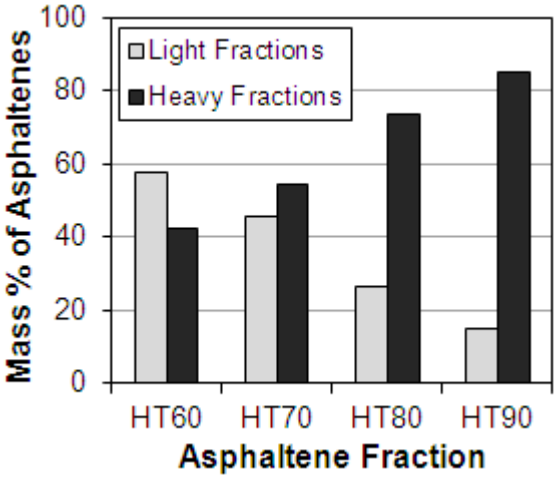

Figure B.9. Mass percentage of heavy and light fractions for Athabasca asphaltenes.

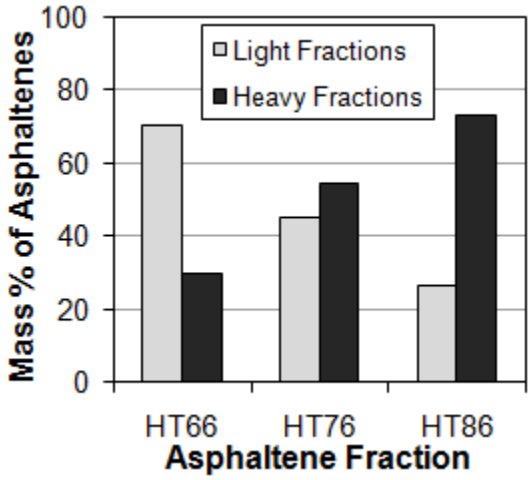

Figure B.10. Mass percentage of heavy and light fractions for Arabian asphaltenes.

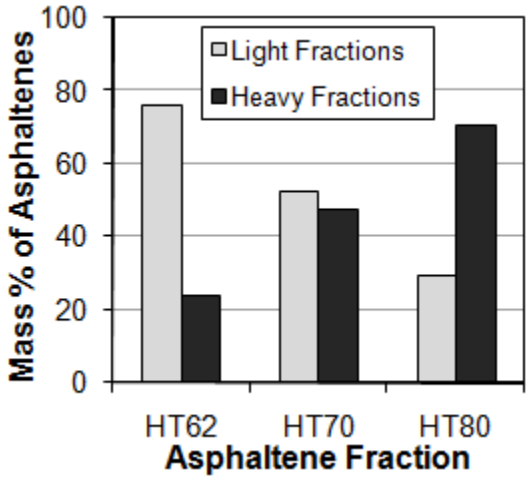

Figure B.11. Mass percentage of heavy and light fractions for Cliffdale asphaltenes.

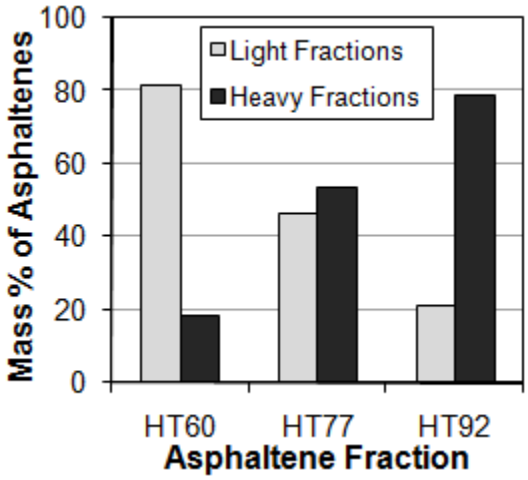

Figure B.12. Mass percentage of heavy and light fractions for Peace River asphaltenes.

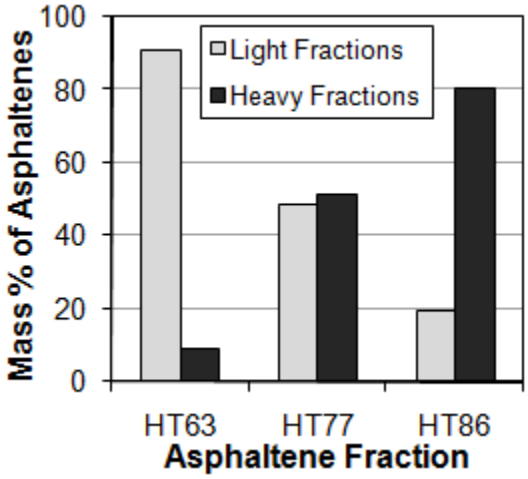

Figure B.13. Mass percentage of heavy and light fractions for 27-168-178 asphaltenes.

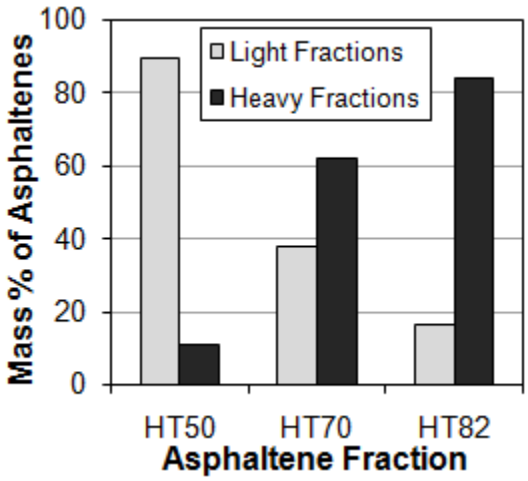

Figure B.14. Mass percentage of heavy and light fractions for 27034-87 asphaltenes.

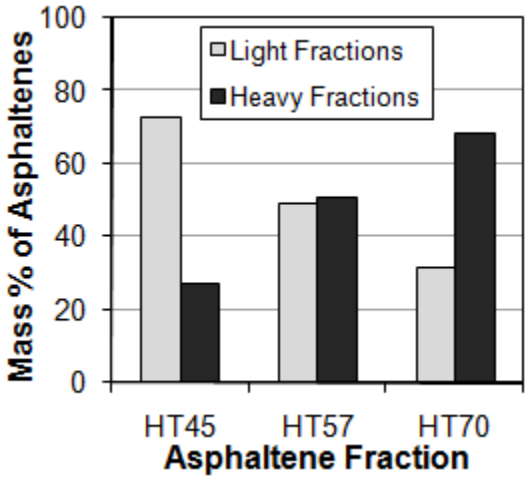

Figure B.15. Mass percentage of heavy and light fractions for 27034-113 asphaltenes.

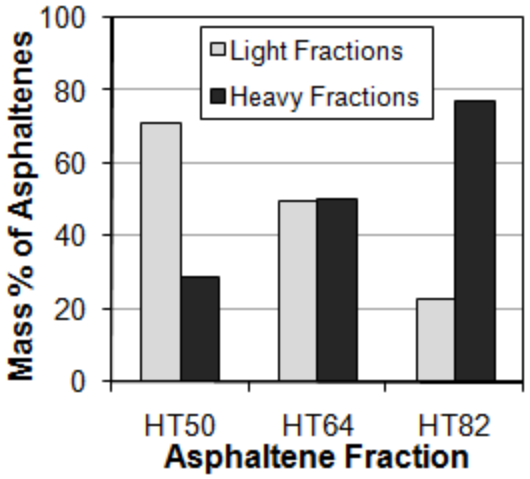

Figure B.16. Mass percentage of heavy and light fractions for 26845 asphaltenes.

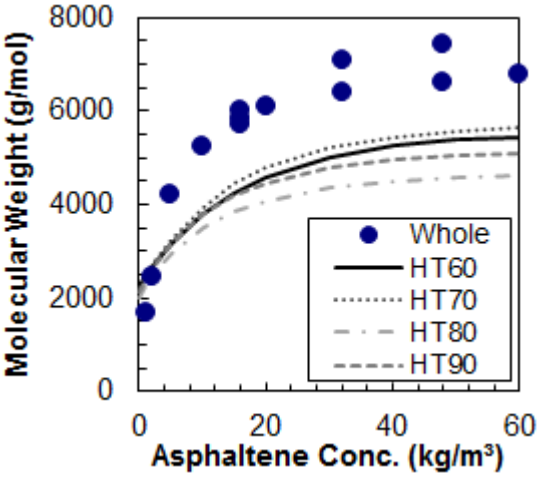

Figure B.17. Recalculation of Athabasca asphaltene molecular weight assuming ideal behavior.

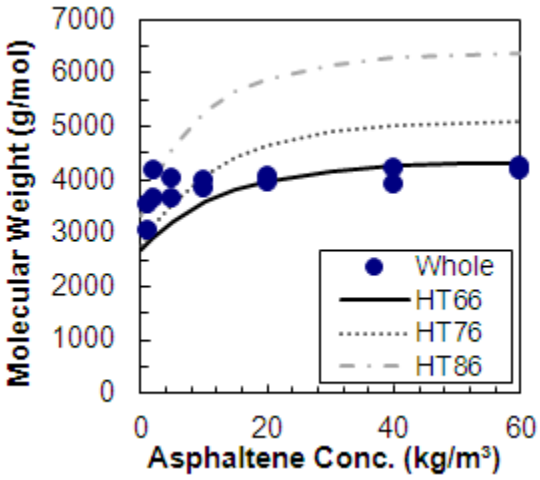

Figure B.18. Recalculation of Arabian asphaltene molecular weight assuming ideal behavior.

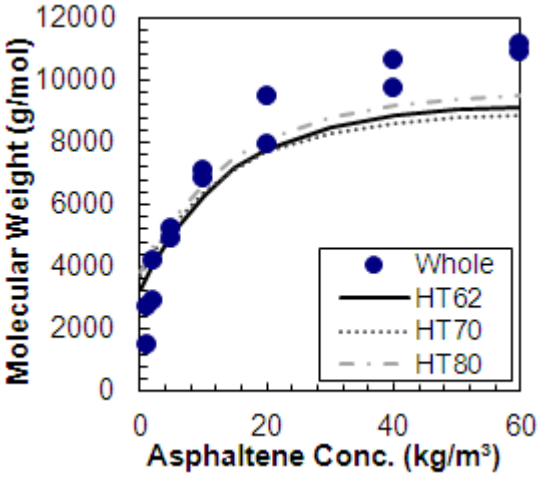

Figure B.19. Recalculation of Cliffdale asphaltene molecular weight assuming ideal behavior.

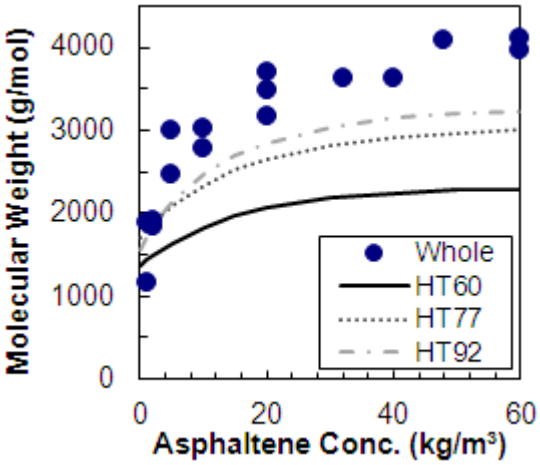

Figure B.20. Recalculation of Peace River asphaltene molecular weight assuming ideal behavior.

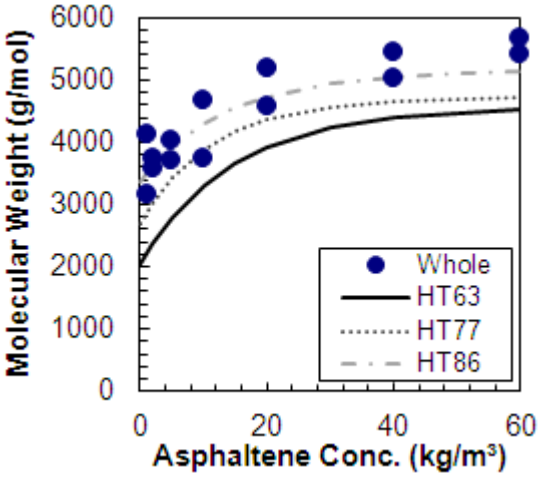

Figure B.21. Recalculation of 27-168-178 asphaltene molecular weight assuming ideal behavior.

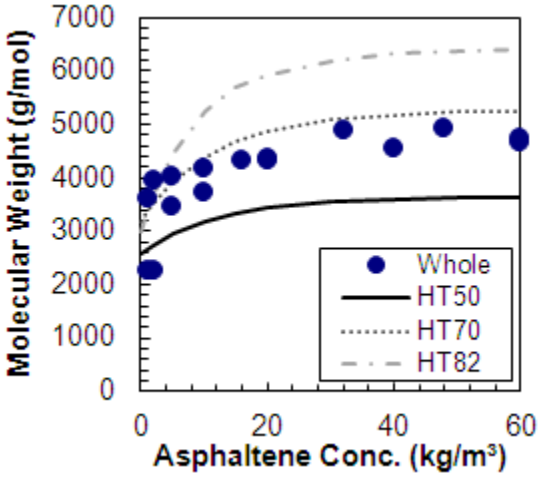

Figure B.22. Recalculation of 27034-87 asphaltene molecular weight assuming ideal behavior.

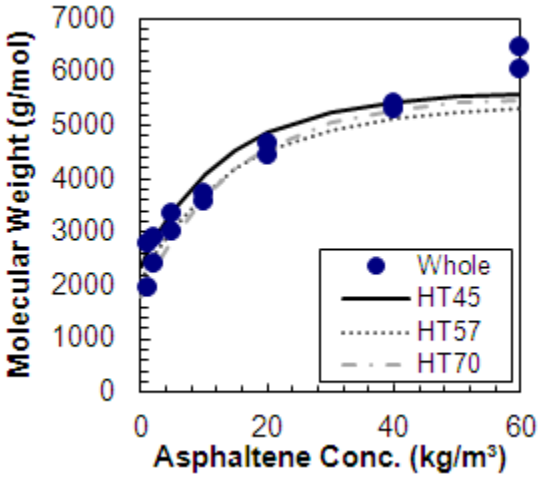

Figure B.23. Recalculation of 27034-113 asphaltene molecular weight assuming ideal behavior.

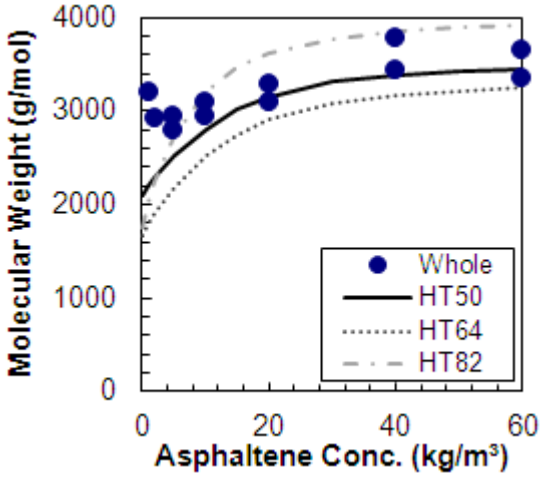

Figure B.24. Recalculation of 26845 asphaltene molecular weight assuming ideal behavior.

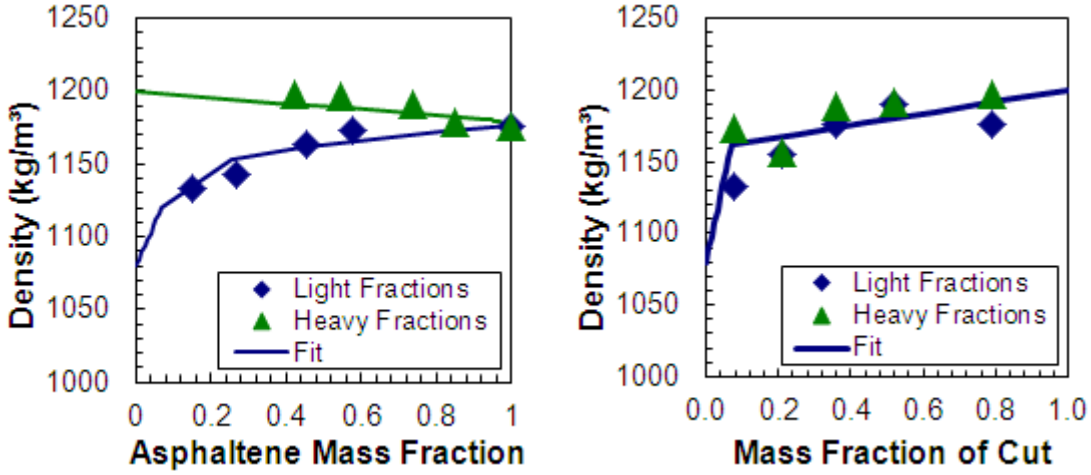

Figure B.25. Density of fractions (left plot) and density distribution for Athabasca asphaltenes (right plot).

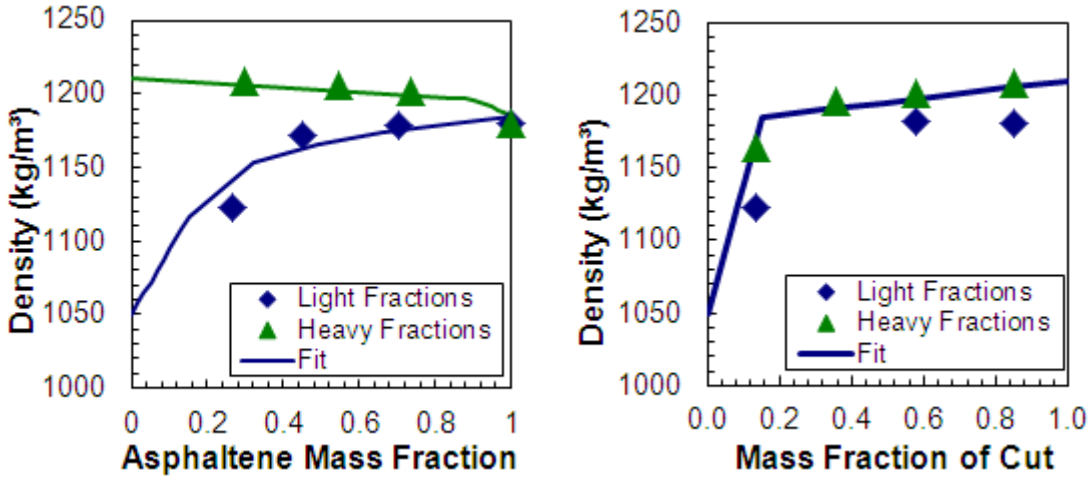

Figure B.26. Density of fractions (left plot) and density distribution for Arabian asphaltenes (right plot).

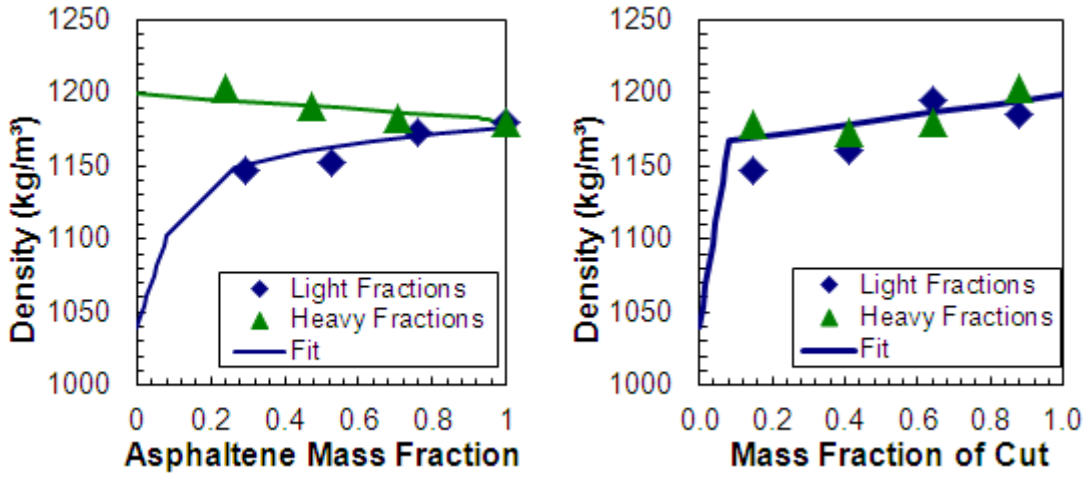

Figure B.27. Density of fractions (left plot) and density distribution for Cliffdale asphaltenes (right plot).

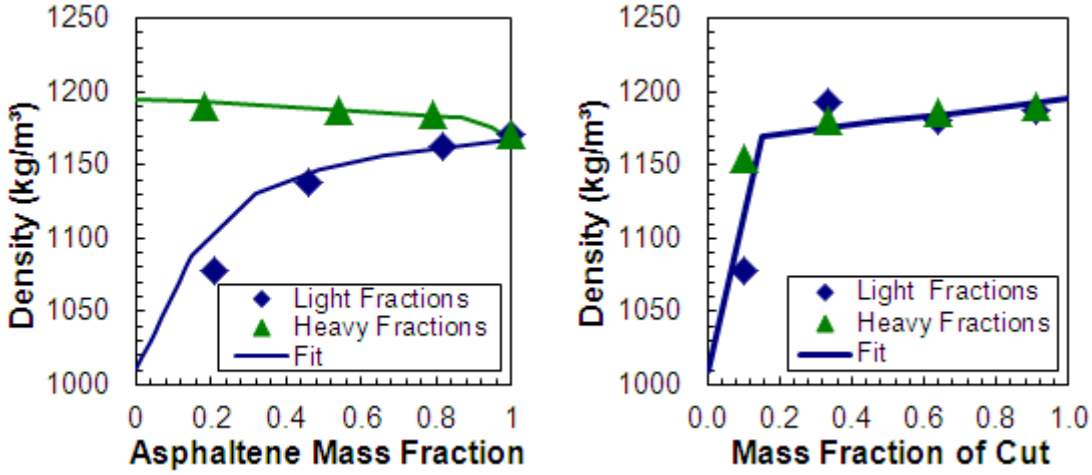

Figure B.28. Density of fractions (left plot) and density distribution for Peace River asphaltenes (right plot).

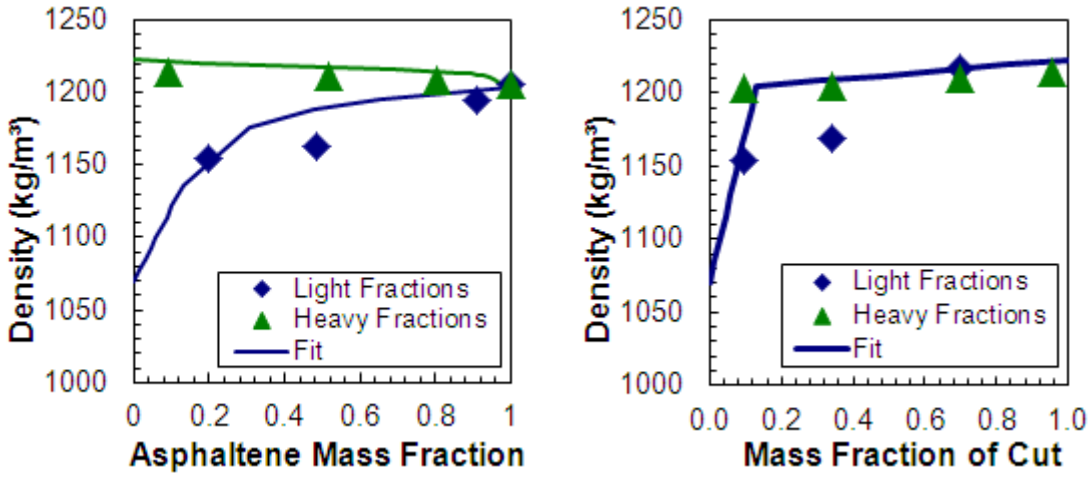

Figure B.29. Density of fractions (left plot) and density distribution for 27-168-178 asphaltenes (right plot).

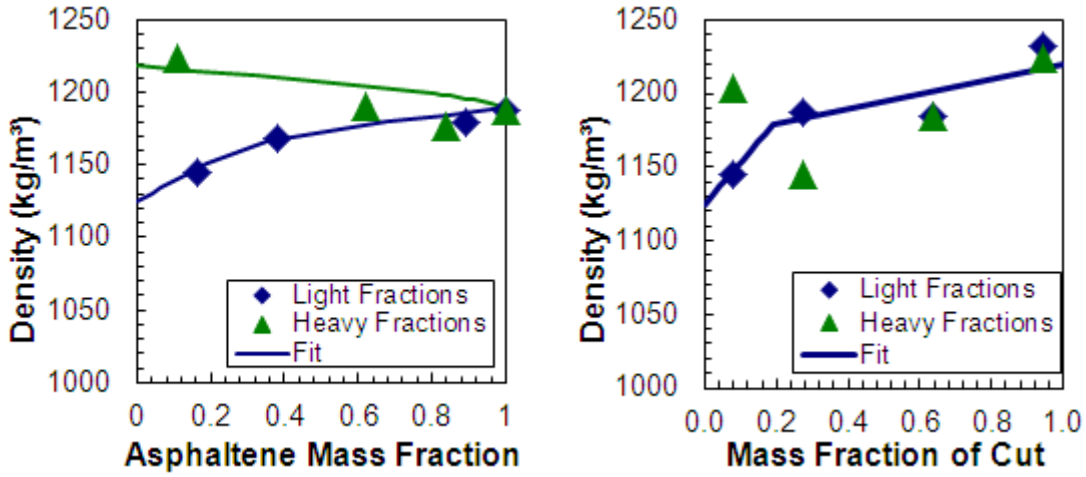

Figure B.30. Density of fractions (left plot) and density distribution for 27034-87 asphaltenes (right plot).

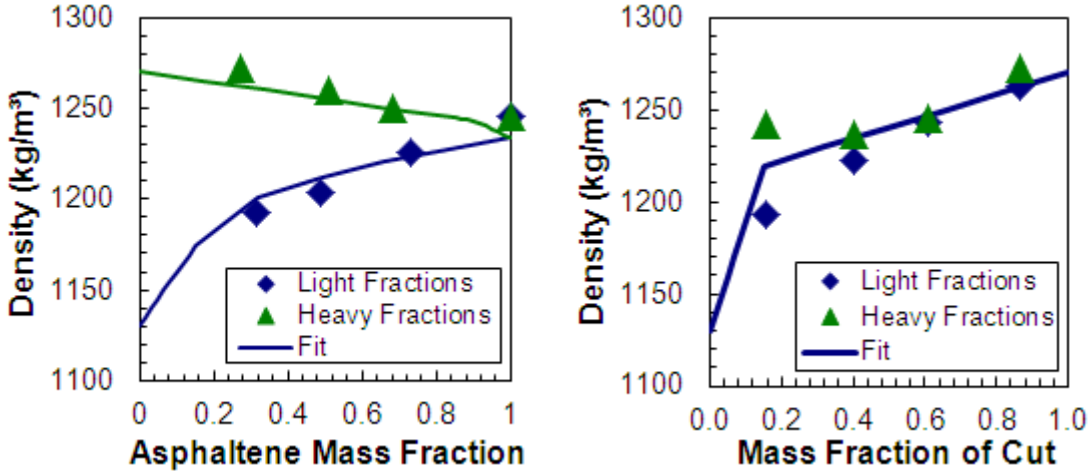

Figure B.31. Density of fractions (left plot) and density distribution for 27034-113 asphaltenes (right plot).

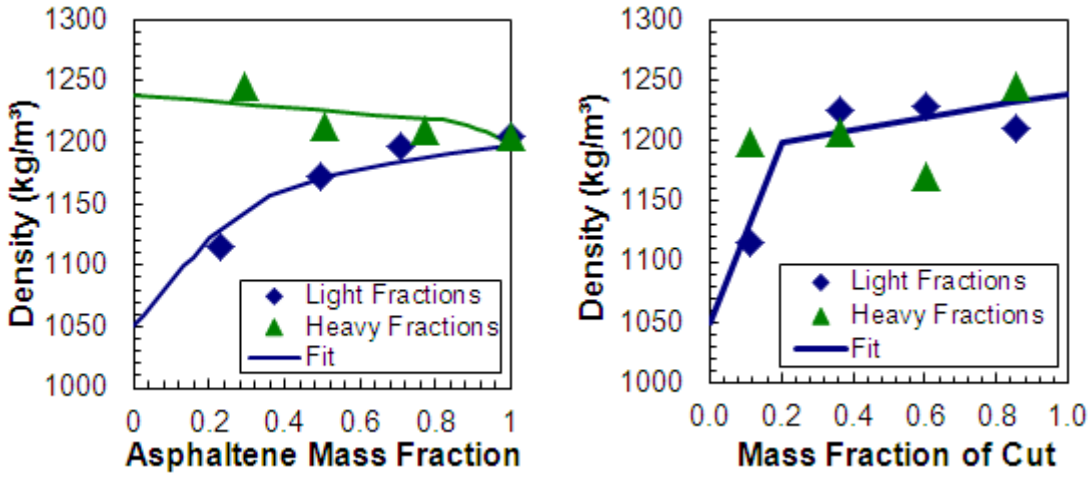

Figure B.32. Density of fractions (left plot) and density distribution for 26845 asphaltenes (right plot).

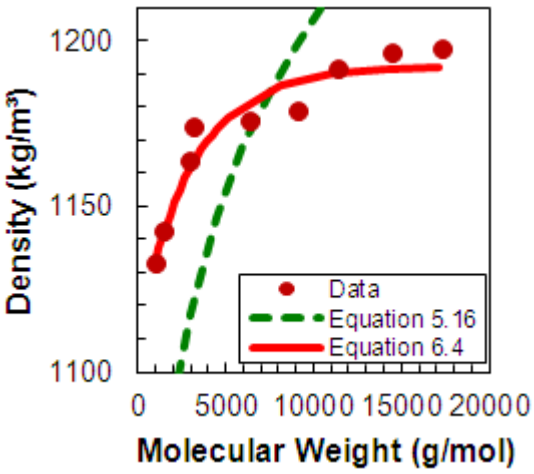

Figure B.33. Density as a function of molecular weight for Athabasca asphaltenes.

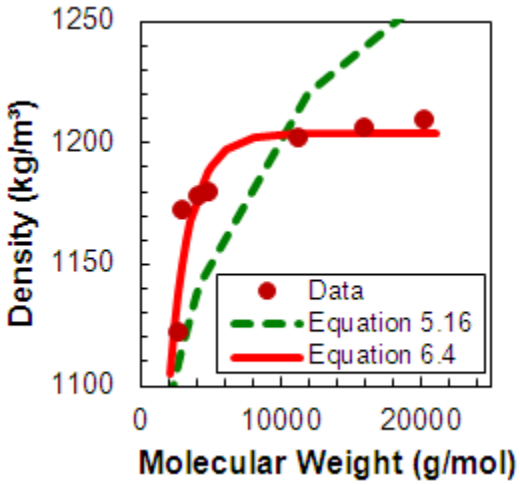

Figure B.34. Density as a function of molecular weight for Arabian asphaltenes.

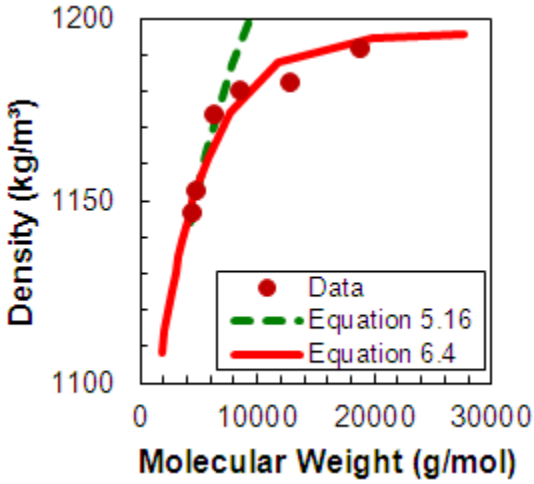

Figure B.35. Density as a function of molecular weight for Cliffdale asphaltenes.

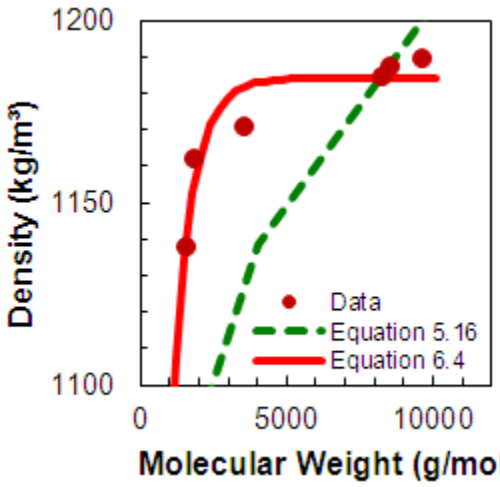

Figure B.36. Density as a function of molecular weight for Peace River asphaltenes.

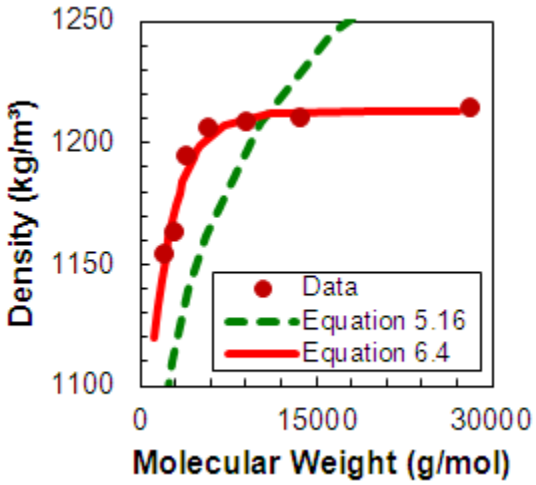

Figure B.37. Density as a function of molecular weight for 27-168-178 asphaltenes.

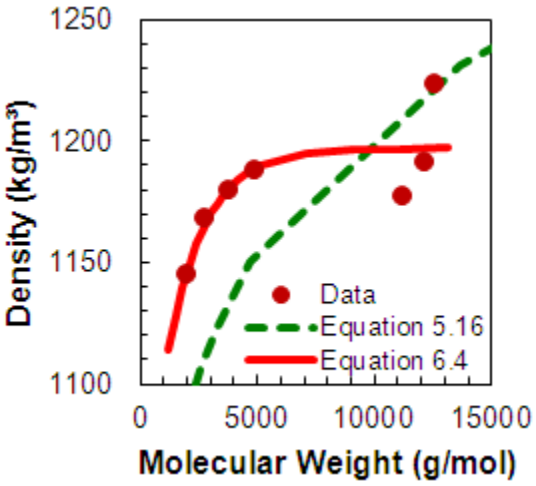

Figure B.38. Density as a function of molecular weight for 27034-87 asphaltenes.

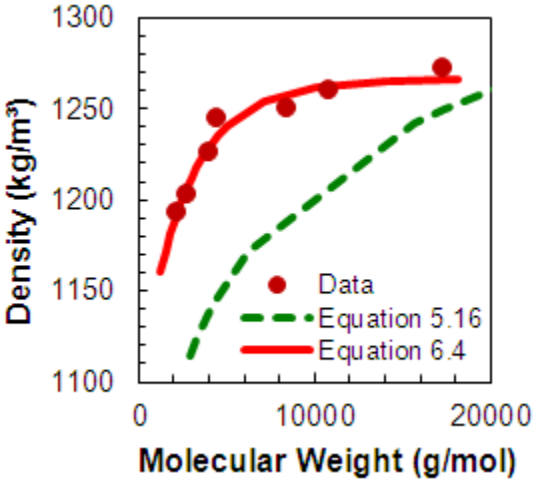

Figure B.39. Density as a function of molecular weight for 27034-113 asphaltenes.

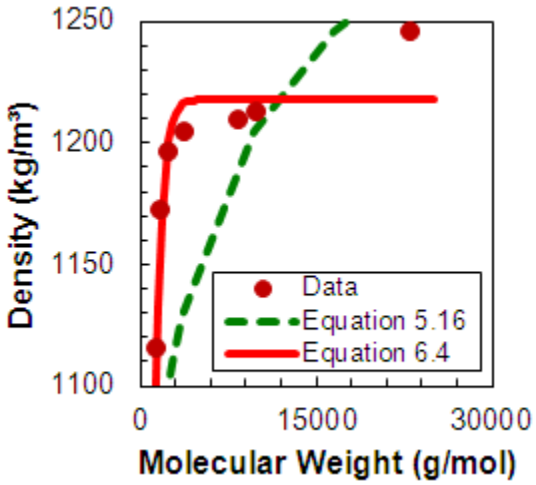

Figure B.40. Density as a function of molecular weight for 26845 asphaltenes.

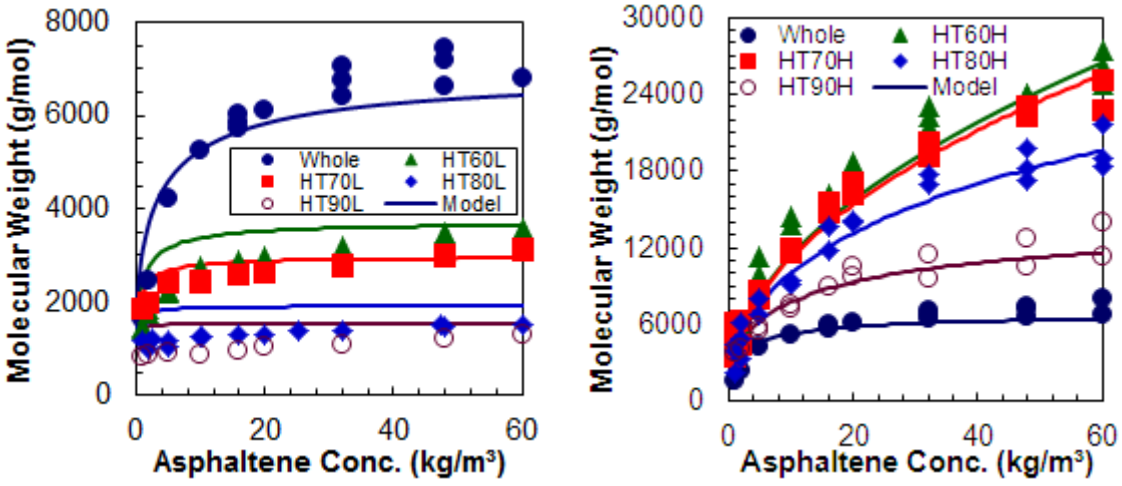

Figure B.41. Fitting of molecular weight data using the single-end termination model for all the fractions and whole Athabasca asphaltenes.

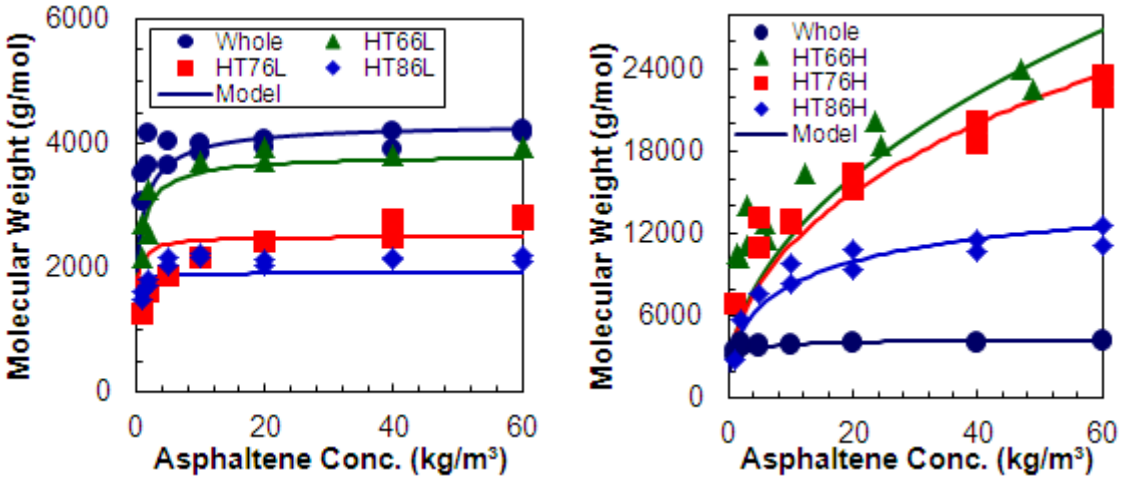

Figure B.42. Fitting of molecular weight data using the single-end termination model for all the fractions and whole Arabian asphaltenes.

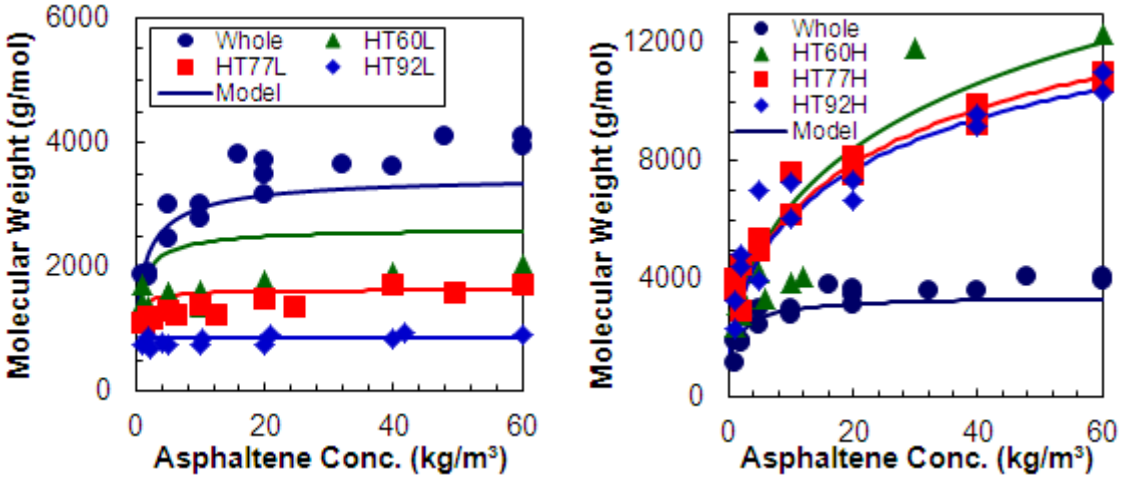

Figure B.43. Fitting of molecular weight data using the single-end termination model for all the fractions and whole Peace River asphaltenes.

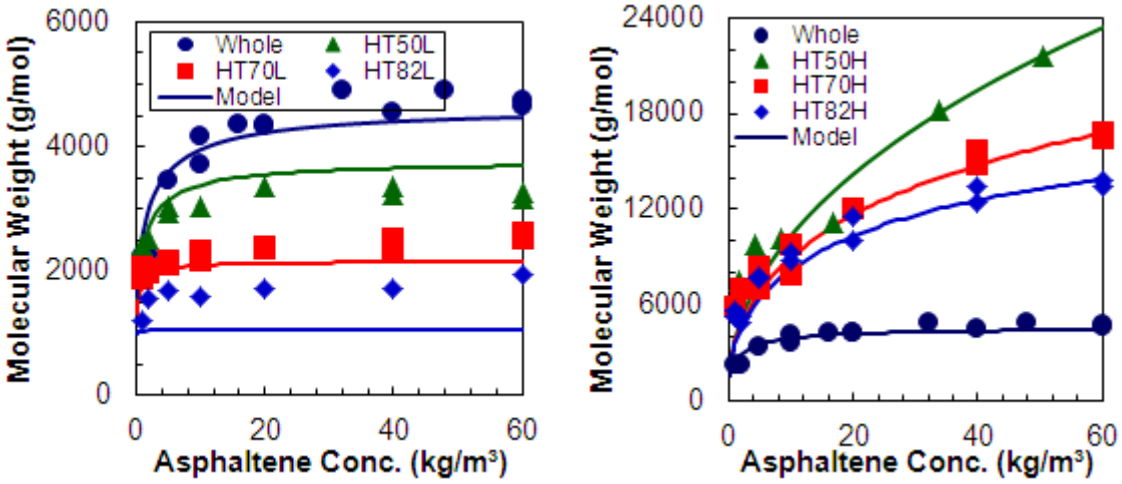

Figure B.44. Fitting of molecular weight data using the single-end termination model for all the fractions and whole 27034-87 asphaltenes.

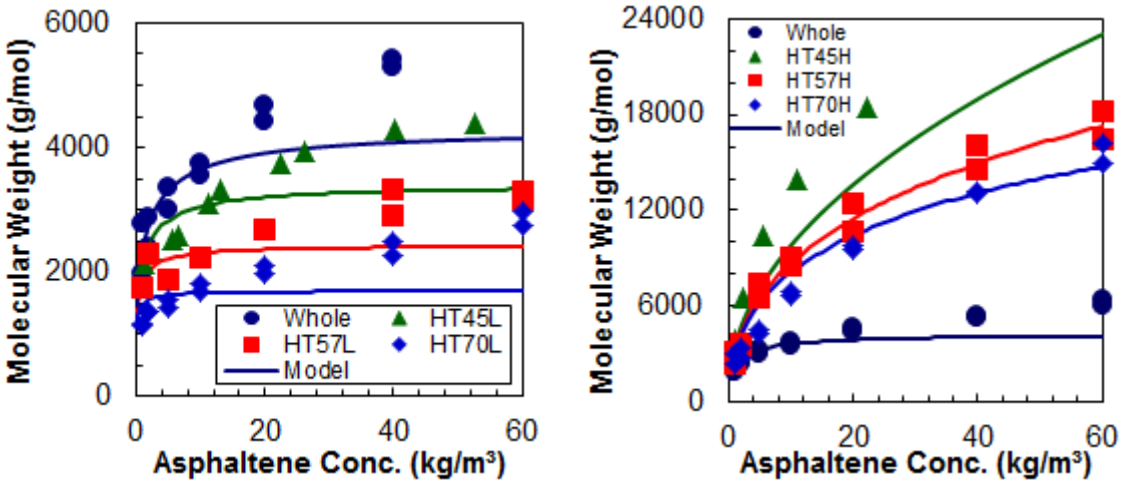

Figure B.45. Fitting of molecular weight data using the single-end termination model for all the fractions and whole 27034-113 asphaltenes.

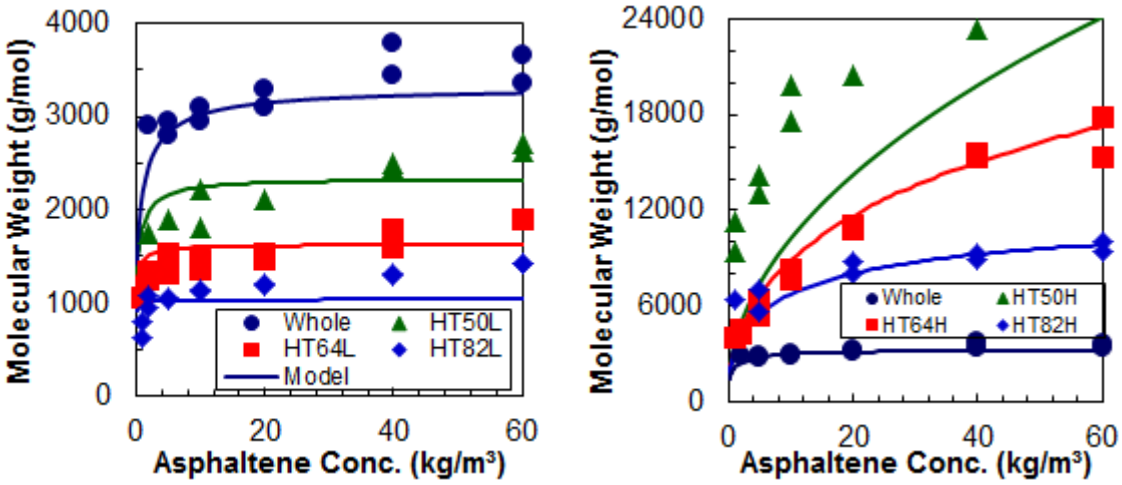

Figure B.46. Fitting of molecular weight data using the single-end termination model for all the fractions and whole 26845 asphaltenes.